Blowoff Velocities of Spherical Flameholders

by Alexander Weir, Jr.,
Donald E. Rogers, and Robert E. Cullen

Project MX-772
USAF Contract W33-038-ac-21100

Willow Run Research Center
Engineering Research Institute
University of Michigan
UMM-74. September 1950

TABLE OF CONTENTS

FOREWARD

The experimental work reported here is part of the experimental work performed by the University of Michigan Engineering Research Institute, Project M772, at the Willow Run Research Center, Willow Run Airport. This work was performed under Air Force Contract No. W33-038-ac-21100, which was initiated in July, 1948, by Mr. G. L. Wander, Fuels and Lubricants Branch, Power Plant Laboratory, Air Materiel Command. In January, 1950, this contract was transferred to the jurisdiction of Mr. D. G. Samaras, Office of Air Research, Wright-Patterson Air Force Base.

The experimental work on Project M772 was supervised by Mr. R. B. Morrison, whose aid and encouragement is sincerely appreciated. The experimental work (and the calculations involved) reported here was performed by A. Weir, D. E. Rogers, and R. E. Cullen. This report was prepared by A. Weir. A. W. Stohrer aided materially with the computations and plots required for this final report. Faculty advisors to Project M772 were Professor E. T. Vincent, Chairman of the Mechanical Engineering Department, and Assistant Professor J. W. Luecht, Aeronautical Engineering Department, University of Michigan.

ABSTRACT

The effect of different variables upon the mass velocity at blowoff of a spherical flameholder was determined. The experiments were performed in an unconfined jet under the following conditions:

Variable	Range
Propane-Air Ratio	0.060 to 0.100 lb propane/lb air
Spherical Flameholder Diameter	0.0625 to 0.189 inches
Ambient Pressure	0.4 to 1.0 atmospheres.
Nozzle Diameter	1/8 to 1 inch
Height of the Flameholder above Nozzle	0 to 1-1/8 inches

An empirical equation was developed which represented the experimental data obtained under the above conditions. In addition to the study of the effect of the above-mentioned variables on the mass velocity at blowoff, several miscellaneous experiments and observations are reported. Flames were extinguished by imposing external sounds over a wide range of frequencies and intensitites. The mass velocity at blowoff was considerably increased by inserting glass wool upstream of the nozzle, probably because of the reduction of resonance between the flame and the upstream vessel, since shadowgraphs indicated the flow conditions were essentially unchanged. In the small "pilot" flame obtained just before blowoff, it was observed that a luminous region in the pilot flame always moved towards the flameholder before blowout occurred under vacuum. Static and total pressure measurements were made throughout the flame region, as well as electrical conductivity measurements. It was found that a cylinder inserted at a certain critical distance downstream of a spherical flameholder increased the flame stability markedly. It was established that removal of the flameholder boundary layer considerably decreased the flame stability limits, and under certain conditions extinguished the flame.

LIST OF ILLUSTRATIONS

LIST OF ILLUSTRATIONS (CONT'D)

LIST OF ILLUSTRATIONS (CONT'D)

LIST OF ILLUSTRATIONS (CONT'D)

I. INTRODUCTION

This paper is a study of some of the factors which change the flame stability limits of a flameholder. This study is important because of the combustion problems experienced with the operation of jet-propulsion devices. A ramjet combustion chamber is simply a duct with a flameholder inserted. The fuel-air mixture enters at one end, is partially burned in the wake of the flameholder, and leaves the combustion chamber with increased momentum due to the addition of heat. However, experiments with these burners indicated that adequate flame stability was necessary to secure operation of the ramjet. In addition, operation at high altitude conditions indicated that pressure was an important variable to be considered in the design of a ramjet combustion chamber. Hence, in order to secure efficient operation of a ramjet, it is necessary to have some understanding of the variables affecting the flame stability limit or blowoff velocity limit of a flameholder.

There are a great number of variables which affect the blowoff velocity of a flameholder. These may be divided into two groups, those variables which are purely physical in nature, and variables whose effect is due to some physico-chemical aspect. These variables are not all independent of each other and there is no clear cut distinction between the two groups. In the first group might be considered variables, such as the shape (sphere, cone, cylinder, grid, orifice, disc, or flat plate) and orientation of the flameholder, the diameter or some characteristic dimension of the flameholder, the distance of the flameholder from the nozzle or jet exit, the diameter of the nozzle, the degree of confinement of the jet, the velocity distribution of the jet, and the turbulence of the jet.

The second group might include such items as the type (paraffin, olefin, etc.) and state (gaseous or liquid) of the fuel, the heating value of the fuel, the droplet size and distribution of a liquid fuel, the homogenuity of the fuel-air mixture, the temperature of the fuel-air mixture, the temperature of the flameholder, the surface material of the flameholder, the presence of combustion products and water of humidity in the fuel-air mixture, the intensity and frequency of external sounds as well as resonance effects due to the flame itself, and the ambient pressure of the atmosphere. While there are probably other factors which also affect the blowoff velocities of flameholders, all of the above experimental variables have been investigated to a greater or lesser extent, either in

this laboratory or at laboratories of other institutions.

In the experimental work reported here, many of the above mentioned variables have been minimized or eliminated in order to reduce the problem of flame stabilization to a more basic level. To that end, a single paraffin fuel, gaseous propane, was used to eliminate the problems inherent with liquid fuels. This fuel was mixed thoroughly with air reasonably free from water vapor or other combustion products. Spherical flameholders were used to eliminate the shape and orientation effects. An unconfined jet with a rectangular velocity distribution was used. Those parameters which were intentionally varied were fuel-air ratio, sphere diameter, ambient pressures below one atmosphere, nozzle or jet diameter, and the height of the flameholder above the nozzle. Some idea of the range of mass velocities* used in this investigation may be seen in figure 1, which shows the effect on the mass velocity at blowoff caused by changing each of the above variables in turn. It is the purpose of this paper to show quantitatively the effect on mass velocity at blowoff of the five variables mentioned above, i.e., flameholder diameter, fuel-air ratio, ambient pressure, nozzle diameter, and flameholder height.

* Mass velocity is defined as the mass flow per unit area of the nozzle (lbs/sec/sq.ft. of nozzle area) and is numerically equal to the product of the average linear jet velocity (ft/sec) and the average density (lbs mass/cu.ft.) of the fuel-air mixture issuing from the jet. It can be regarded as proportional to the thrust of a ramjet.

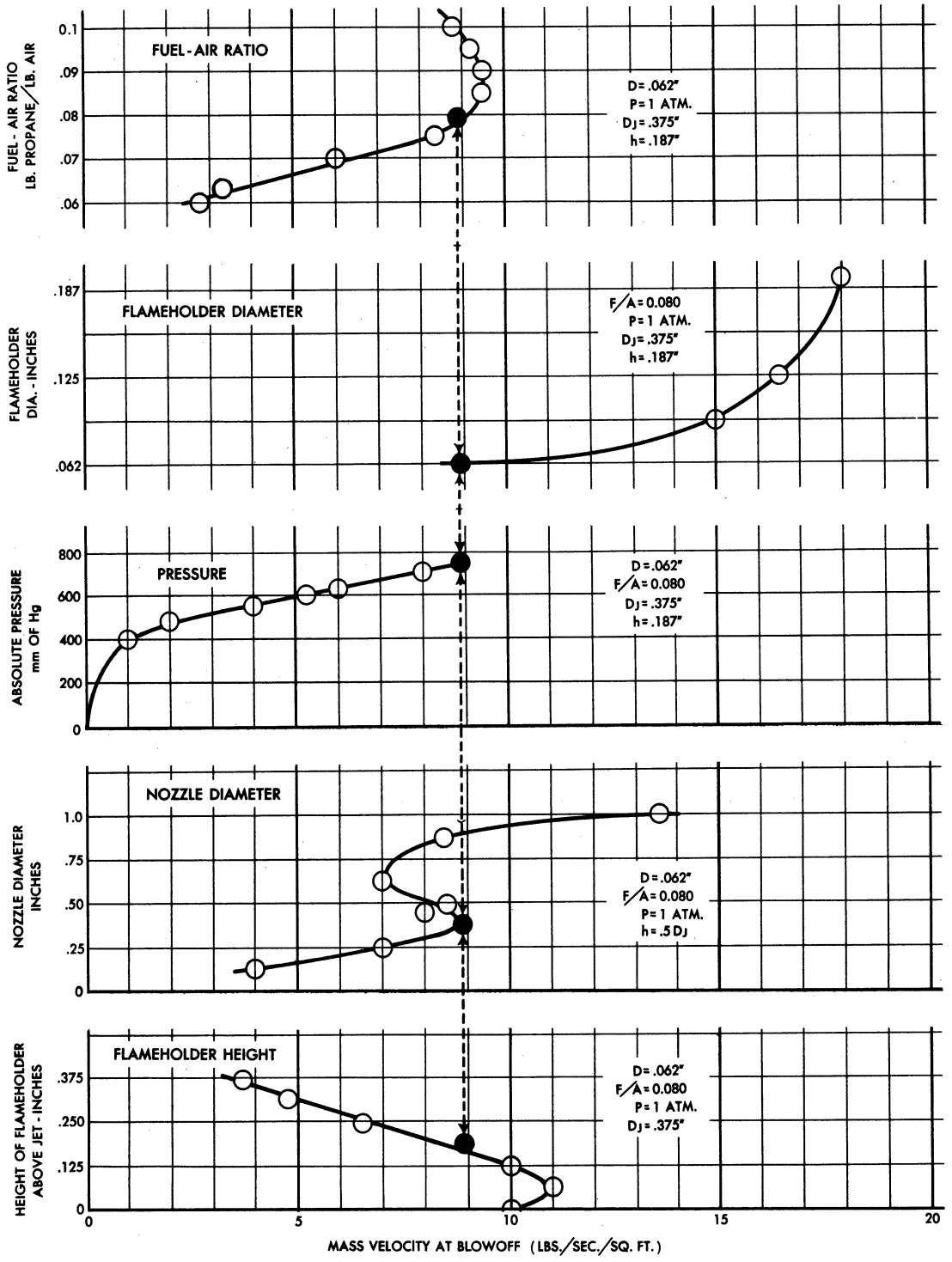

FIG. 1 VARIABLES AFFECTING MASS VELOCITY AT BLOWOFF OF SPHERICAL FLAME HOLDERS

II. DESCRIPTION OF APPARATUS, MATERIALS, AND METHOD OF TESTING

The equipment used during this investigation was designed to measure the mass velocity at blowoff for various fuel-air ratios and ambient pressures, the physical variables (i.e., spherical flame holder diameter, nozzle diameter, and height of the flame holder above the nozzle) being held constant. These physical variables could then be changed and the experiments repeated.

Two different systems were used during this investigation. In System 1, a schematic diagram of which may be seen in figure 2, the fuel mass rate and the air mass rate could be varied during operation, the ambient pressure (atmospheric) being held constant. Blowoff of the flame was obtained in this system by setting some air flow and then changing very slowly the fuel flow rate until blowoff occurred. Identical values were obtained if the fuel flow rate was set and the air flow rate changed slowly.

A schematic diagram of the second system used, System 2, may be seen in figure 3. In the operation of this system under vacuum, it was found advantageous to let the fuel-air ratio be held constant during an experiment by using a premised fuel and air mixture of known composition. The total mass flow and the ambient pressure could be varied during the experiment. Blowoff would occur in this system if the pressure were maintained constant and the mass flow increased, but operation was simpler if a certain flow of fuel-air mixture was set on the rotameter and then the pressure decreased slowly until blowoff occurred.

In both System 1 and System 2 a stable pilot flame was observed just before blowoff except when blowoff occurred at low jet velocities or when the flame was accoustically disturbed. In figure 4 may be seen photographs of a flame burning from a holder at jet velocities of 186 and 268 ft/sec. As evidenced by these photographs, it may be seen that at the jet velocity of 186 ft/sec., steady state combustion is maintained far downstream of the holder while at the higher jet velocity combustion is confined to a very small region immediately downstream of the spherical flame holder. The photograph on the right in figure 4 (i.e., at the higher jet velocity) is a typical photograph of the pilot flame seen before blowoff.

An observation concerning this pilot flame was made during the experiments performed in System 2 under vacuum. This observation, which enabled

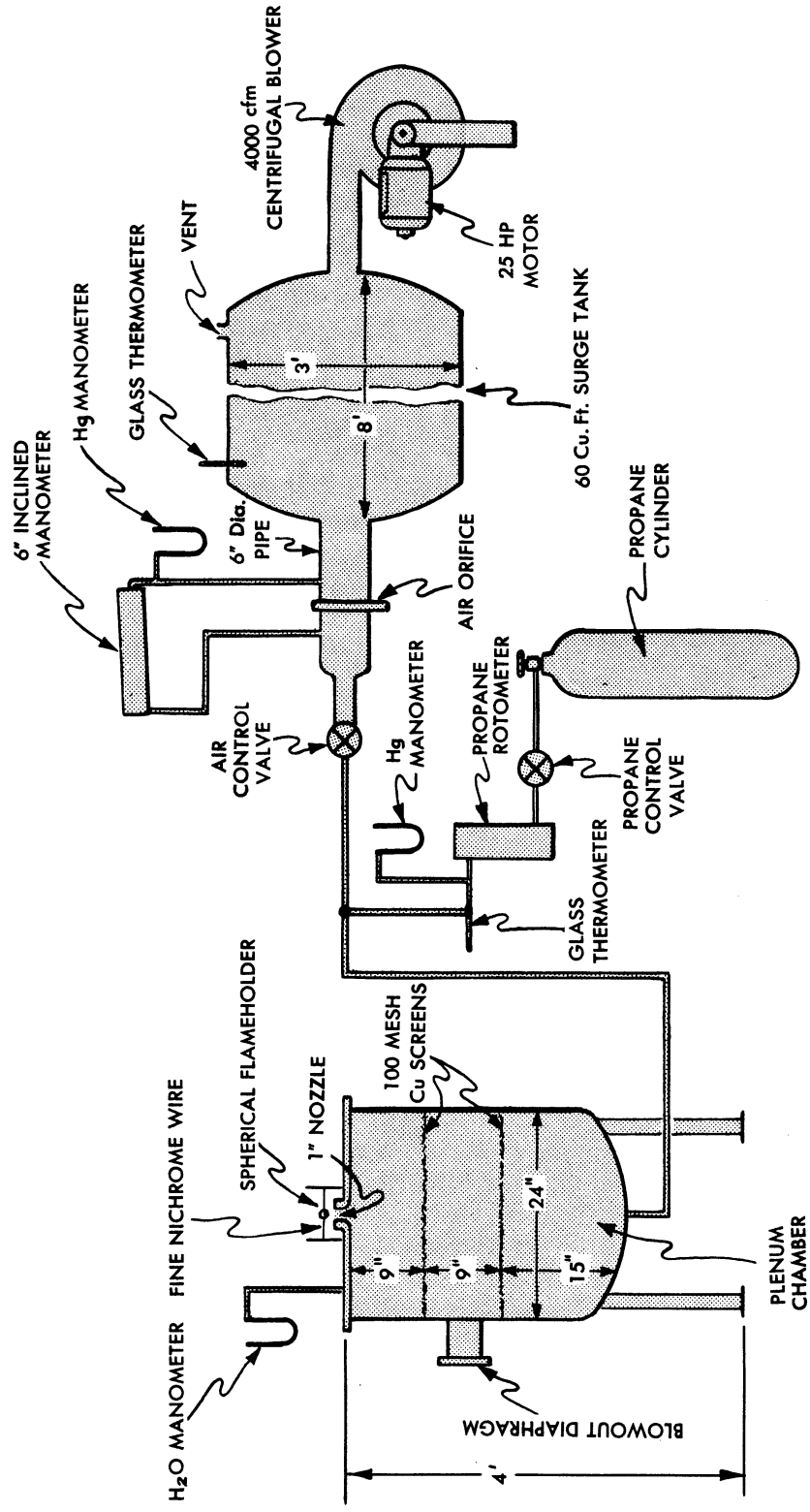

FIG. 2 SCHEMATIC DIAGRAM OF SYSTEM 1

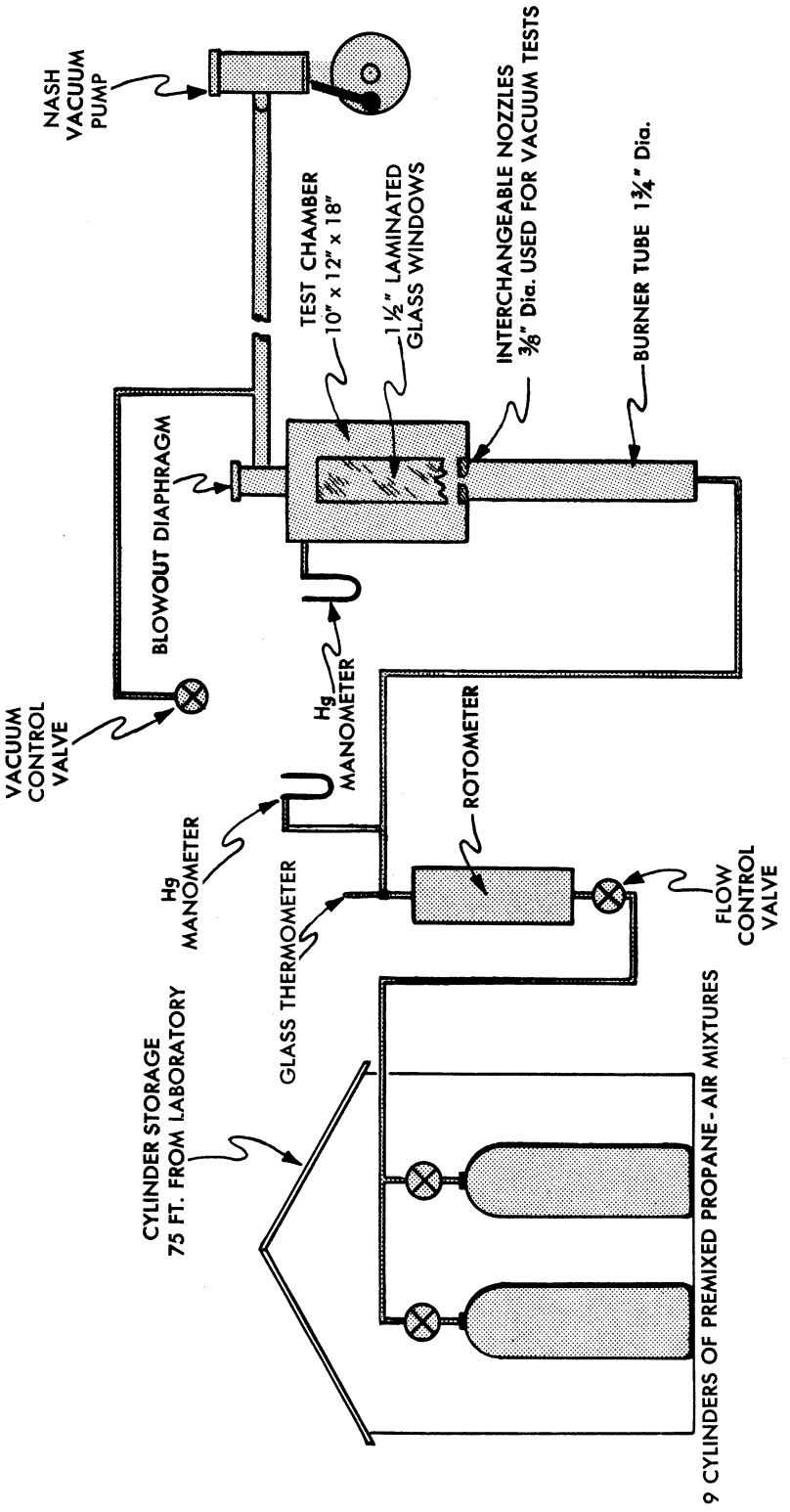

FIG. 3 SCHEMATIC DIAGRAM OF SYSTEM 2.

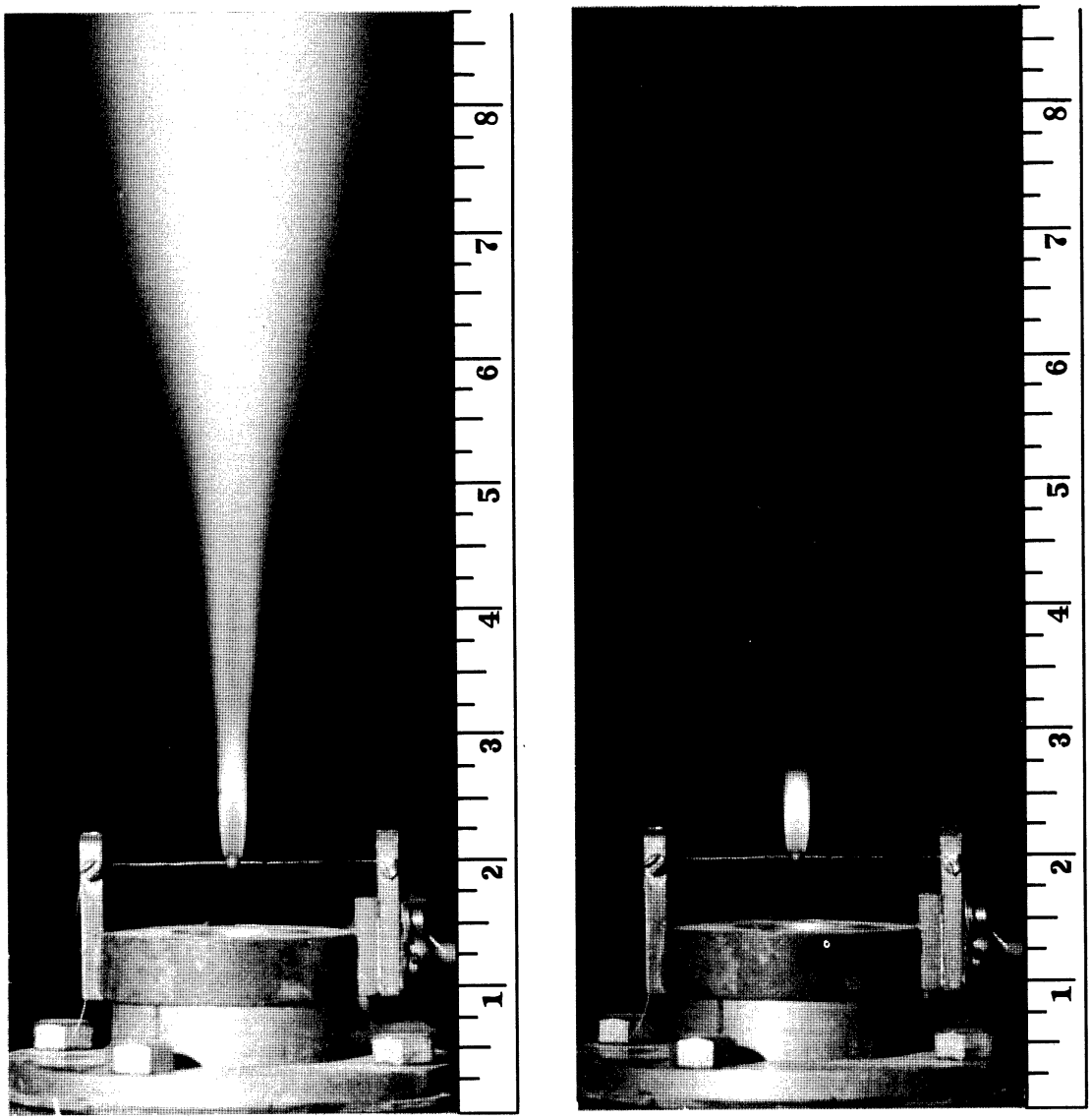

(4a) Typical intermediate velocity flame
Jet velocity - 186 ft./sec.

(4b) Typical pilot flame
Jet velocity - 268 ft./sec.

FIG. 4 TYPICAL FLAME PHOTOGRAPHS

Propane-air ratio = 0.05
Nozzle dia. = 1 in.
Height of flameholder = 1/2 in.
Flameholder dia. = 1/8 in.
Pressure = 1 atm.

FIG. 4 TYPICAL FLAME PHOTOGRAPHS.

the experimenters to eliminate premature blowoff points, was that a zone of violently agitated and burning gas moved toward the flame holder before blowoff. A sequence of six pictures approaching the blowoff point is reproduced in figure 5. Photographs A, B, C, D, E, and F were taken at increasing velocity and decreasing pressure from left to right with photograph F taken just prior to blowoff. In these photographs of the pilot flame region, the agitated region appears luminous (or white). The agitated region is very close to the holder just before blowoff and moves about quite rapidly. At the instant this region touched the downstream side of the flame holder, blowoff occurred. This phenomena was noted during the atmospheric blowoff runs, however there was not enough contrast between the wake and the agitated zone to allow a photograph or a close observation of the occurrence.

During early experiments, an electric spark was passed through the mixture, after blowoff had occurred, to determine whether or not the mixture was combustible. This "spark test" was not used a great deal during the later experiments, since the appearance of the pilot flame aided materially in the determination of the blowoff point.

A schematic diagram of System 2 was previously shown in figure 2. Several photographs of this system are shown if figure 6. The upper photograph shows the 4000 cfm. blower, the 60 cu. ft. surge tank and the propane cylinder, while the lower photograph shows the metering instruments and the plenium chamber.

The rotameter used to meter the propane, manufactured by Fischer and Porter, was calibrated with propane by a volumetric displacement method as well as by measuring the change in weight of a propane cylinder over five minute intervals.

The flat plate, square edged, brass orifice used to meter the air was designed in accordance with the Report of the ASME Research Committee on Fluid Meters and was then calibrated, with the section of six inch pipe and the radius taps used, against a standard orifice in the Ford Research Laboratory, Dearborn, Michigan, through the courtesy of Mr. W. G. Was. The values obtained in the calibration agreed with the values predicted by the ASME Formulas.

A schematic diagram of System 2 was previously shown in figure 3. A photograph of this system is shown in figure 7 while figure 8 shows

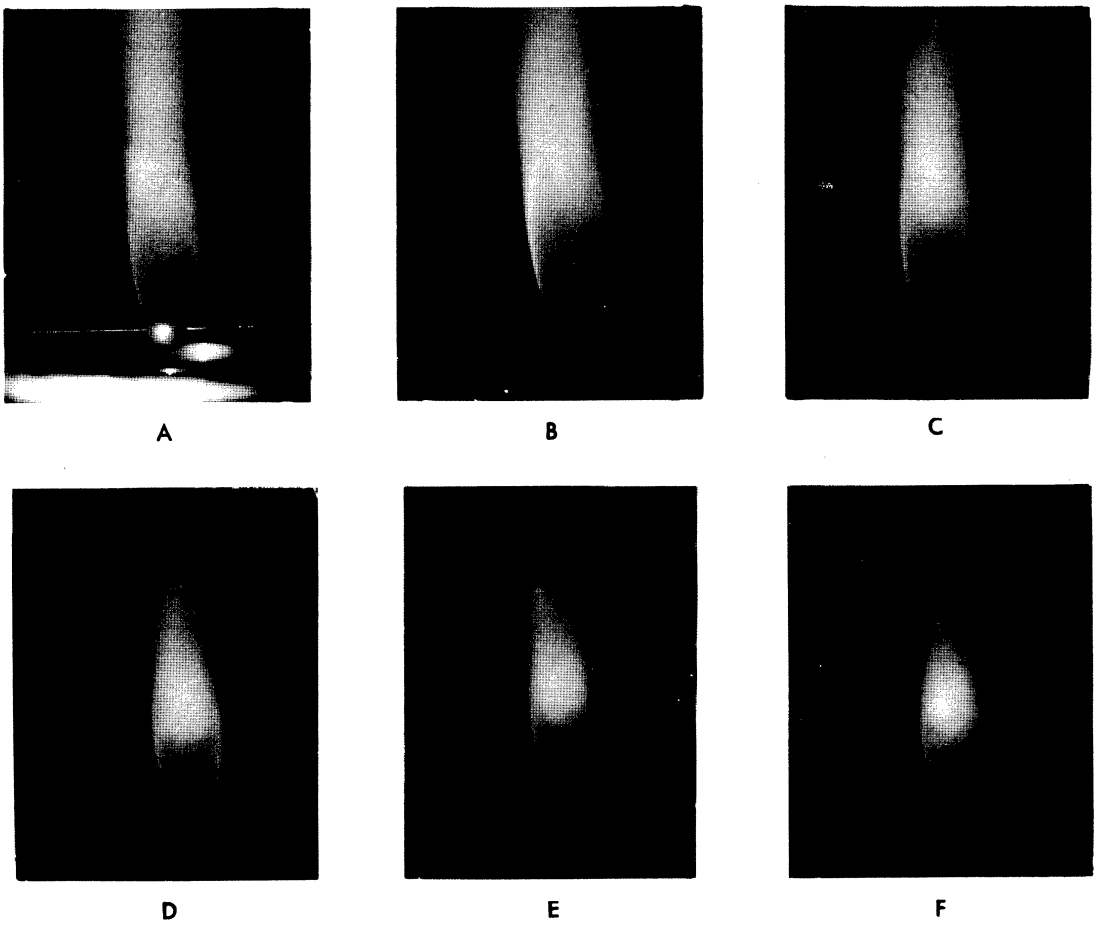

FLAMEHOLDER HEIGHT - 3/16"
FUEL AIR RATIO - 0.080"
NOZZLE DIA. - 3/8"
SPHERE DIA. - 3/16"

PHOTOGRAPH No.	ABS PRESSURE mm of Hg
A	680
B	465
C	412
D	359
E	333
F	307

FIG. 5 PHOTOGRAPHS OF BURNING FROM A SPHERICAL FLAME HOLDER UNDER VACUUM.

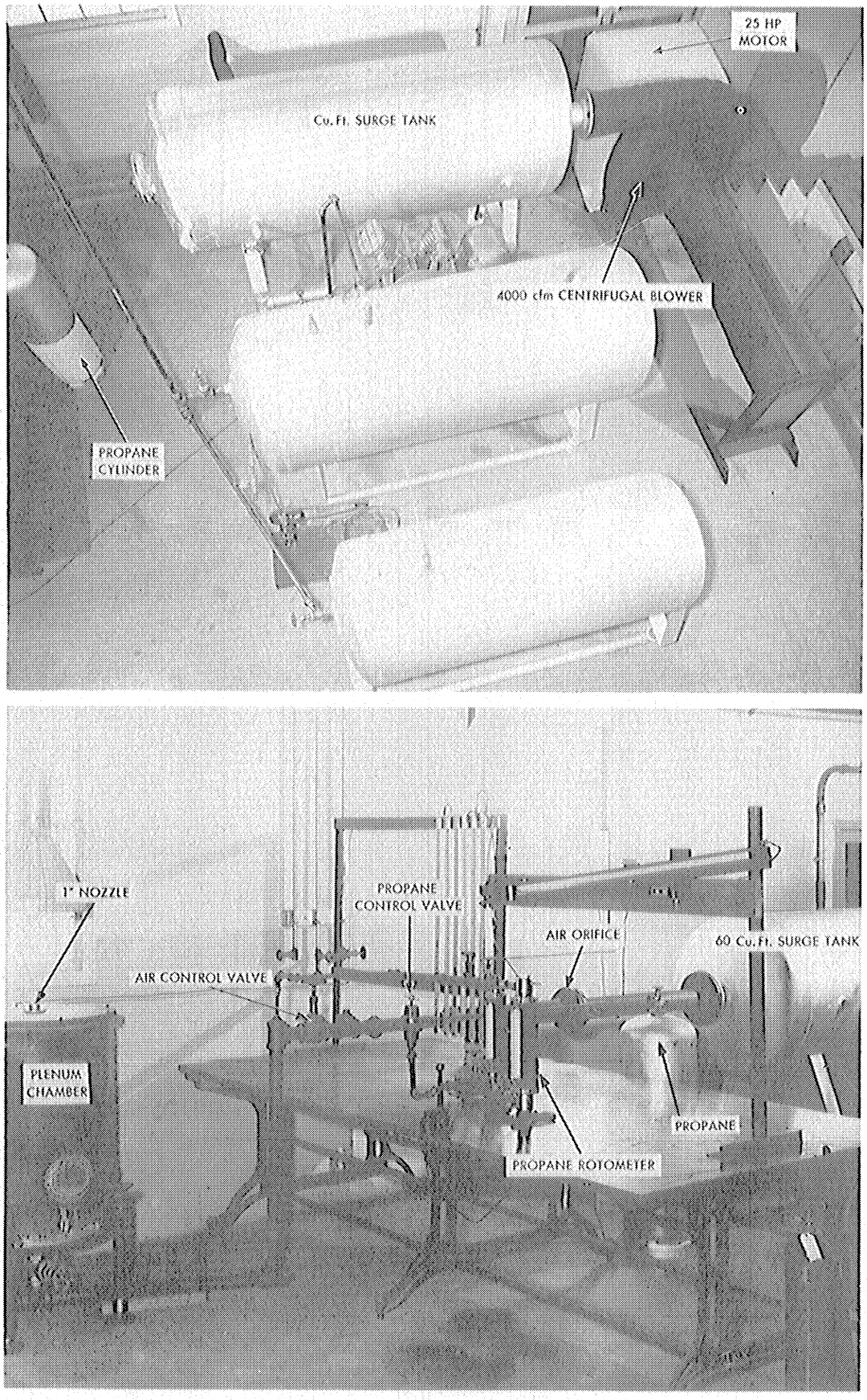

FIG. 6 PHOTOGRAPHS OF SYSTEM 1.

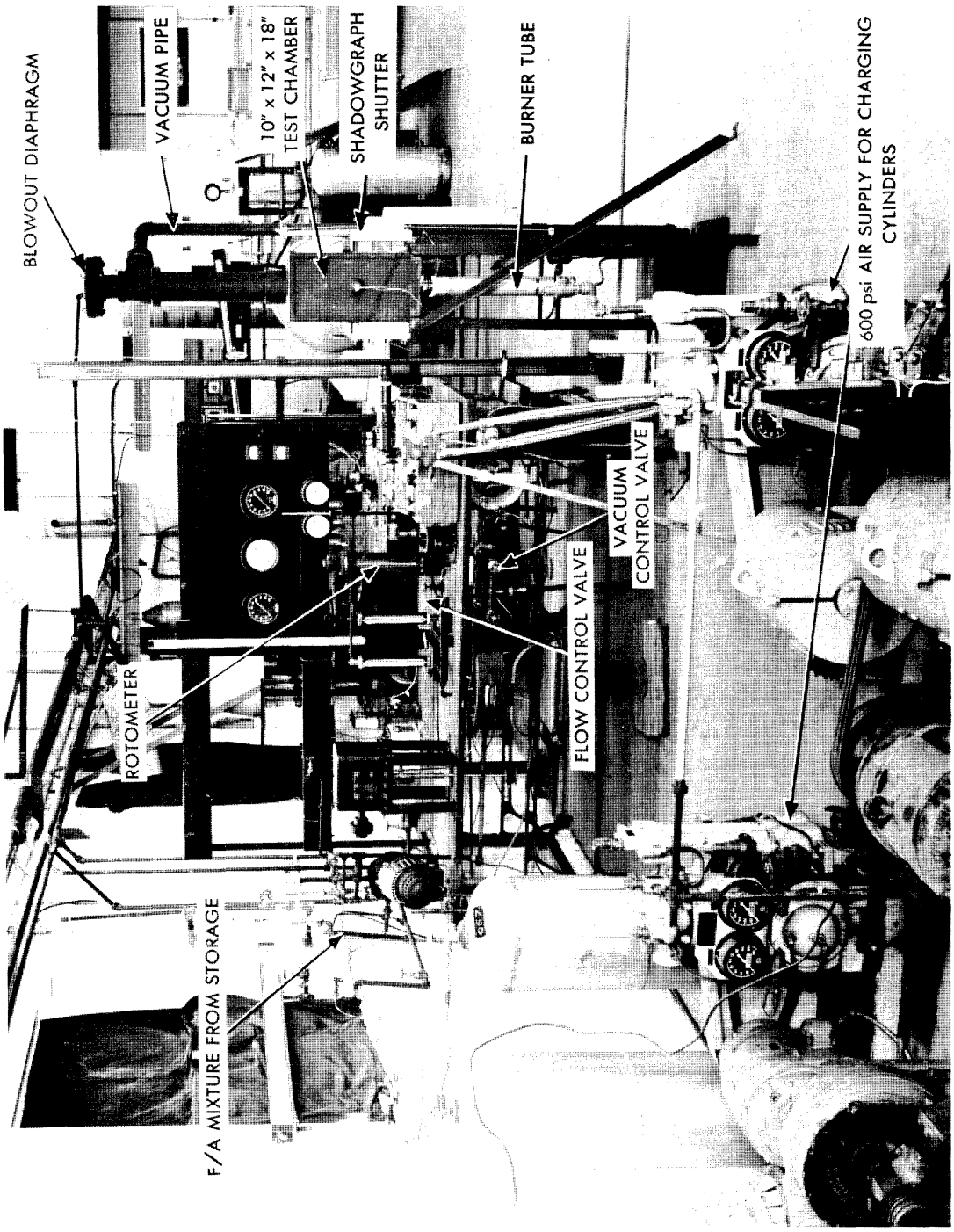

FIG. 7 PHOTOGRAPHS OF SYSTEM 2.

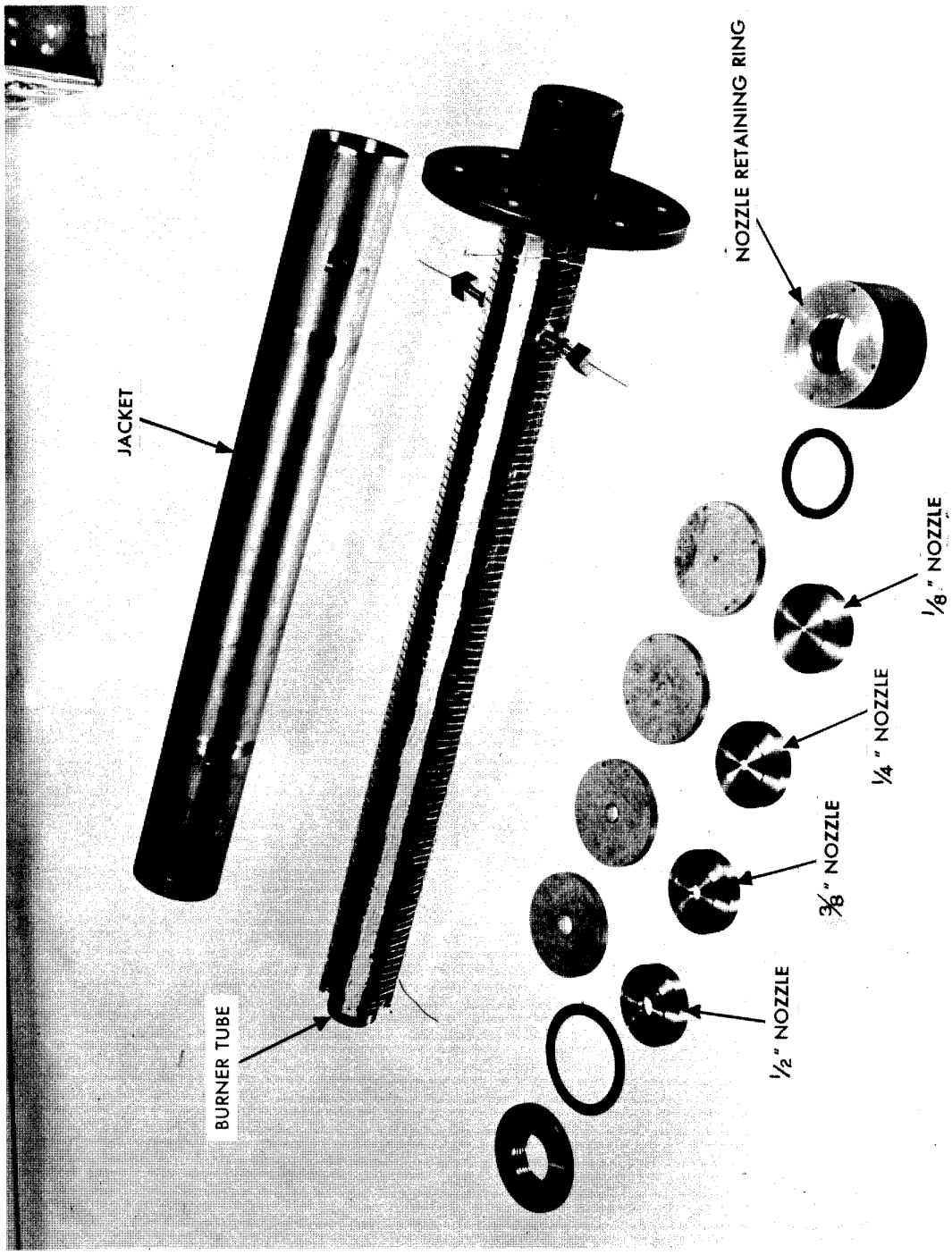

FIG. 8 PHOTOGRAPH OF BURNER ASSEMBLY IN SYSTEM 2.

an exploded view of the burner tube and the nozzles. The nichrome wire shown on the inner tube was not used during this investigation.

The rotameter used, manufactured by Schute and Koettering, was calibrated with an 0.080 fuel-air mixture by a volumetric displacement method at atmospheric pressure. This calibration was checked against previously calibrated rotameters in this laboratory. There is some indication that at very low pressures, the square root of the density ratio method of computing the rotameter flow is slightly in error. Also, at very low pressures, the mass velocity at blowoff is also very low, giving a reading near the bottom of the rotameter scale where the accuracy of the rotameter is in doubt. However, at mass velocities over 2 lbs/sec/sq.ft. of nozzle area it is believed that the rotameter calibration is correct.

The fuel used in this investigation was commercially pure propane (95 per cent propane and propylene) obtained from the Flamegas Corporation, Detroit, Michigan. The majority of the data was obtained in System 2, and the propane used in this system was obtained from a single cylinder. The cylinder contents were not analyzed. Several cylinders were used in the investigation in System 1. However, no difference in blowoff velocities was observed when different cylinders were used. The air, supplied in System 1 by means of the 4000 cfm. blower shown in figure 6, had a relatively low humidity when measured in the 60 cu.ft. surge tank shown in figure 6. After the blower had been in operation for several minutes, the air temperature was ca. 100°F which probably accounted for the low humidity (0.01 lb. water/lb. bone dry air) of the air.

As was previously stated, in the operation of System 2 under vacuum, it was found advantageous to use a premixed fuel and air mixture of known fuel-air ratio. Accordingly, cylinders containing propane-air ratios (by weight) of 0.060, 0.0637 (stoichiometric ratio), 0.070, 0.075, 0.080, 0.085, 0.090, 0.095, and 0.100 were prepared. The cylinders were filled with gaseous propane, evacuated to 15 mm Hg abs., filled with propane and evacuated a second time, and then filled with propane to a predetermined pressure. The temperature of the cylinder wall was measured at this time with a Leeds and Northrup Galvanometer and a chromel-alumel thermocouple. Air, from a 600 psig source, was then charged into the cylinder in such a fashion, so that when the cylinder was at the same temperature as that recorded during the propane charging, the total pressure was 240 psig. Measurements of the humidity of the air to be charged (which was at

600 psig and ca. 110°F) indicated that the humidity was less than 0.01 lb. water/lb. bone dry air. The compressibility factors for air and propane, used in calculating the amount of propane to be charged for some desired fuel-air ratio, were obtained from a plot of compressibility factors with parameters of reduced pressure and reduced temperature.[1]

The cylinders of propane-air mixtures were placed in a shed ca. 75 ft. from the laboratory building where they were connected to System 2 inside the laboratory.

The flame holders used in this investigation were steel ball bearings obtained (before the hardening process) through the courtesy of the Hoover Ball Bearing Co., Ann Arbor, Michigan. Four different size spheres were used, 0.0625, 0.0937, 0.1250, and 0.1890 inches in diameter. No. 80 drill holes were made through an axis of the sphere and the spheres were mounted on 0.005 in. diameter nichrome wire. Various methods were used to mount the sphere on the wire, including knotting the wire in the center of the sphere as well as the use of adhesives, such as sodium silicate ("water glass") or "X-pando" pipe cement. The latter methods were preferable. The spherical flame holders were mounted in the center of the jet as is shown in figure 4. Various heights of the flame holder above the nozzle were used. At low jet velocities, with nichrome wires larger in diameter than 0.013, the flame tended to burn from the wire as well as from the flame holder, but this tendency was not observed with the 0.005 diameter wire used.

The diameter of the nozzle used in System 1 was 1 inch. A 3/8 inch diameter nozzle was used in the vacuum experiments in System 2, but nozzles with diameters of 1/8, 1/4, 7/16, 1/2, and 5/8 inch were also used with this system. The radius of curvature of each of these nozzles was equal to the diameter of the nozzle in each case.

It is believed that the usual criterion for testing nozzles, i.e., a rectilinear velocity distribution, was met with all of these nozzles. In Table 1 is shown nozzle coefficients which were determined by means of a total head tube.

Table 1 follows on the next page.

TABLE 1

Nozzle Coefficients of 3/8-inch Diameter Nozzle
at 1/2 Nozzle Diameter Above Jet

Mass Velocity lb/sec/sq.ft. of Nozzle Area	Nozzle Coefficient = Average Velocity / Maximum Velocity
4	0.954
6	0.963
10	0.964
14	0.966
18	0.968
22	0.970

Comparable values were obtained with the 1/2 inch diameter nozzle in System 2 and the 1 inch diameter nozzle in System 1.

III. SPHERICAL FLAME HOLDER EXPERIMENTAL DATA

The data obtained with System 1 at atmospheric pressure is shown in figure 9. The diameter of the nozzle used was 1 inch and the flame holders were tested at a height of 1/2 nozzle diameter (1/2 inch). The experimental data was smoothed on this mass velocity plot since it is essentially a plot of the two experimental variables measured during this set of experiments. The area inside of the curves shown in figure 9 represents a condition in which it is possible to maintain stable burning, while the area outside of these curves represents a condition in which it is not possible to secure combustion under the test conditions. As may be seen from figure 9, the fuel-rich blowoff limit is the same curve for the four spherical flame holders tested.

Because of the experimental technique used, greater weight was given to points near the outside of the curve since a large number of variables (gusts of wind, vibrations or noises in the laboratory, etc.) may cause premature blowoff, but only errors in observation or measurement will cause higher values of the blowoff velocity.

The experimental data which was obtained under vacuum in System 2 is presented in figures 10, 11, 12, and 13. The diameter of the nozzle used in these experiments was 3/8 inch and the height of the flame holder above the jet was 1/2 nozzle diameter (3/16 inch). The data obtained with the 1/16 inch diameter spherical flame holder is shown in figure 10, which contains plots of the absolute pressure versus the mass velocity at blowoff for the nine fuel-air ratios tested. Similar data for the 0.0937, 0.125, and 0.189 inch diameter flame holders are shown in figures 11, 12, and 13.

Data obtained from the smoothed curves shown in figure 10 was used to obtain the mass velocity plot shown in figure 14. This plot is similar to figure 9 except that parameters of pressure rather than flame holder diameter are used. It is to be noted that, as in the case involving flame holder diameter, the curves are concurrent on the fuel-rich side. Curves similar to figure 14, except for other diameter flame holders, are shown in figures 15, 16, and 17.

However, the data obtained in System 2, although showing the same trends, did not have the same numerical values as the data obtained in

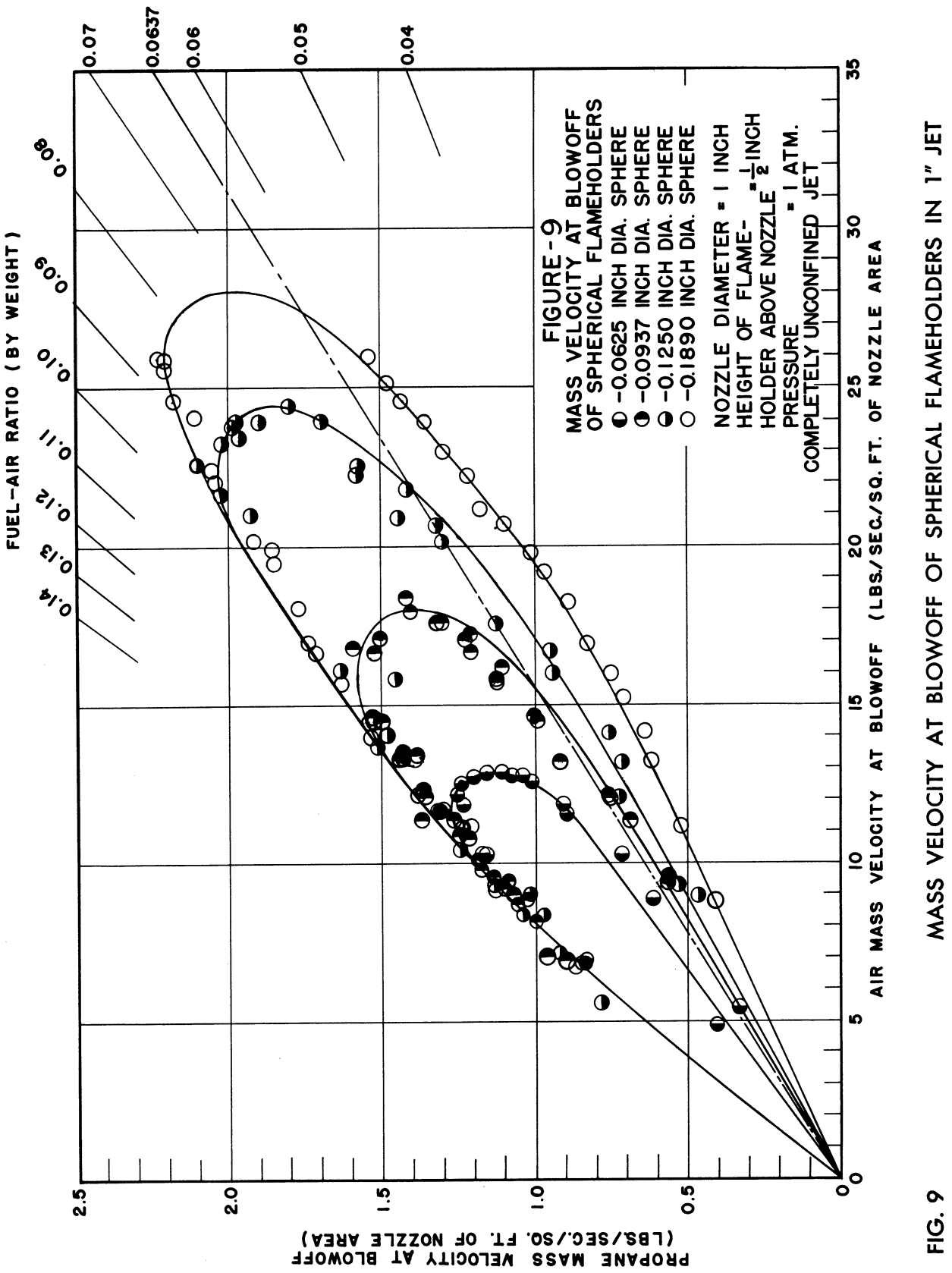

FIG. 9 MASS VELOCITY AT BLOWOFF OF SPHERICAL FLAMEHOLDERS IN 1" JET AT ATMOSPHERIC PRESSURE

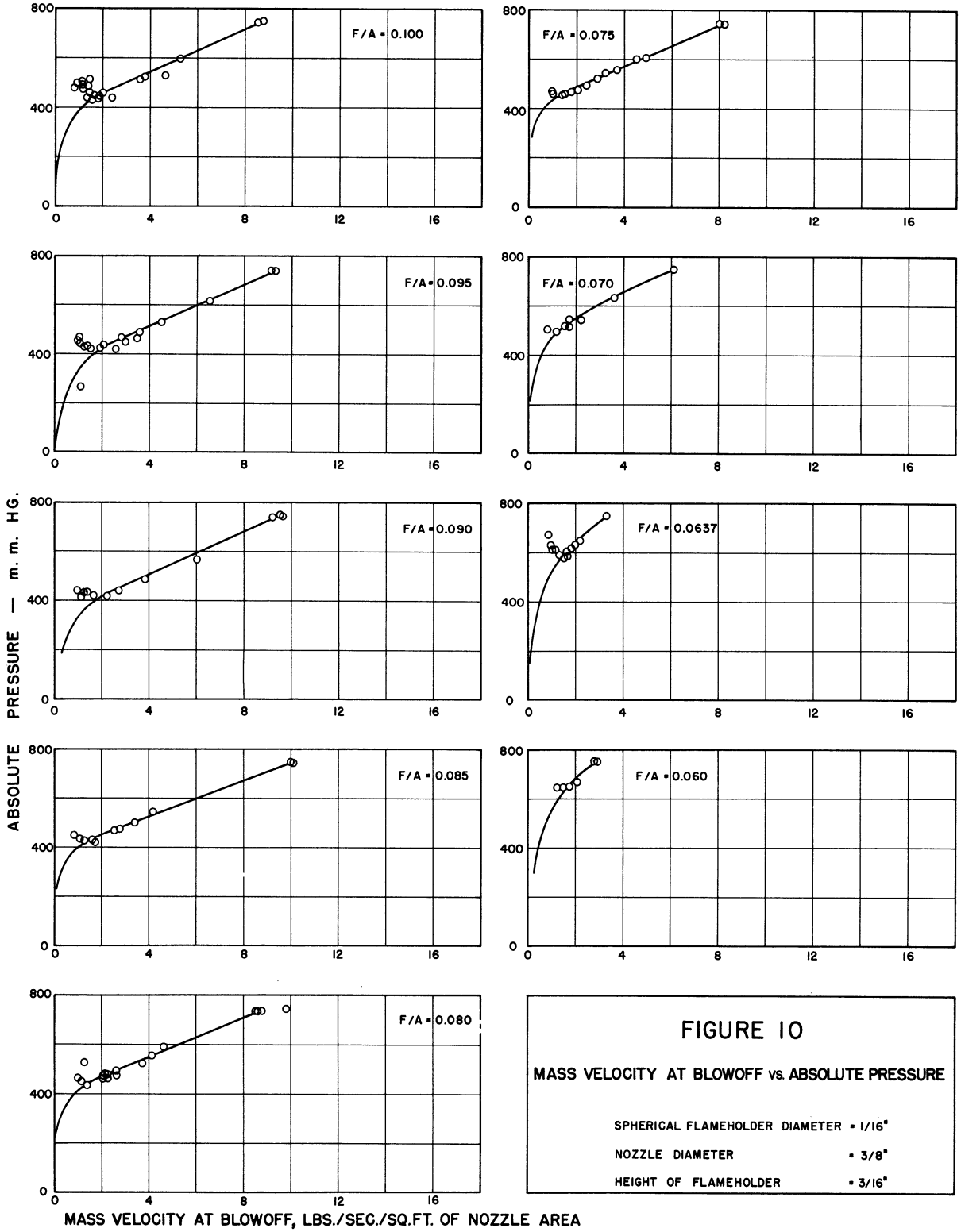

FIG. 10 MASS VELOCITY AT BLOWOFF VERSUS ABSOLUTE PRESSURE FOR .0625 IN. DIAMETER SPHERICAL FLAME HOLDERS.

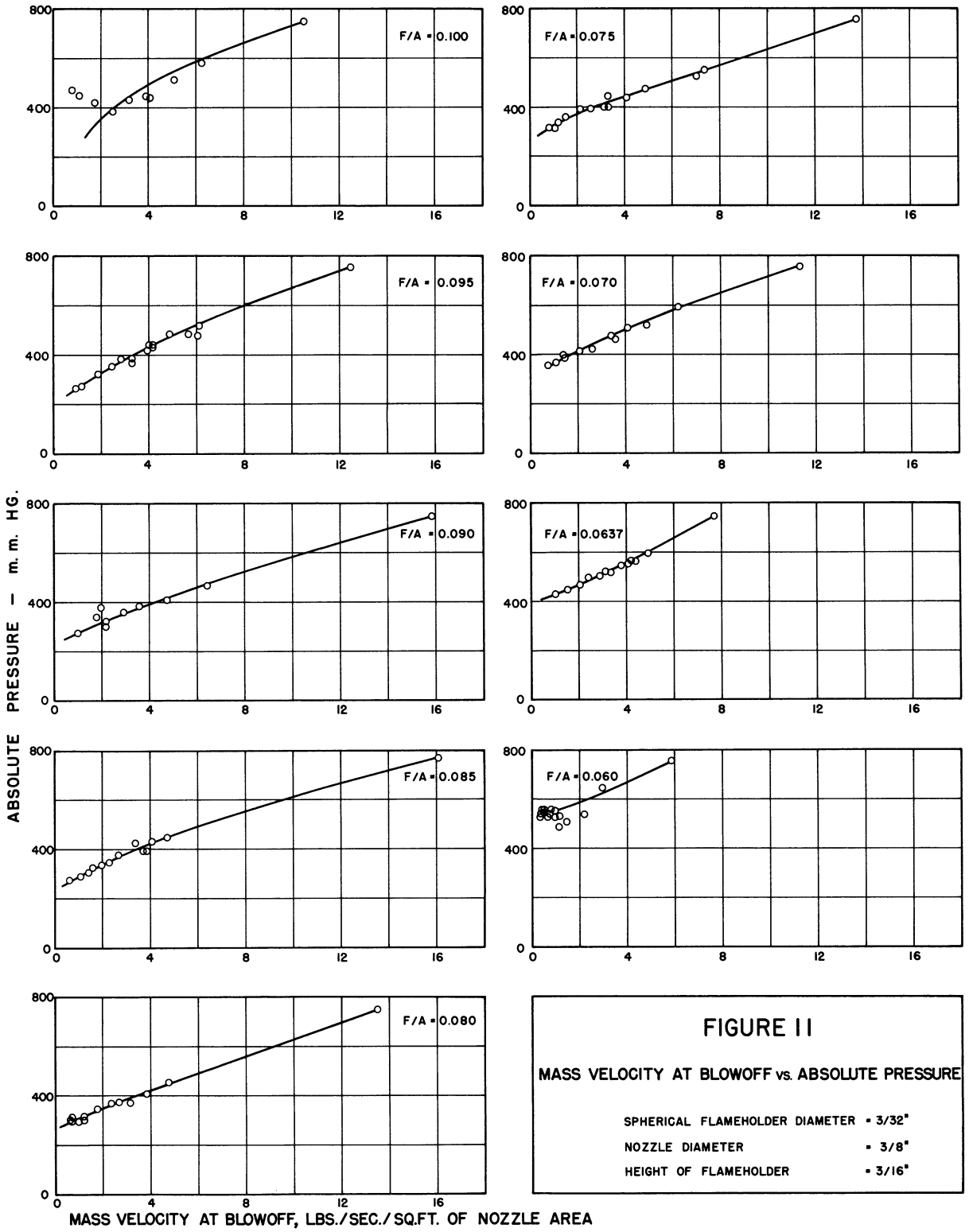

FIG. 11 MASS VELOCITY AT BLOWOFF VERSUS ABSOLUTE PRESSURE FOR .094 IN. DIAMETER SPHERICAL FLAME HOLDERS.

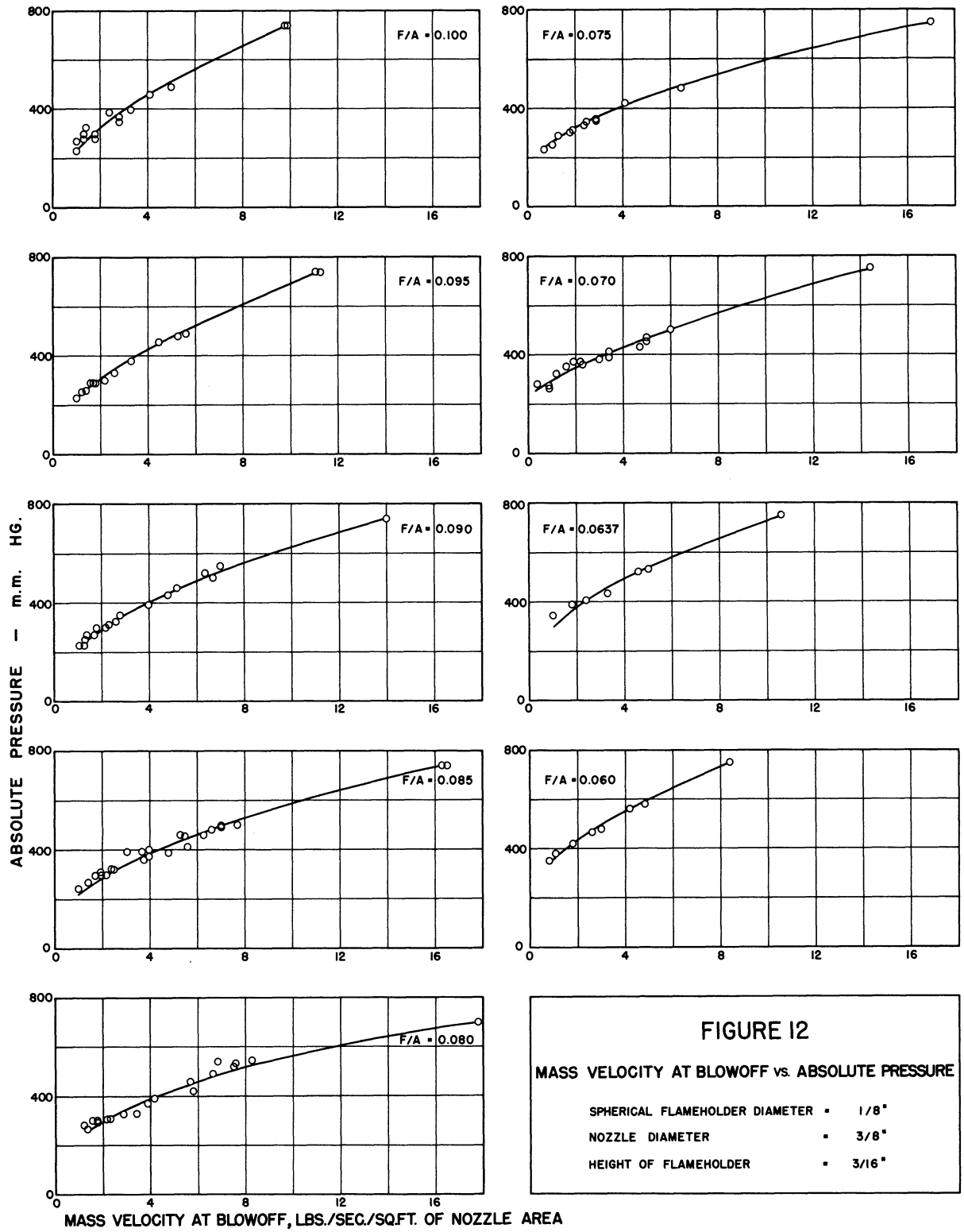

FIGURE 12

MASS VELOCITY AT BLOWOFF vs. ABSOLUTE PRESSURE

SPHERICAL FLAMEHOLDER DIAMETER = 1/8"
NOZZLE DIAMETER = 3/8"
HEIGHT OF FLAMEHOLDER = 3/16"

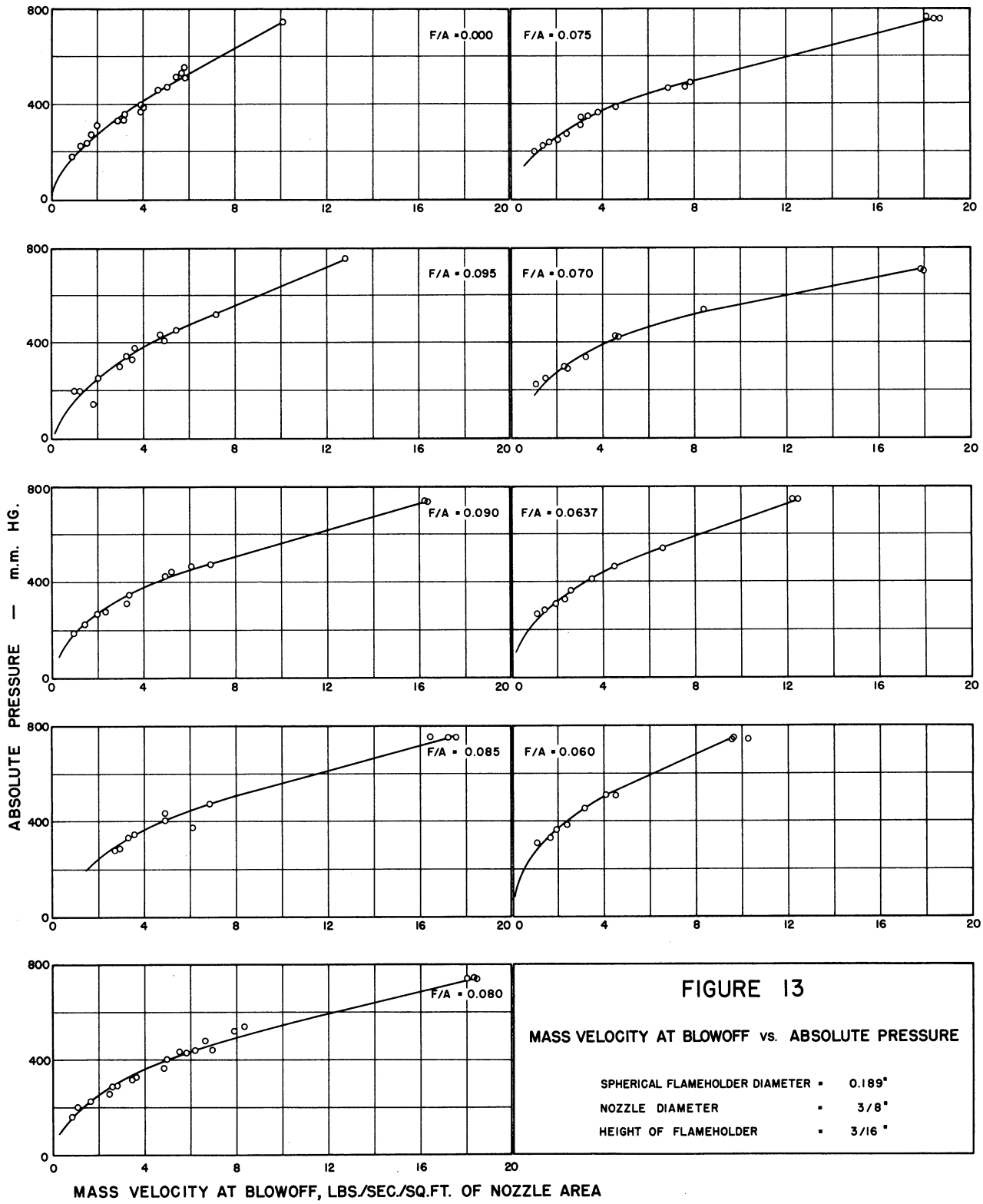

FIGURE 13

MASS VELOCITY AT BLOWOFF vs. ABSOLUTE PRESSURE

SPHERICAL FLAMEHOLDER DIAMETER = 0.189"
NOZZLE DIAMETER = 3/8"
HEIGHT OF FLAMEHOLDER = 3/16"

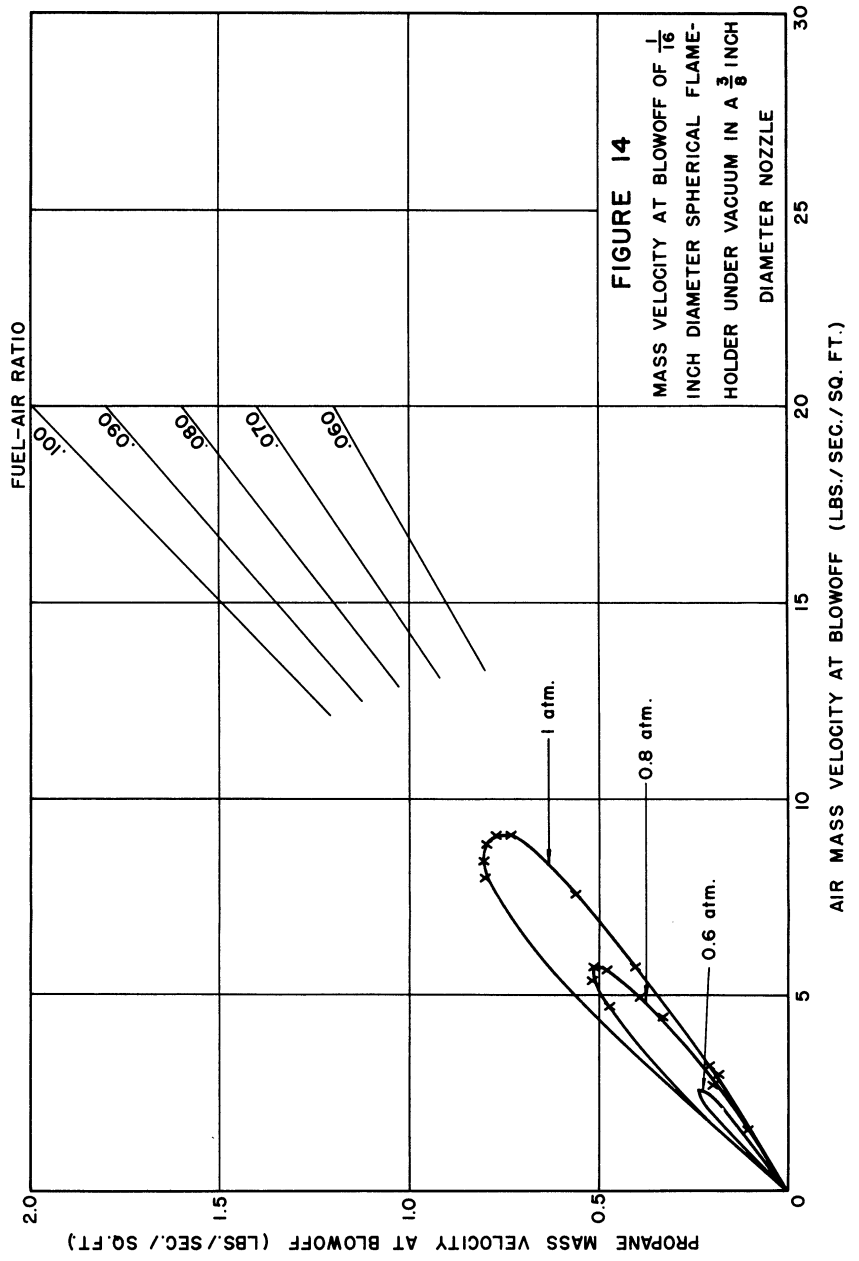

FIG. 14 MASS VELOCITY AT BLOWOFF FOR .0625 FLAME HOLDER UNDER VACUUM.

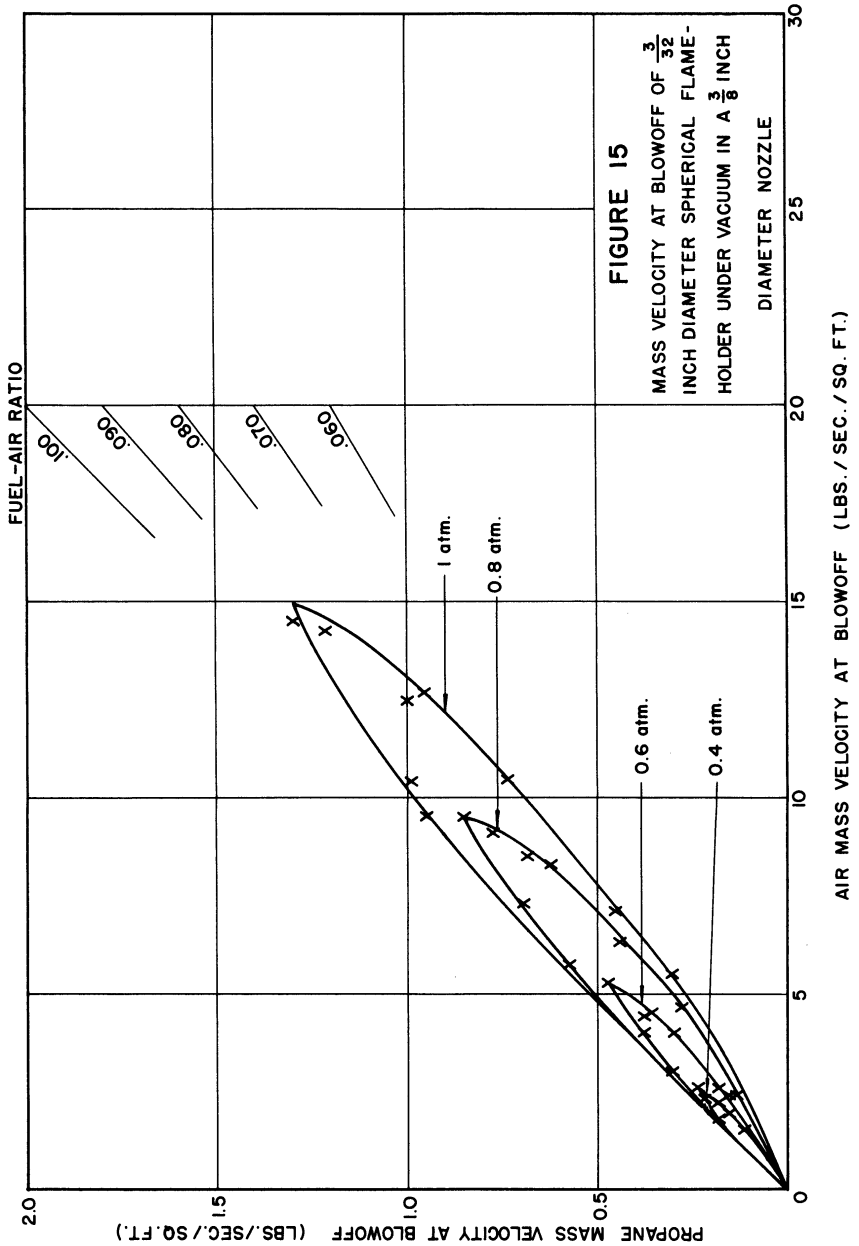

FIG. 15 MASS VELOCITY AT BLOWOFF FOR .094 FLAME HOLDER UNDER VACUUM.

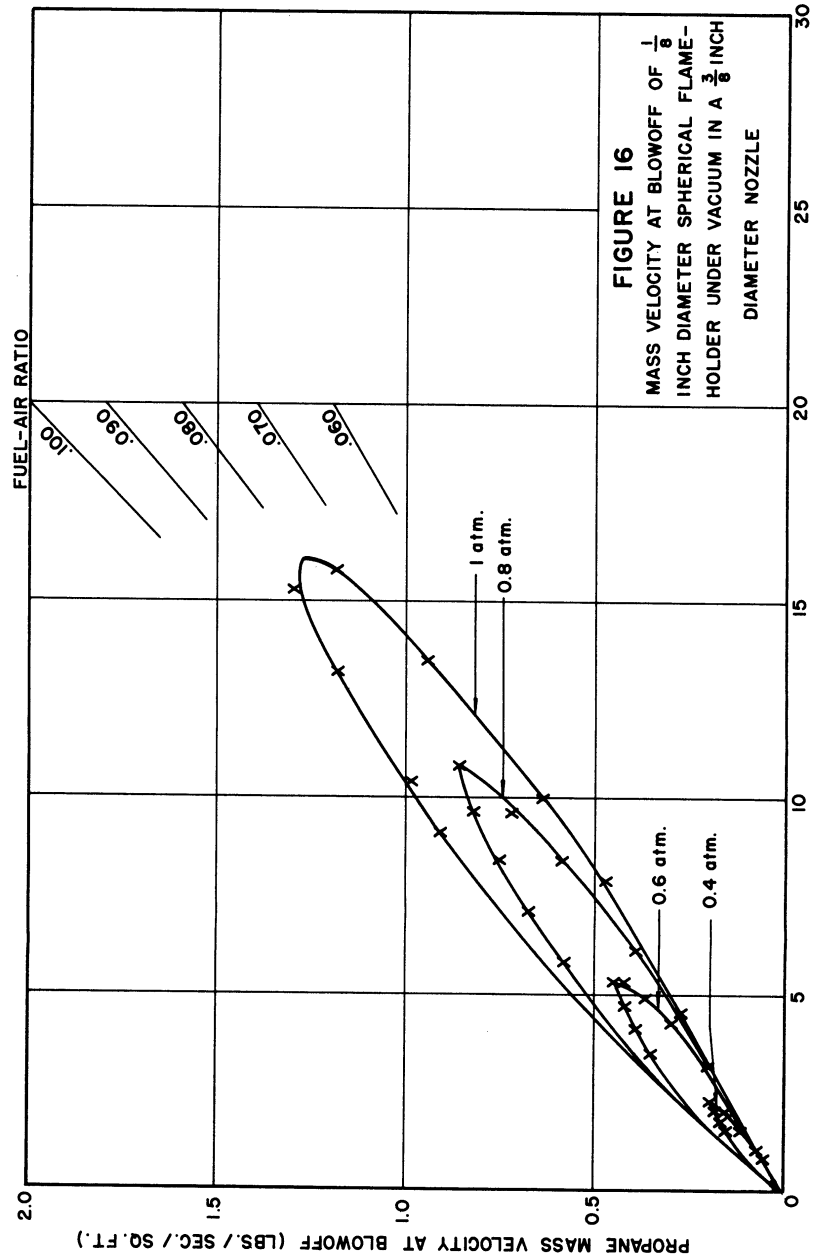

FIG. 16 MASS VELOCITY AT BLOWOFF FOR .125 FLAME HOLDER UNDER VACUUM.

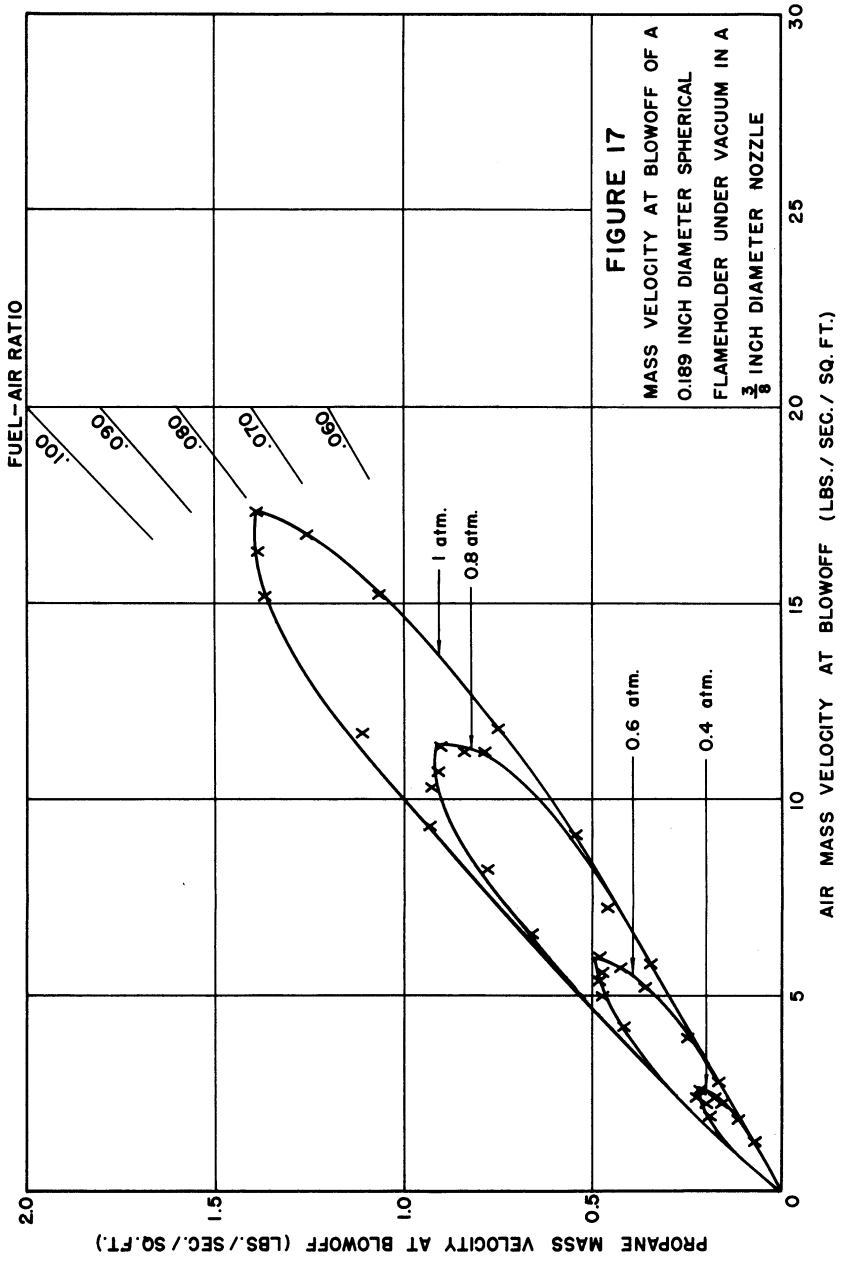

FIG. 17 MASS VELOCITY AT BLOWOFF FOR .189 FLAME HOLDER UNDER VACUUM.

System 1. The essential difference between the two systems was that the nozzle diameter in System 1 was 1-inch, while the nozzle diameter in System 2 was 3/8-inch. As was previously stated, the velocity distribution in both jets was essentially rectilinear. Accordingly, an investigation of the effects of nozzle diameter was performed. Tests were made in System 2 at atmospheric pressure and with a fuel-air ratio of 0.080 with nozzle diameters of 1/8, 1/4, 3/8, 7/16, 1/2, and 5/8 inch diameter nozzles. In each case the flame holder was placed 1/2 nozzle diameter above the nozzle. The data obtained with this series of experiments is shown in figure 18. The data obtained in System 1 with a 1-inch jet is also shown in figure 18.

In figures 20, 21, and 22 are shown shadow photographs of the various jets at their indicated conditions. The height of the completely laminar zone may be seen to decrease as the mass velocity increases, and these shadowgraphs indicate qualitatively the degree of turbulence in the jet at the various conditions.

It may be seen in figure 18, that for the four flame holders tested in System 2, the largest values of the mass velocity at blowoff were obtained with the 3/8 inch diameter nozzle. However, the values obtained in System 1 with a 1-inch diameter nozzle were greater than any obtained in System 2. In System 2 the increase in blowoff velocity with increasing nozzle diameter up to the 3/8 inch diameter nozzle can be explained logically by blocking of the jet by the flame holder. However, the decrease in blowoff velocity in System 2 with nozzle diameters greater than 3/8 inch diameter cannot be accounted for by this explanation.

As was previously shown in Table 1, the usual criterion for testing nozzles, i.e. a rectilinear velocity distribution, was met. This would seem to indicate than an unsteady state, rather than a steady state, phenomenon was causing lower blowoff velocities in the 7/16, 1/2, and 5/8 inch diameter nozzles. To confirm this supposition, total head measurements were made upstream of the nozzle at the moment blowoff occurred. This data is presented in figure 23. The similarity of the curve in figure 23 to the curves in figure 18 is evident.

Since the phenomenon appeared to be of an unsteady-state nature, an external sound was imposed on the flame with an audio oscillator, amplifier, and a speaker. It appeared that at low jet velocities, ca. 100 ft/sec, the

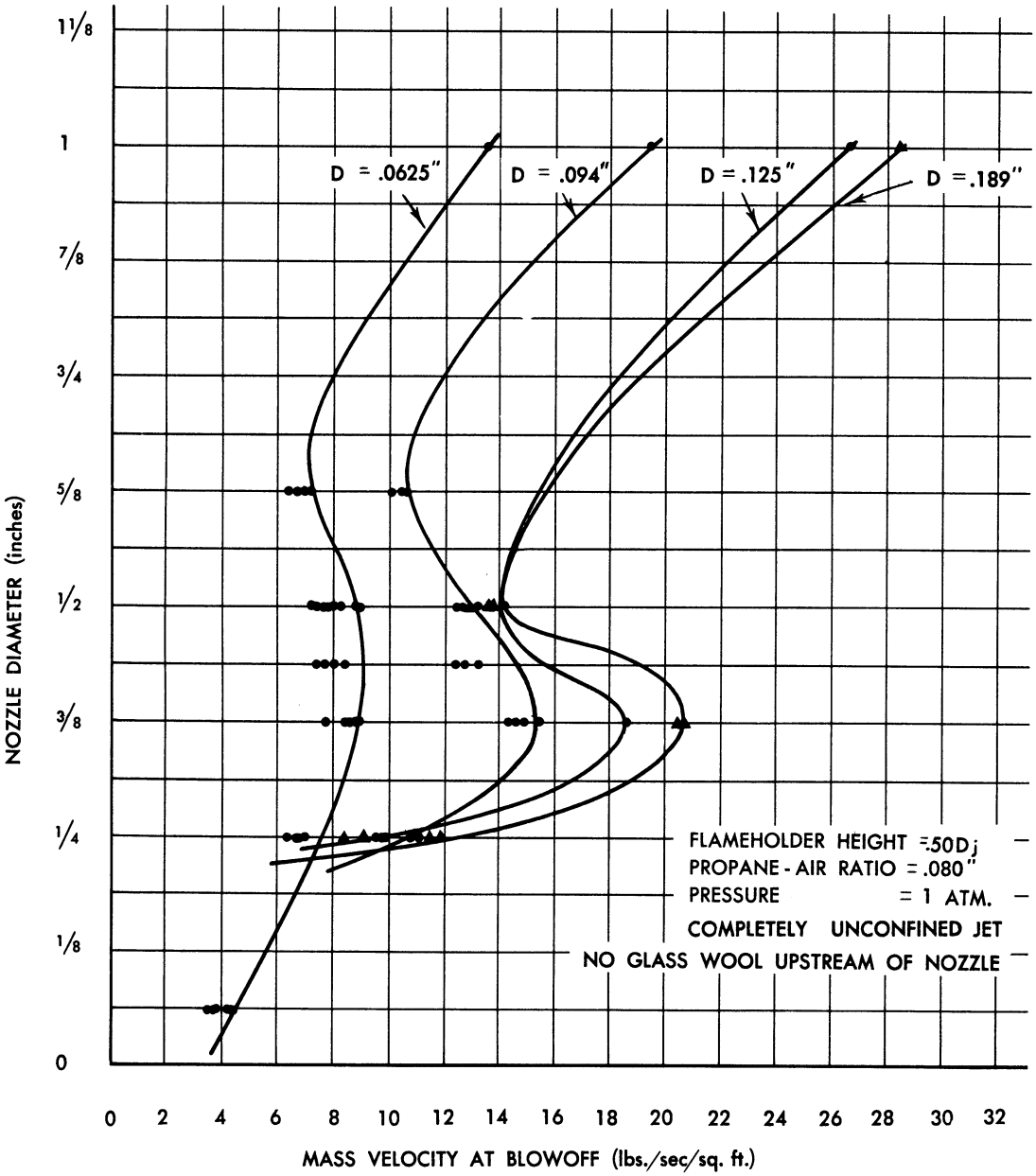

FIG. 18 MASS VELOCITY AT BLOW OFF VERSUS NOZZLE DIAMETER- NO GLASS WOOL UPSTREAM OF NOZZLE.

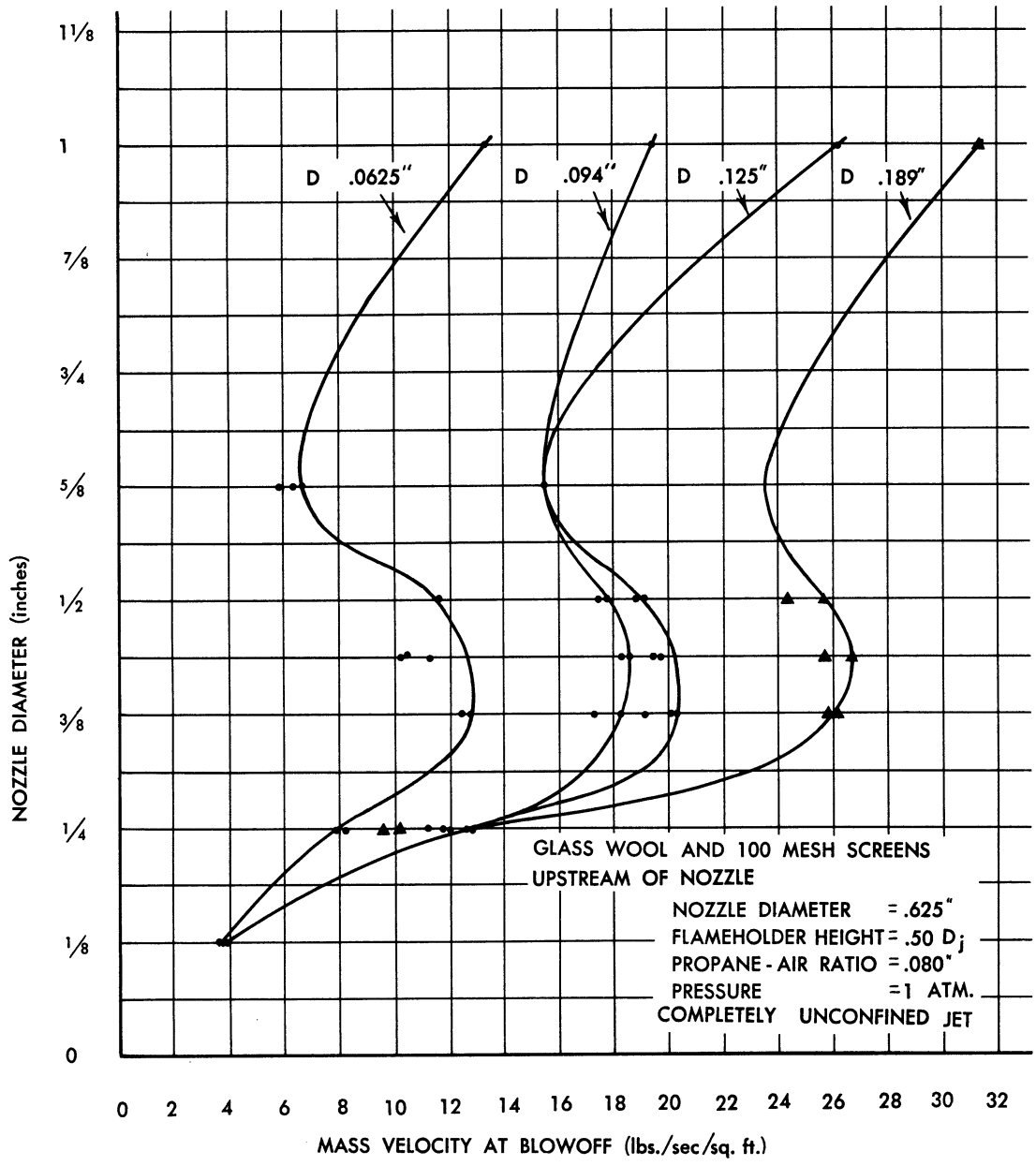

FIG. 19 MASS VELOCITY AT BLOW OFF VERSUS NOZZLE DIAMETER- WITH GLASS WOOL UPSTREAM OF NOZZLE.

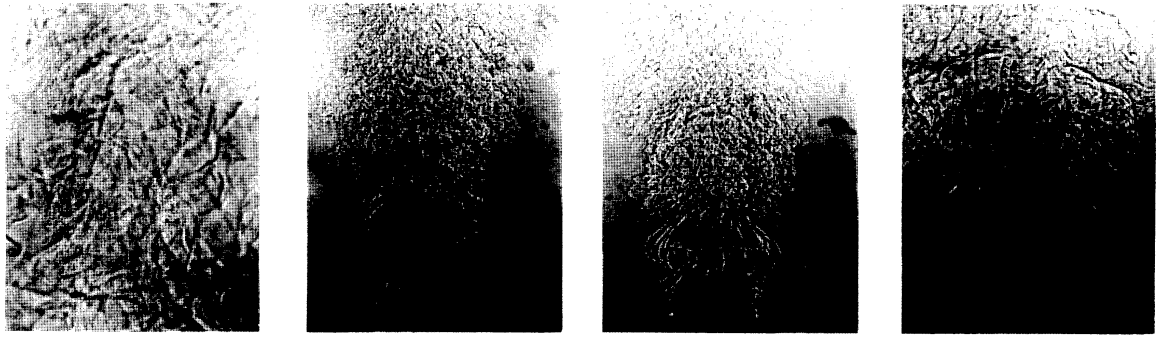

Without glass wool and 100 mesh screens upstream of nozzle				
Mass velocity (lbs./sec./sq. ft. of nozzle area)	16.1	6.7	3.8	1.8
Reynolds' Number	71,400	29,700	16,600	7,800

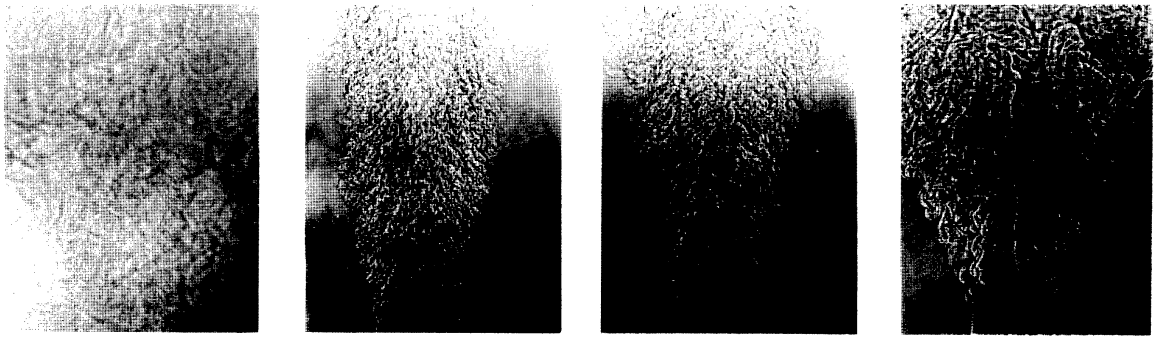

With glass wool and 100 mesh screens upstream of nozzle				
Mass velocity (lbs./sec./sq. ft. of nozzle area)	13.7	6.9	3.9	2.8
Reynolds' Number	60,800	30,400	17,200	8,061

Propane-air mixture 0.080 (by weight) Pressure 1 atmosphere

FIG. 20 SHADOWGRAPHS SHOWING VARIATION OF HEIGHT OF COMPLETELY LAMINAR ZONE WITH DIFFERENT MASS VELOCITIES — FOR .625 IN. DIA. NOZZLE.

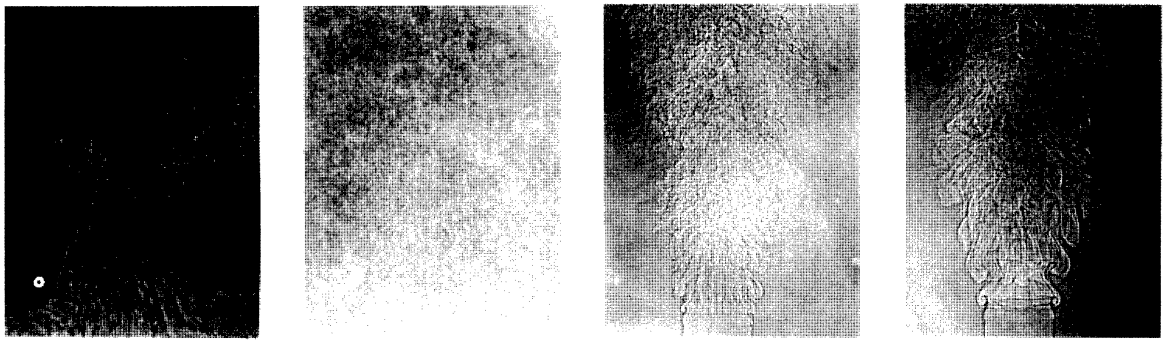

Without glass wool and 100 mesh screens upstream of nozzle				
Mass velocity (lbs./sec./sq. ft. of nozzle area)	23.7	10.5	5.6	2.9
Reynolds' Number	83,900	37,100	19,900	10.100

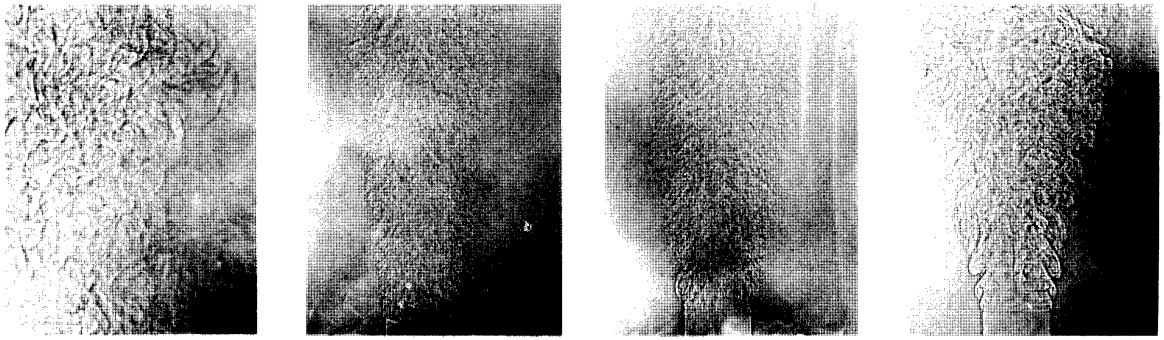

With glass wool and 100 mesh screens upstream of nozzle				
Mass velocity (lbs./sec./sq. ft. of nozzle area)	21.5	10.9	6.1	2.8
Reynolds' Number	76,200	38,700	21,600	10,000

Propane-air mixture 0.080 (by weight) Pressure 1 atmosphere

FIG. 21 SHADOWGRAPHS SHOWING VARIATION OF HEIGHT OF COMPLETELY LAMINAR ZONE WITH DIFFERENT MASS VELOCITIES — FOR .500 IN. DIA. NOZZLE.

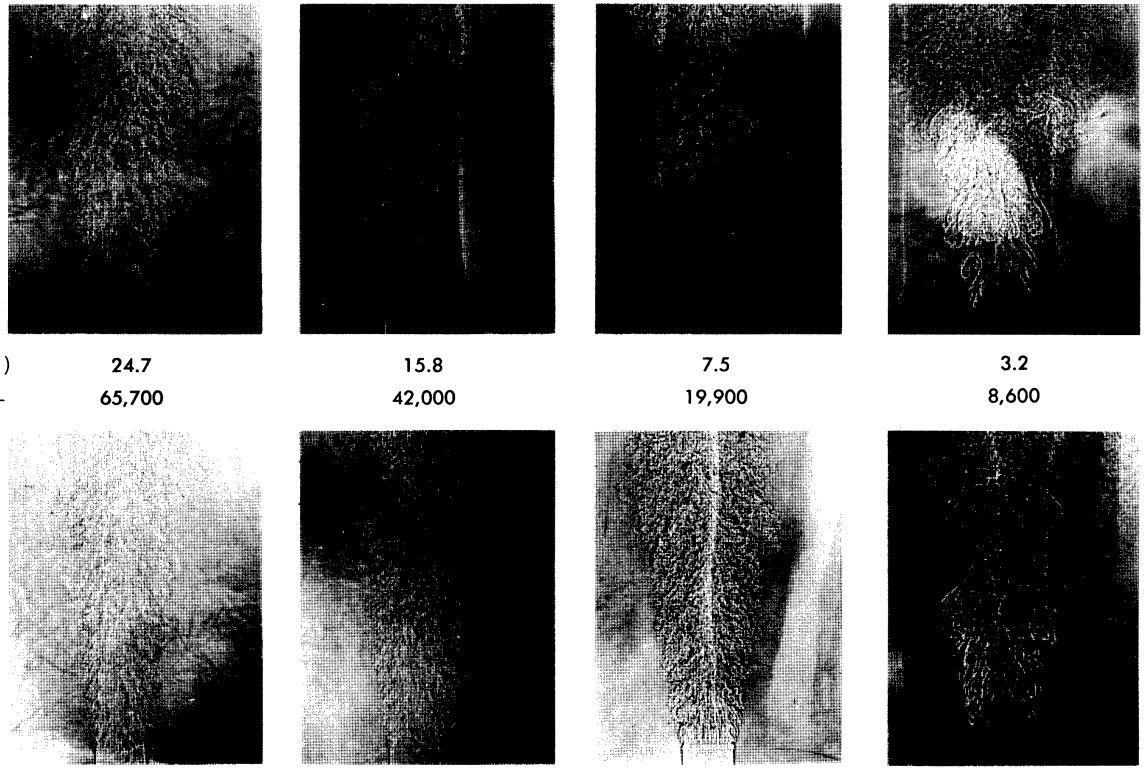

Propane-air mixture 0.080 (by weight) Pressure 1 atmosphere

FIG. 22 **SHADOWGRAPHS SHOWING VARIATION OF HEIGHT OF COMPLETELY LAMINAR ZONE WITH DIFFERENT MASS VELOCITIES — FOR .375 IN. DIA. NOZZLE.**

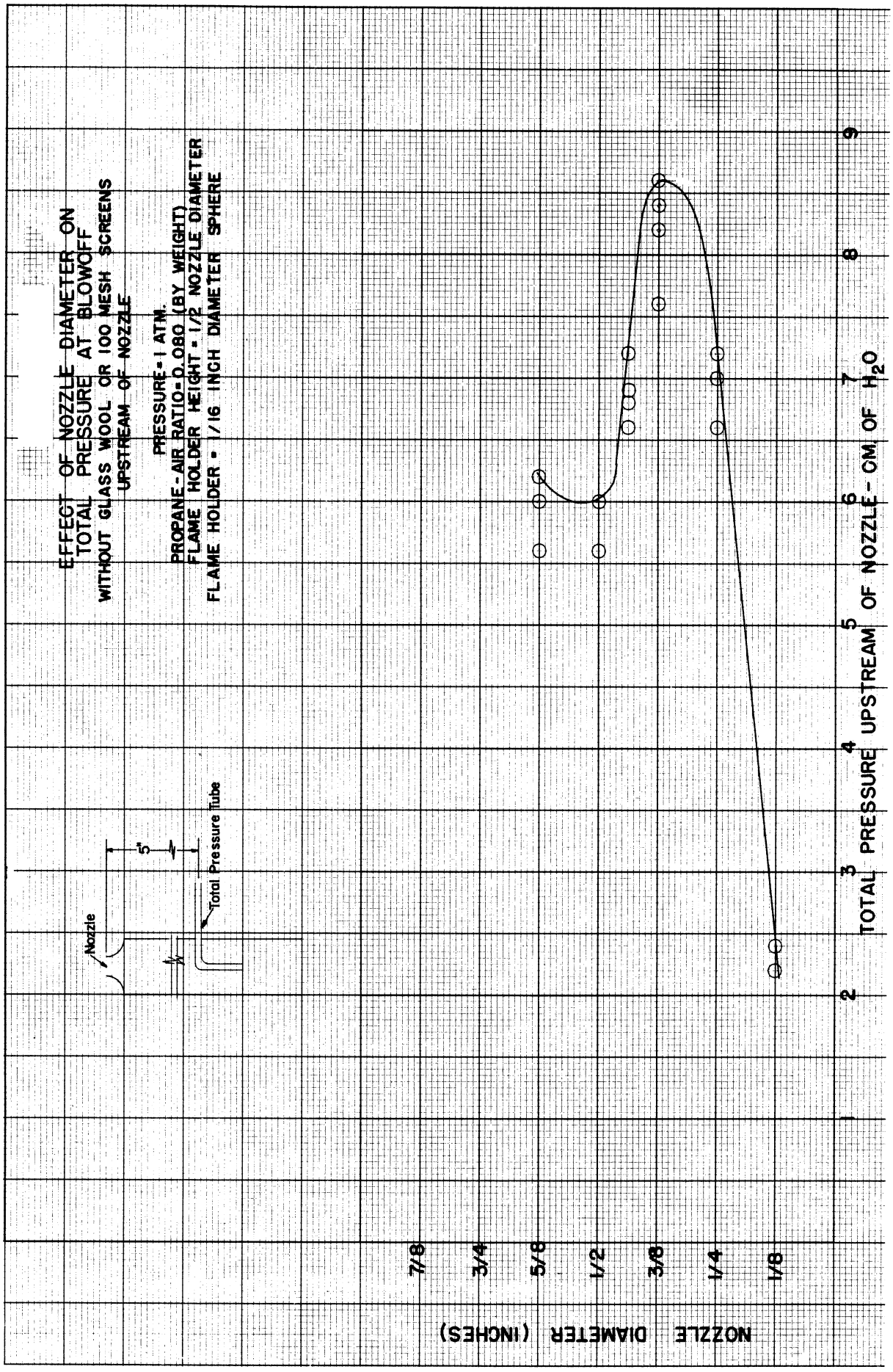

FIG. 23 EFFECT OF NOZZLE DIAMETER ON TOTAL PRESSURE AT BLOWOFF.

flame was visibly affected most by certain frequencies, but at higher jet velocities, the flame could be extinguished well below its normal blow-off velocity by any frequency between 500 cycles/sec and 10,000 cycles/sec, provided the intensity was great enough.

In an attempt to isolate this unsteady state phenomenon, a packing of glass wool retained by several layers of 100 mesh copper screen was placed in the tube immediately upstream of the convergent nozzle. This reduced the noise level of the flame (probably caused by resonance between the upstream tube and the flame itself) and probably tended to decrease the turbulence of the jet. The data obtained with this glass wool inserted upstream of the nozzle is presented in figure 19 which is a plot of nozzle diameter versus the mass velocity at blowoff for the four flame holders tested. The blowoff data shown in figure 23, together with the data presented in figure 18, is replotted in figure 24, which shows the increase in mass velocity caused by the insertion of the glass wool for the four flame holders tested. In figure 25 is shown the height of the completely laminar zone plotted against the mass velocity for the three jets tested. This height was obtained from the shadowgraphs shown in figures 18 and 19, while figure 26 shows the same data plotted as h/D versus Re. From figure 26 it may be seen that insertion of the glass wool does not have an appreciable effect on the height of the completely laminar zone, but it does have a great deal of effect on the mass velocity at blowoff. This would seem to indicate that the action of the glass wool in decreasing the noise level of the flame was more important than any effect the insertion of glass wool had on the turbulence of the jet. Since another investigator in this laboratory, Mr. R. A. Dunlap[2] , was studying the effects of resonance on flames, no further investigation of noise level was performed by this group.

Since the shadowgraphs shown in figures 20, 21, and 22 indicated that the height of the completely laminar zone was a function of the nozzle diameter, as well as the mass velcoity, it became apparent that the height of the flame holder above the nozzle would be an important variable. All of the preceding experiments had been performed at a value of 1/2 of the ratio $\frac{\text{height of the flame holder above nozzle}}{\text{nozzle diameter}}$. Accordingly, various experiments were performed using this flame holder height as one of the variables, while keeping the fuel-air ratio, ambient pressure, and flame holder diameter constant. In figure 27 may be seen a plot of mass velocity at blowoff versus flame holder height for the 3/8 inch diameter nozzle without the glass wool inserted upstream of the nozzle. A similar

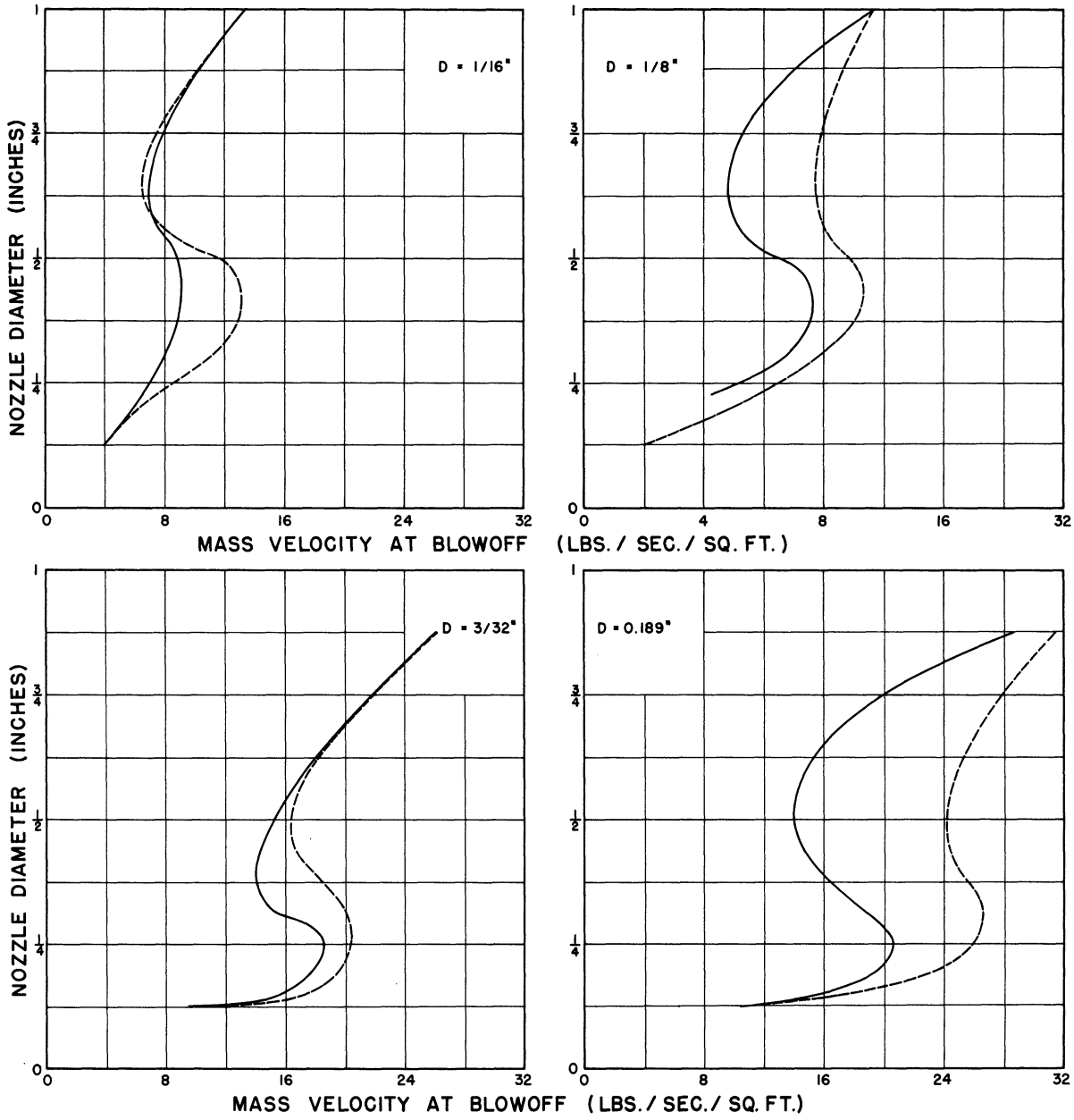

FIG. 24 EFFECT OF INSERTION OF GLASS WOOL ON MASS VELOCITY AT BLOWOFF

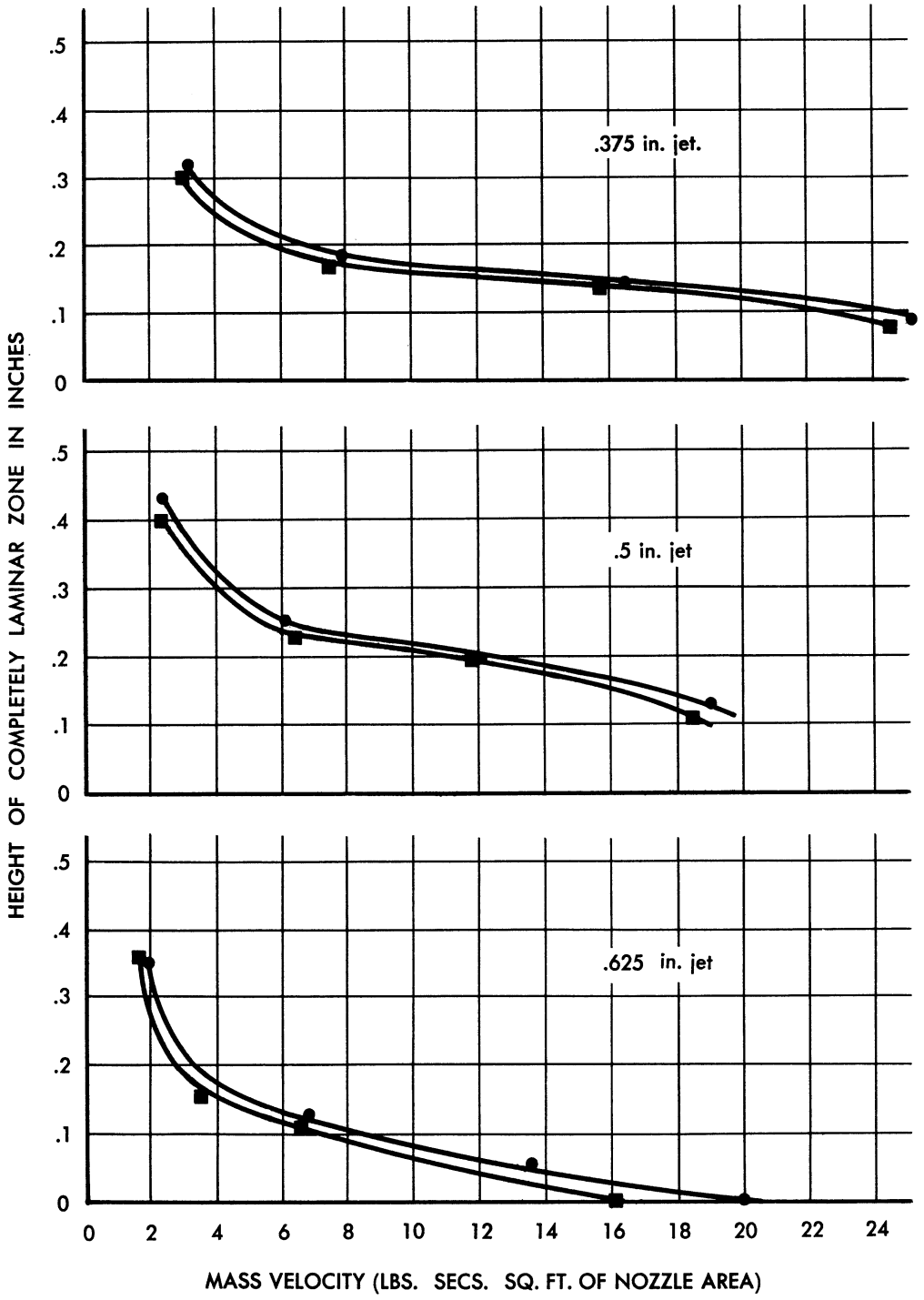

FIG. 25 MASS VELOCITY VS. HEIGHT OF COMPLETELY LAMINAR ZONE.

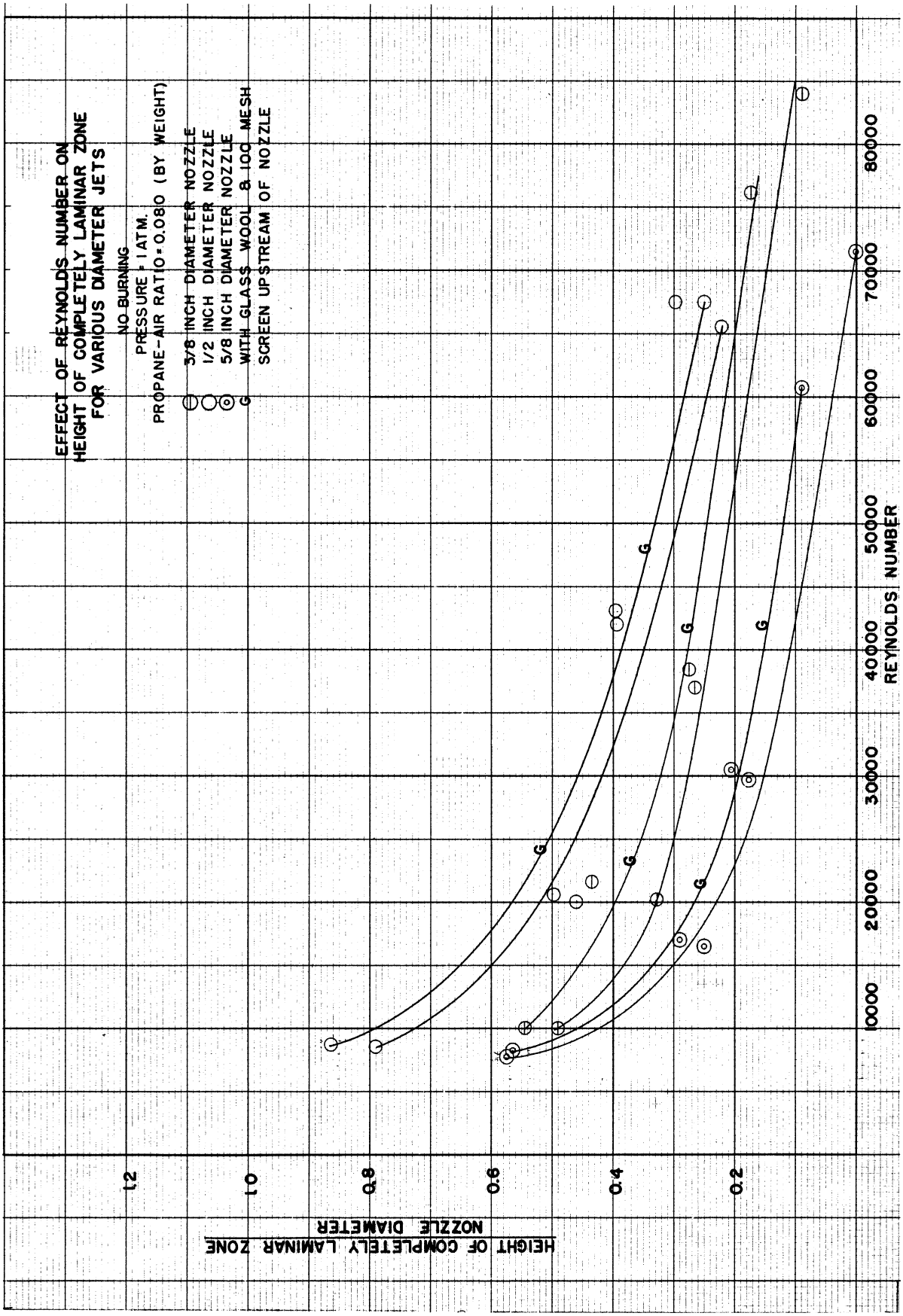

FIG. 26 EFFECT OF REYNOLDS NUMBER ON HEIGHT OF COMPLETELY LAMINAR ZONE FOR VARIOUS DIAMETER JETS.

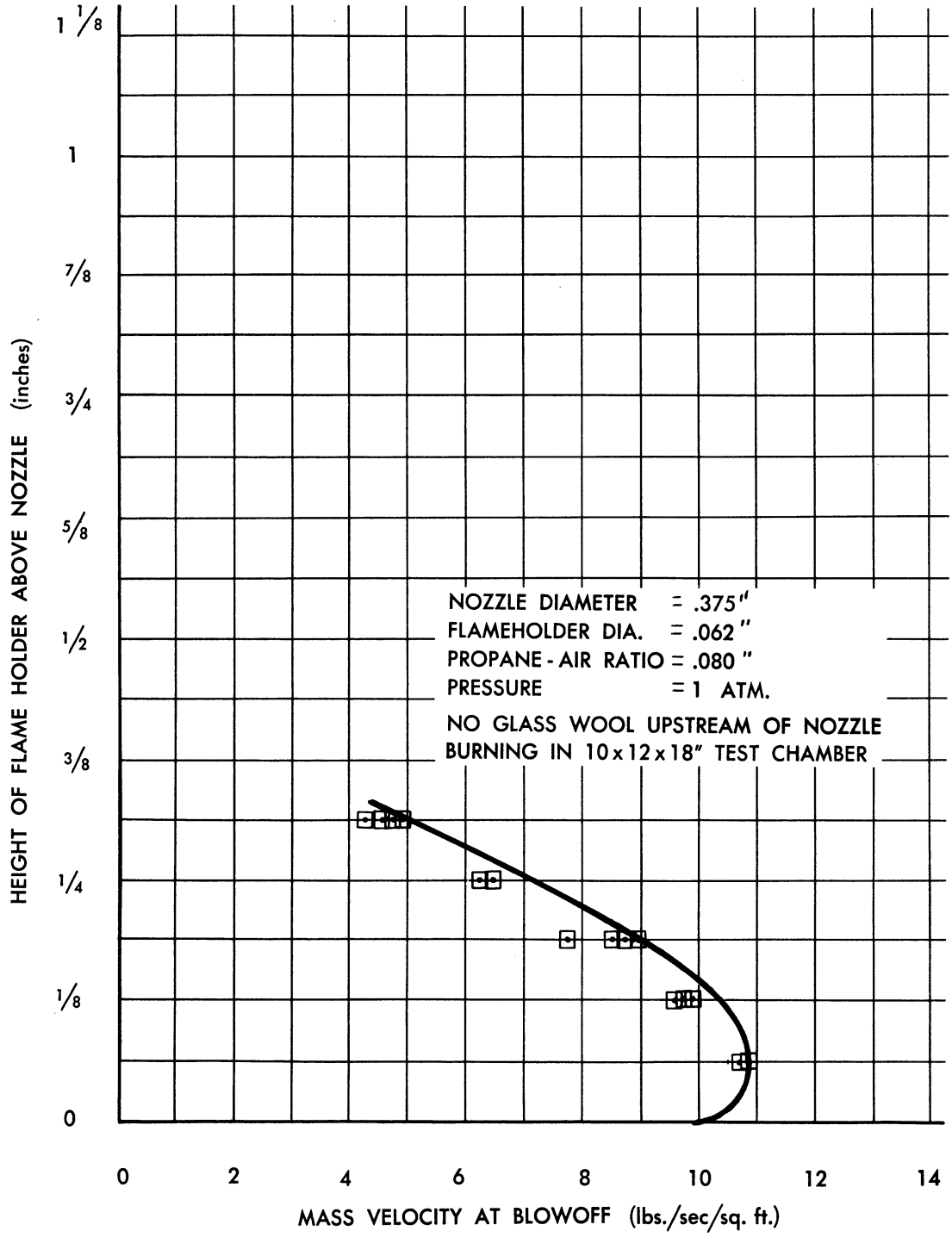

FIG. 27 EFFECT OF FLAME HOLDER HEIGHT ON MASS VELOCITY AT BLOWOFF .375 IN. NOZZLE, NO GLASS WOOL, IN TEST CHAMBER.

picture is shown in figure 28, except that in these experiments the glass wool was inserted upstream of the nozzle. Shadowgraphs showing burning at indicated conditions with the 3/8 inch diameter nozzle are shown in figures 29, 30, and 31.

The data shown in figures 27 and 28 may be compared in figure 32 which shows the effect of adding glass wool on the height of the flame holder versus mass velocity curve. The data shown in figures 27, 28, and 32 was obtained with the 3/8 inch jet inside of the 10 x 12 x 18 inch test chamber, as was the data obtained under vacuum. In order to determine the effect of this confinement of the jet when using the 3/8 inch nozzle, blowoff experiments were performed in and out of this test chamber, and, as may be seen in figure 27, there is no appreciable difference between the two cases when no glass wool is inserted upstream of the nozzle, but there is some effect of confinement when the glass wool is inserted upstream of the nozzle, as may be seen in figure 34.

The data in figure 33 seems to indicate that jet confinement effects were not present to any appreciable extent in the data obtained under vacuum. The vacuum data, as was previously stated, was obtained in the test chamber with a 3/8 inch diameter nozzle with no glass wool upstream of the nozzle. While the data presented in figure 27 was obtained at only one pressure, atmospheric, one fuel-air ratio, 0.080, and with one flame holder diameter, 1/16 inch, it might be assumed that the data obtained with other fuel-air ratios and pressures would not be altered appreciably if the 3/8 inch jet were completely unconfined. This statement, of course, applies only to the 3/8 inch diameter jet with no glass wool upstream of the nozzle.

Experiments similar to those performed with the 3/8 inch nozzle were also performed with the 5/8 inch diameter nozzle. Figure 35 shows the mass velocity at blowoff as a function of flame holder height in an unconfined 5/8 inch diameter nozzle. Figure 36 is similar to figure 35, except that in these experiments, glass wool is inserted upstream of the nozzle. Figures 37, 38, and 39 are shadowgraphs of burning in the 5/8 inch diameter nozzle. Figure 40 allows the data presented in figures 35 and 36 to be compared.

However, when the 5/8 inch diameter jet is confined in the 10 x 12 x 18 inch test chamber, a large effect of jet confinement is observed. When no glass wool is inserted upstream of the 5/8 inch nozzle, it is impossible to ignite the fire in the test chamber at any flame holder height.

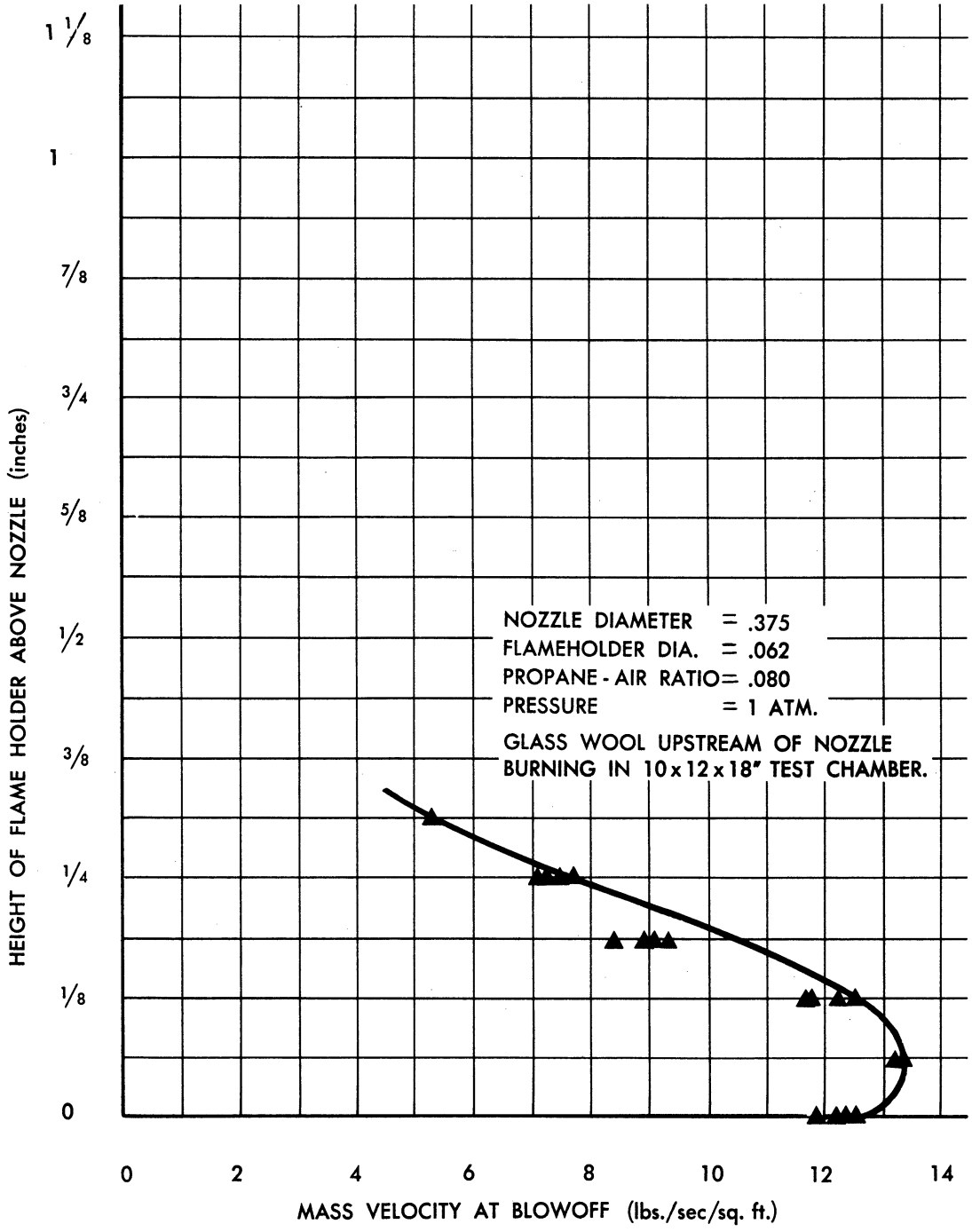

FIG. 28 EFFECT OF FLAME HOLDER HEIGHT ON MASS VELOCITY AT BLOWOFF 375 IN NOZZLE, WITH GLASS WOOL, IN TEST CHAMBER.

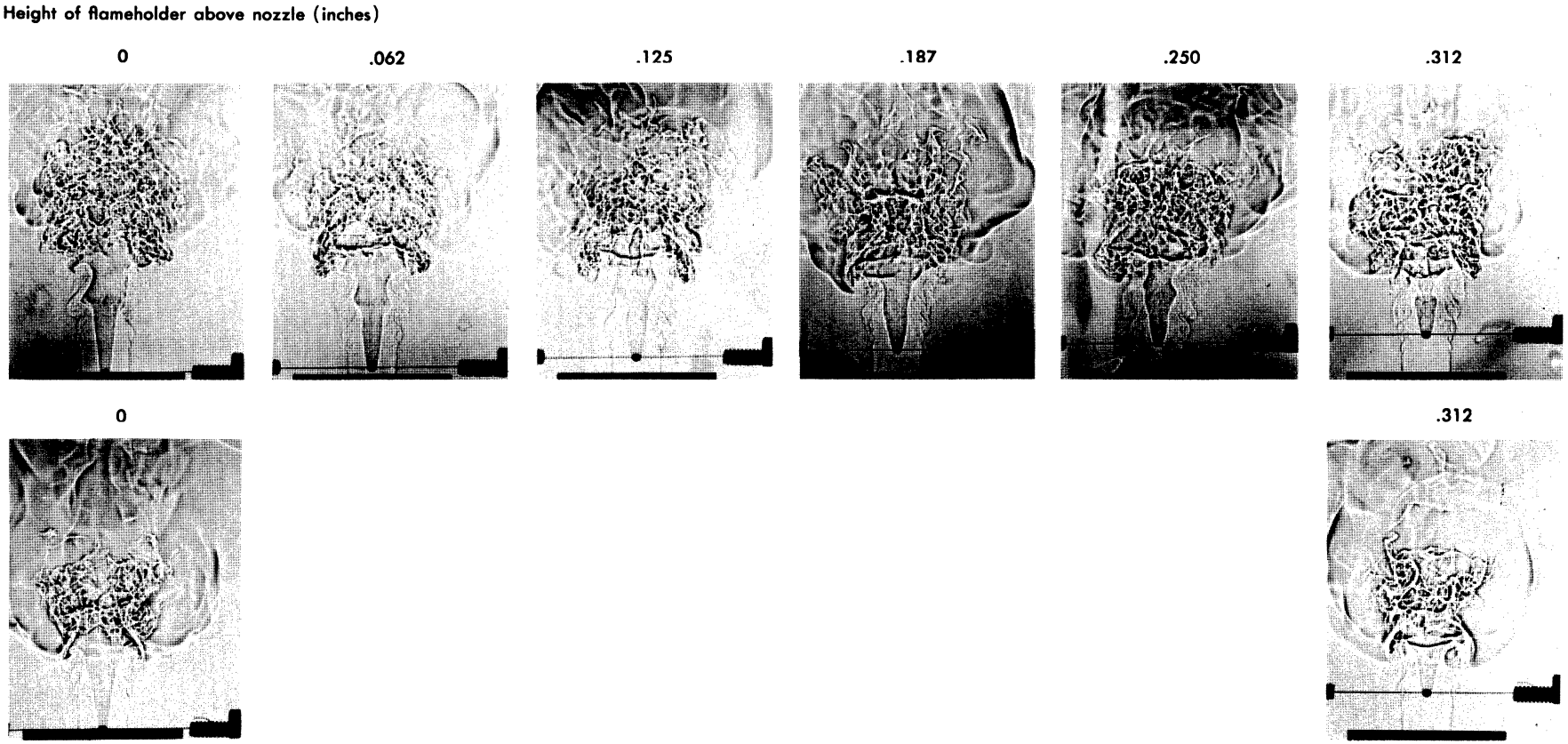

SHADOWGRAPHS SHOWING EFFECT OF HEIGHT OF FLAME HOLDER ABOVE NOZZLE ON COMBUSTION FOR A MASS VELOCITY RANGE OF 3.1 TO 3.2 LB./SEC./SQ. FT. OF NOZZLE AREA REYNOLDS NUMBER ≅ 8,500

Spherical flameholder dia. 1/16 in. Propane-air mixture 0.080 (by weight)
Nozzle diameter 3/8 in. Pressure 1 atmosphere

FIG. 29 SHADOWGRAPHS SHOWING EFFECT OF HEIGHT OF FLAMEHOLDER ABOVE .375" NOZZLE ON COMBUSTION FOR A MASS VELOCITY RANGE OF 3.1 - 3.2.

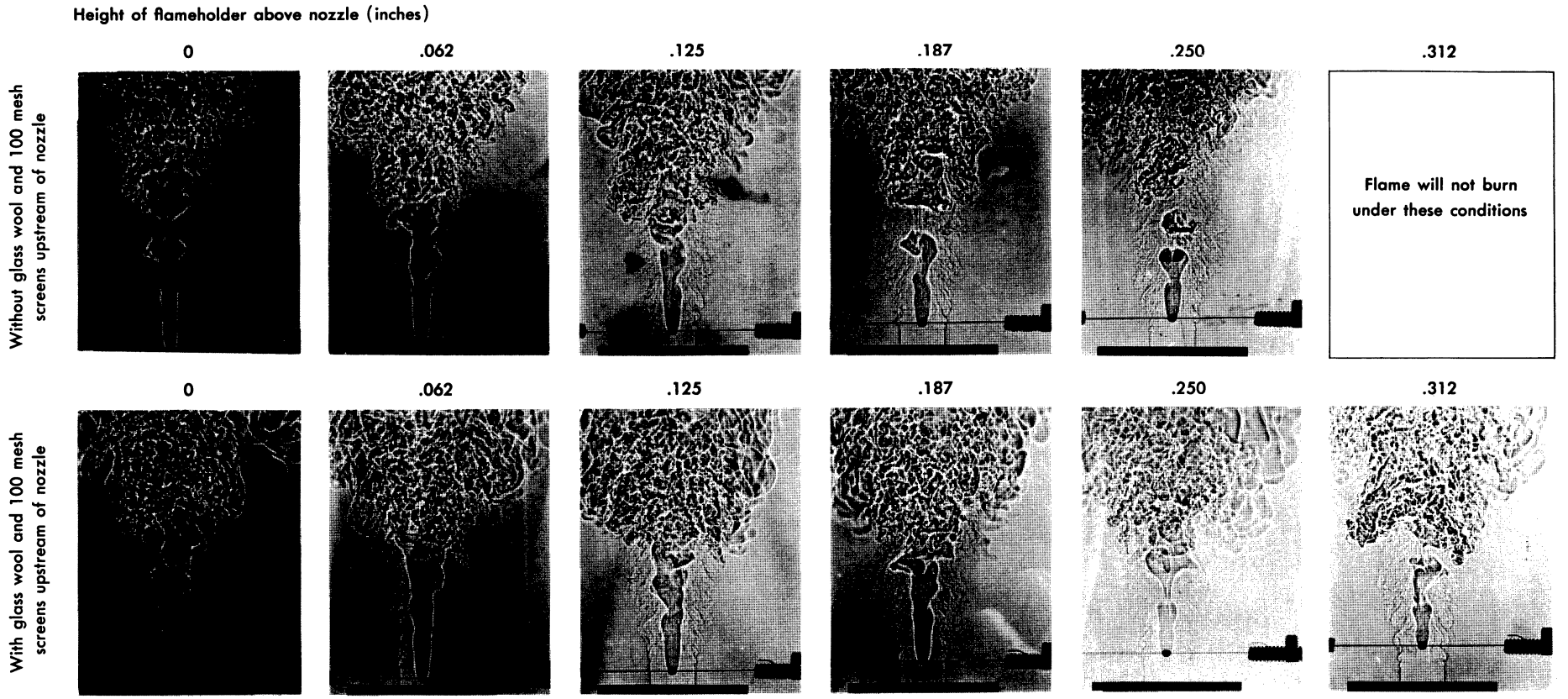

SHADOWGRAPHS SHOWING EFFECT OF HEIGHT OF FLAME HOLDER ABOVE NOZZLE ON COMBUSTION FOR A MASS VELOCITY RANGE OF 5.7 TO 6.0 LB./SEC./SQ. FT. OF NOZZLE AREA REYNOLDS NUMBER≅ 15,000

Spherical flameholder dia. 1/16 in. Propane-air mixture 0.080 (by weight)
Nozzle diameter 3/8 in. Pressure 1 atmosphere

FIG. 30 SHADOWGRAPHS SHOWING EFFECT OF HEIGHT OF FLAMEHOLDER ABOVE .375" NOZZLE ON COMBUSTION FOR A MASS VELOCITY RANGE OF 5.7 - 6.0

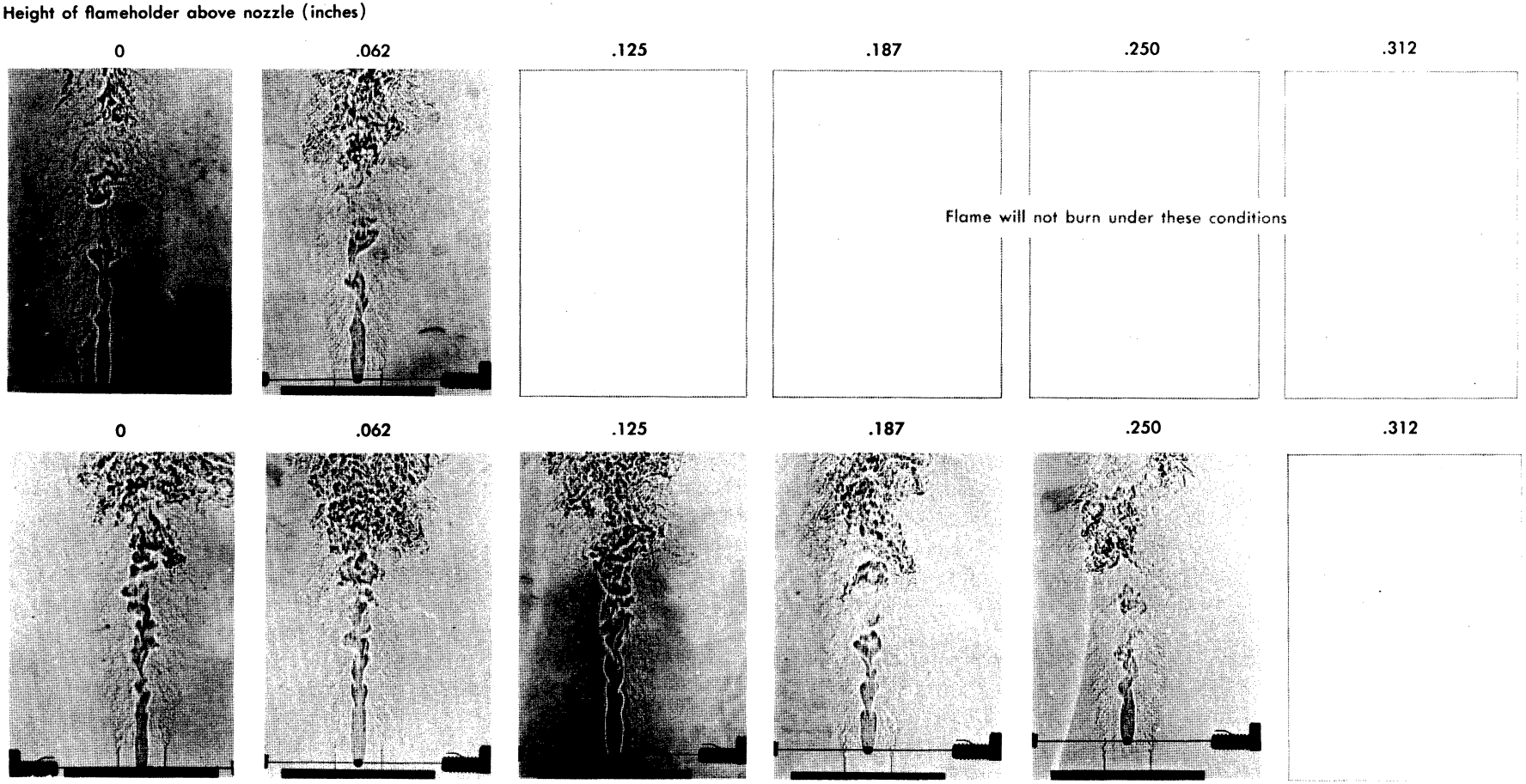

SHADOWGRAPHS SHOWING EFFECT OF HEIGHT OF FLAME HOLDER ABOVE NOZZLE ON COMBUSTION FOR A MASS VELOCITY RANGE OF 9.4 TO 9.7 LB./SEC./SQ. FT. OF NOZZLE AREA REYNOLDS NUMBER ≅ 25,000

Spherical flameholder dia. 1/16 in. Propane-air mixture 0.080 (by weight)
Nozzle diameter 3/8 in. Pressure 1 atmosphere

FIG. 31

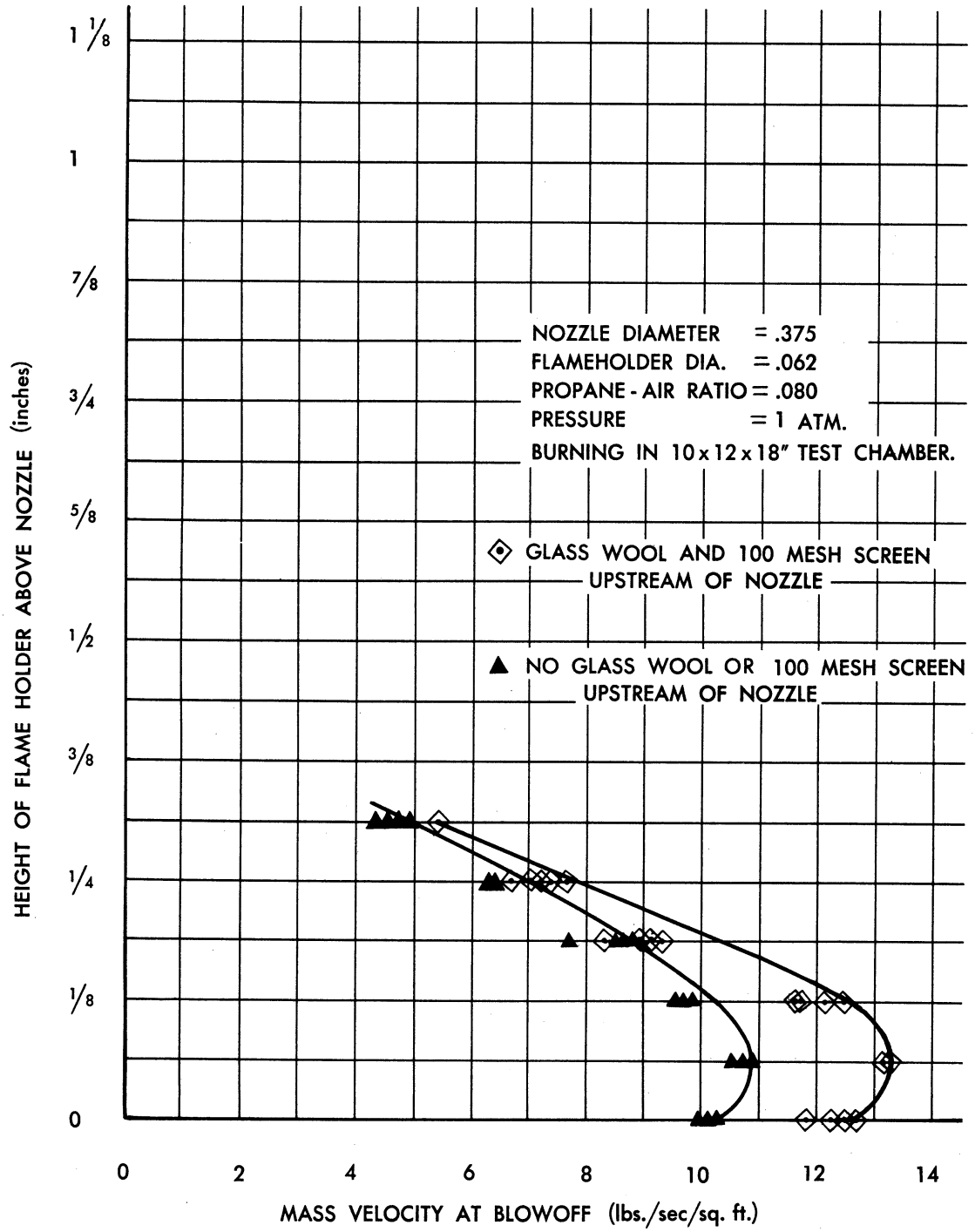

FIG. 32 EFFECT OF INSERTION OF GLASS WOOL ON FLAME HOLDER HEIGHT VS. MASS VELOCITY PLOT - .375 IN. NOZZLE.

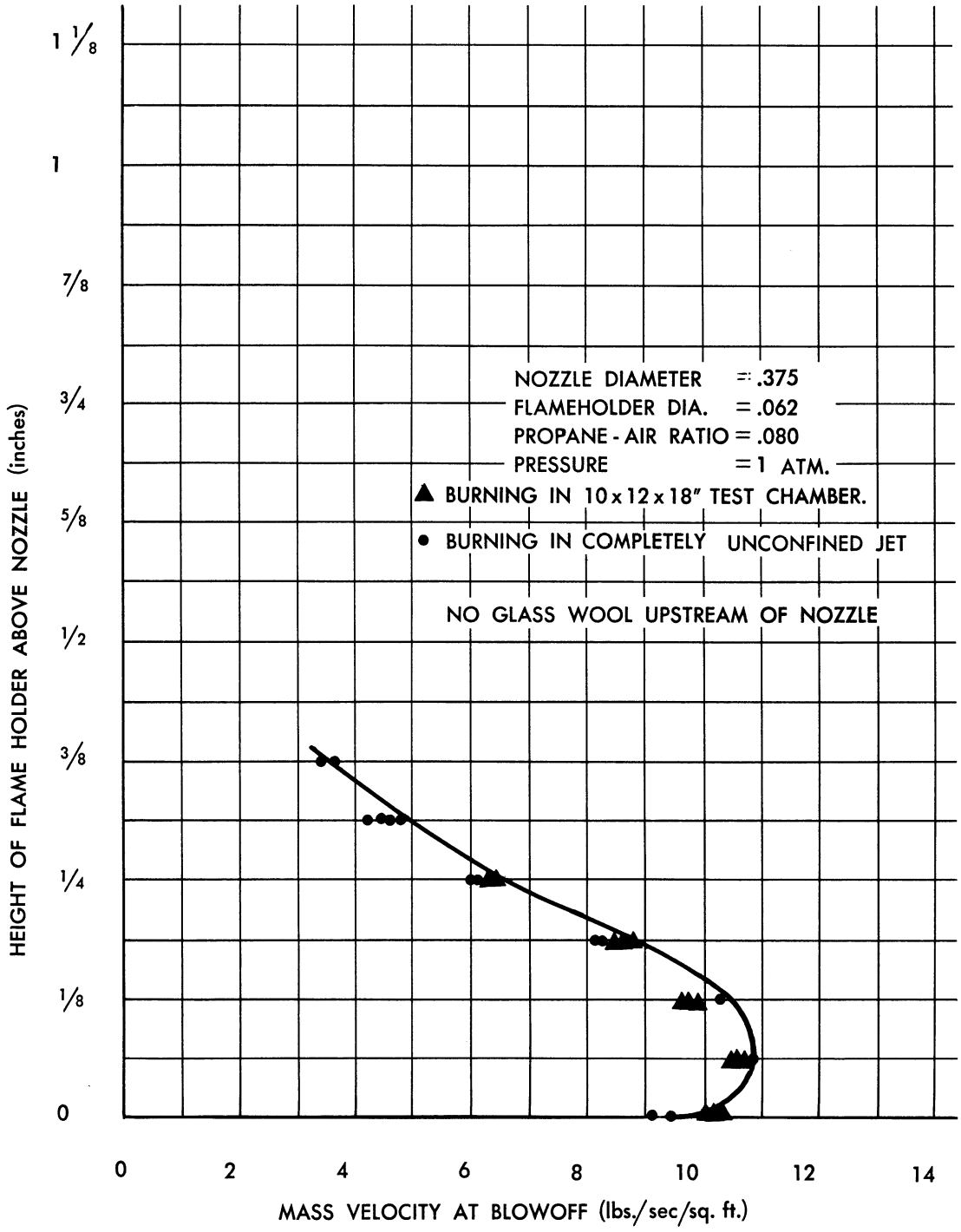

FIG. 33 EFFECT OF JET CONFINEMENT ON MASS VELOCITY AT BLOWOFF .375 IN. NOZZLE, - NO GLASS WOOL.

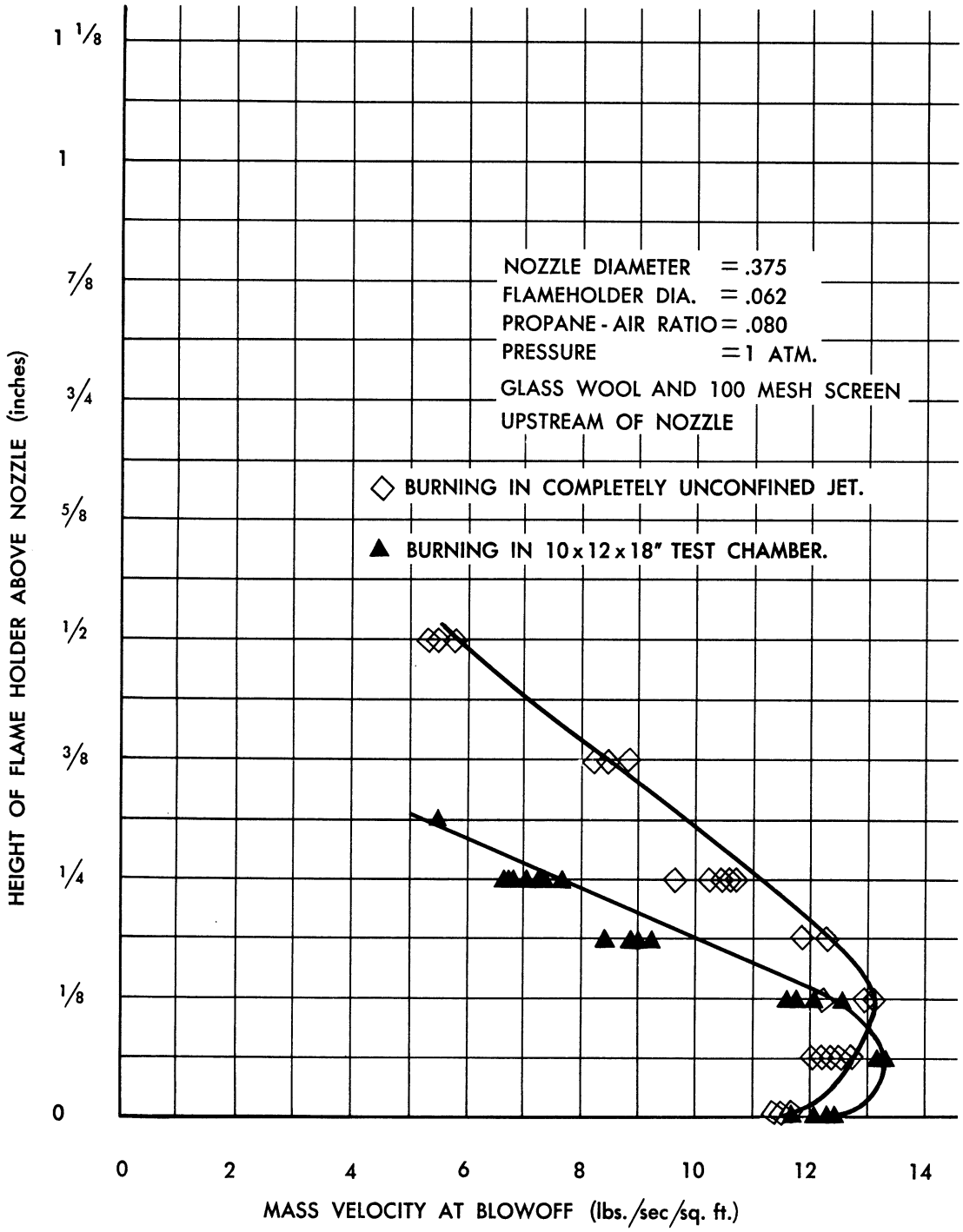

FIG. 34 EFFECT OF JET CONFINEMENT ON MASS VELOCITY AT BLOWOFF .375 IN. NOZZLE, WITH GLASS WOOL.

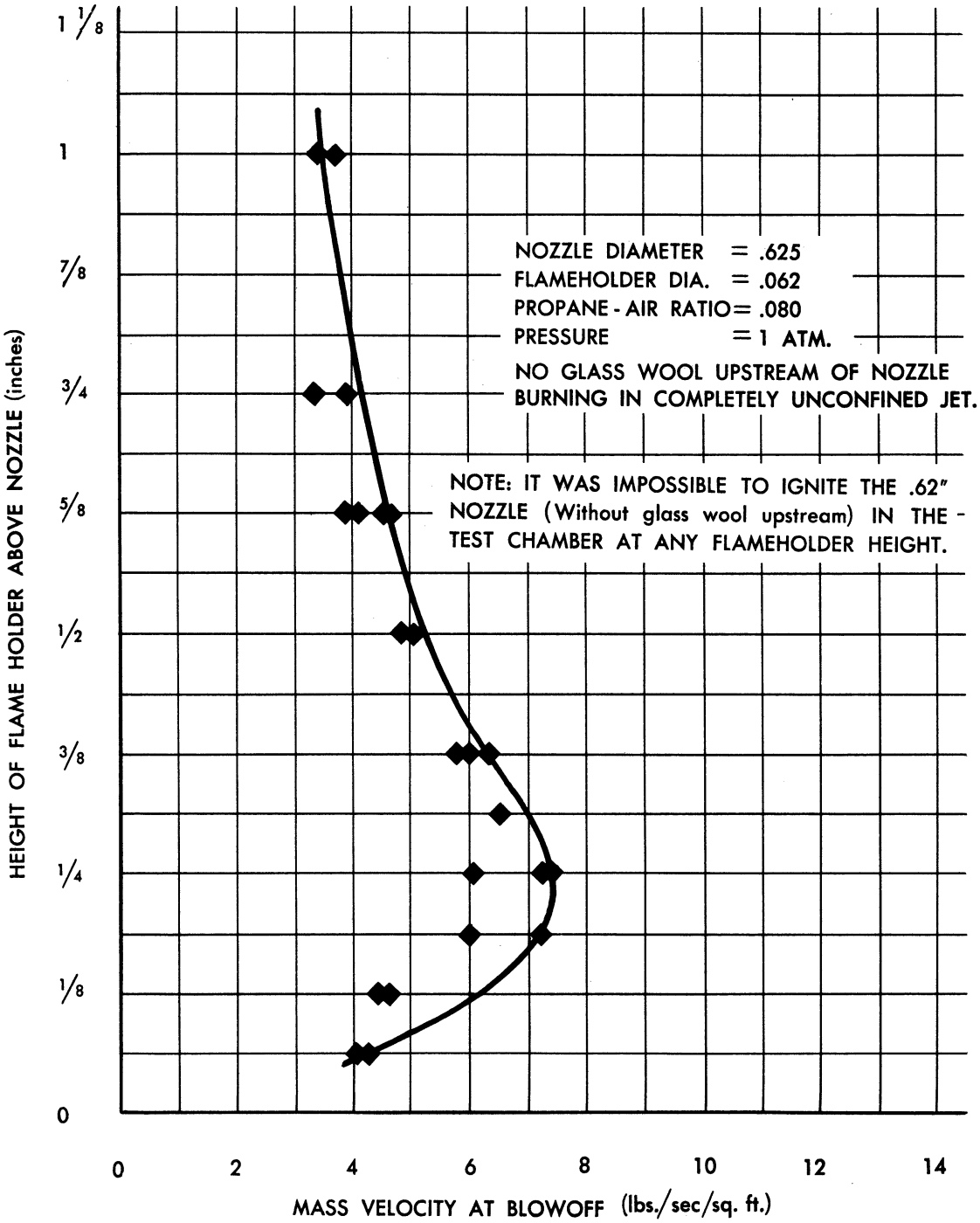

FIG. 35 EFFECT OF FLAME HOLDER HEIGHT ON MASS VELOCITY AT BLOWOFF .625 IN. NOZZLE, NO GLASS WOOL, UNCONFINED JET.

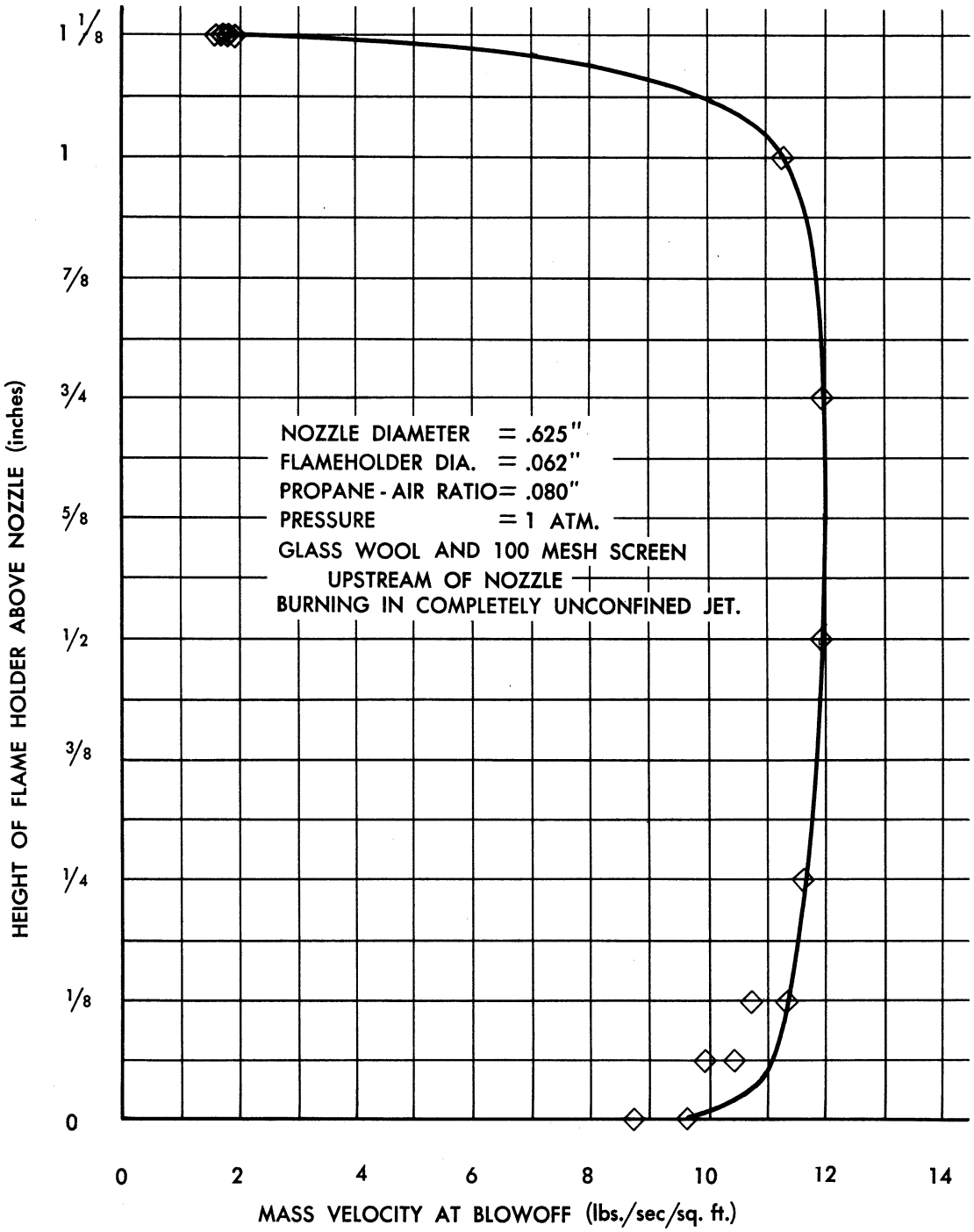

FIG. 36 EFFECT OF FLAME HOLDER HEIGHT ON MASS VELOCITY AT BLOWOFF .625 IN NOZZLE, GLASS WOOL, UNCONFINED JET.

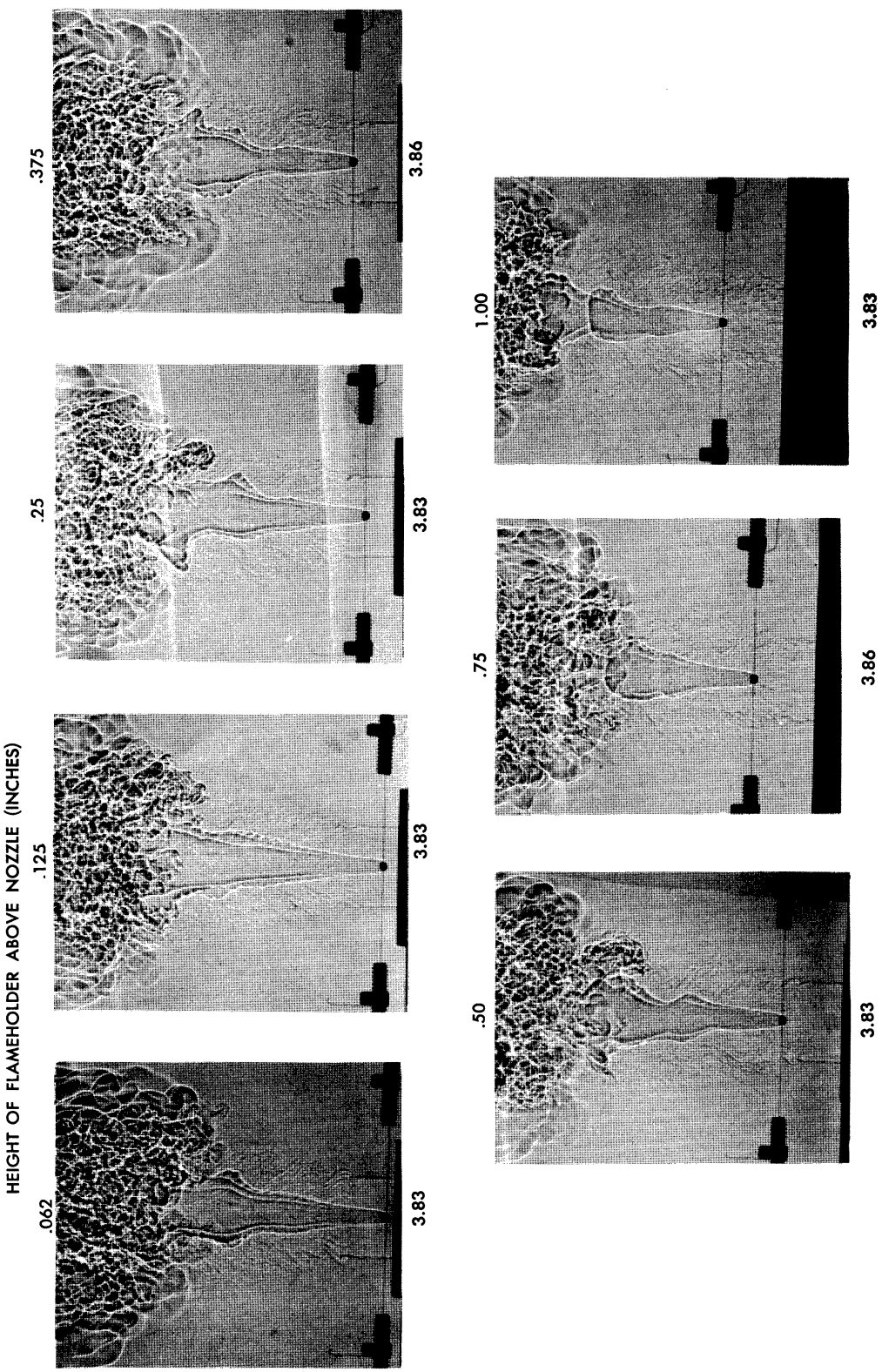

GLASS WOOL AND 100 MESH SCREENS UPSTREAM OF NOZZLE
SPHERICAL FLAMEHOLDER DIA. 1 16 IN. PROPANE AIR MIXTURE .080 (BY WT.)
NOZZLE DIAMETER 5 8 IN. PRESSURE 1 ATMOSPHERE

FIG. 37 SHADOWGRAPHS SHOWING EFFECT OF HEIGHT OF FLAMEHOLDER ABOVE .625" NOZZLE ON COMBUSTION FOR A MASS VELOCITY RANGE OF 3.83 - 3.86 WITH GLASS WOOL UPSTREAM OF NOZZLE.

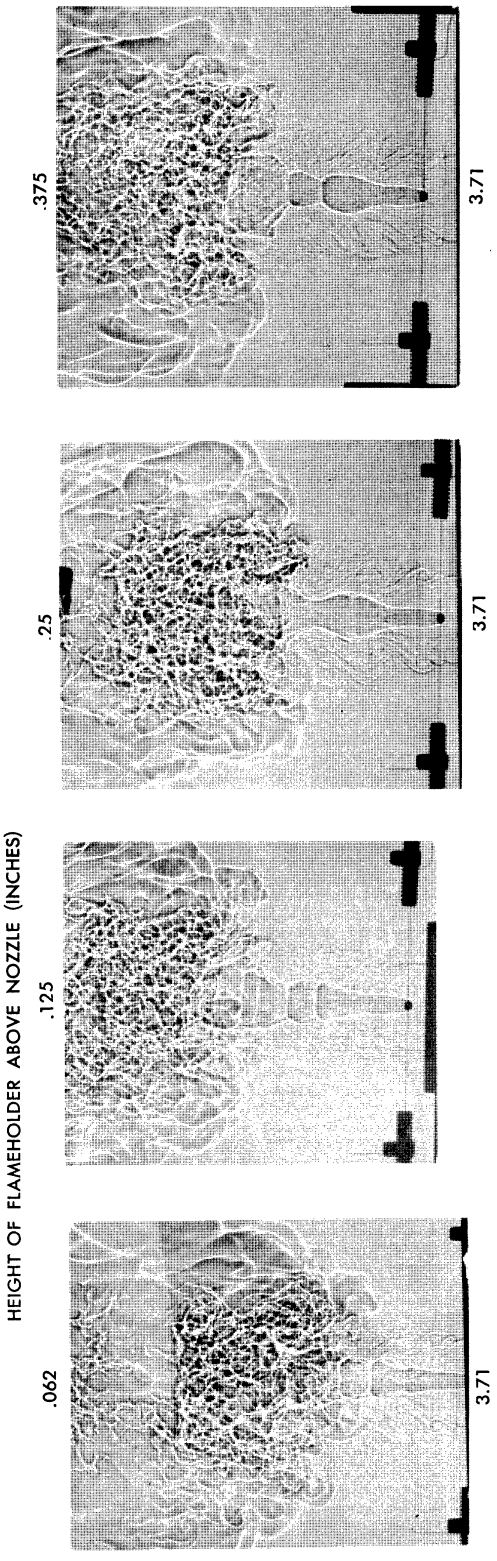

WITHOUT GLASS WOOL OR 100 MESH SCREENS UPSTREAM OF NOZZLE
SPHERICAL FLAMEHOLDER DIA. 1 16 IN. PROPANE AIR MIXTURE .080 (BY WT.)
NOZZLE DIAMETER 5 8 IN. PRESSURE 1 ATMOSPHERE

FIG. 38 SHADOWGRAPHS SHOWING EFFECT OF HEIGHT OF FLAMEHOLDER ABOVE .625" NOZZLE ON COMBUSTION FOR A MASS VELOCITY RANGE OF 3.70 - 3.71 WITHOUT GLASS WOOL UPSTREAM OF NOZZLE.

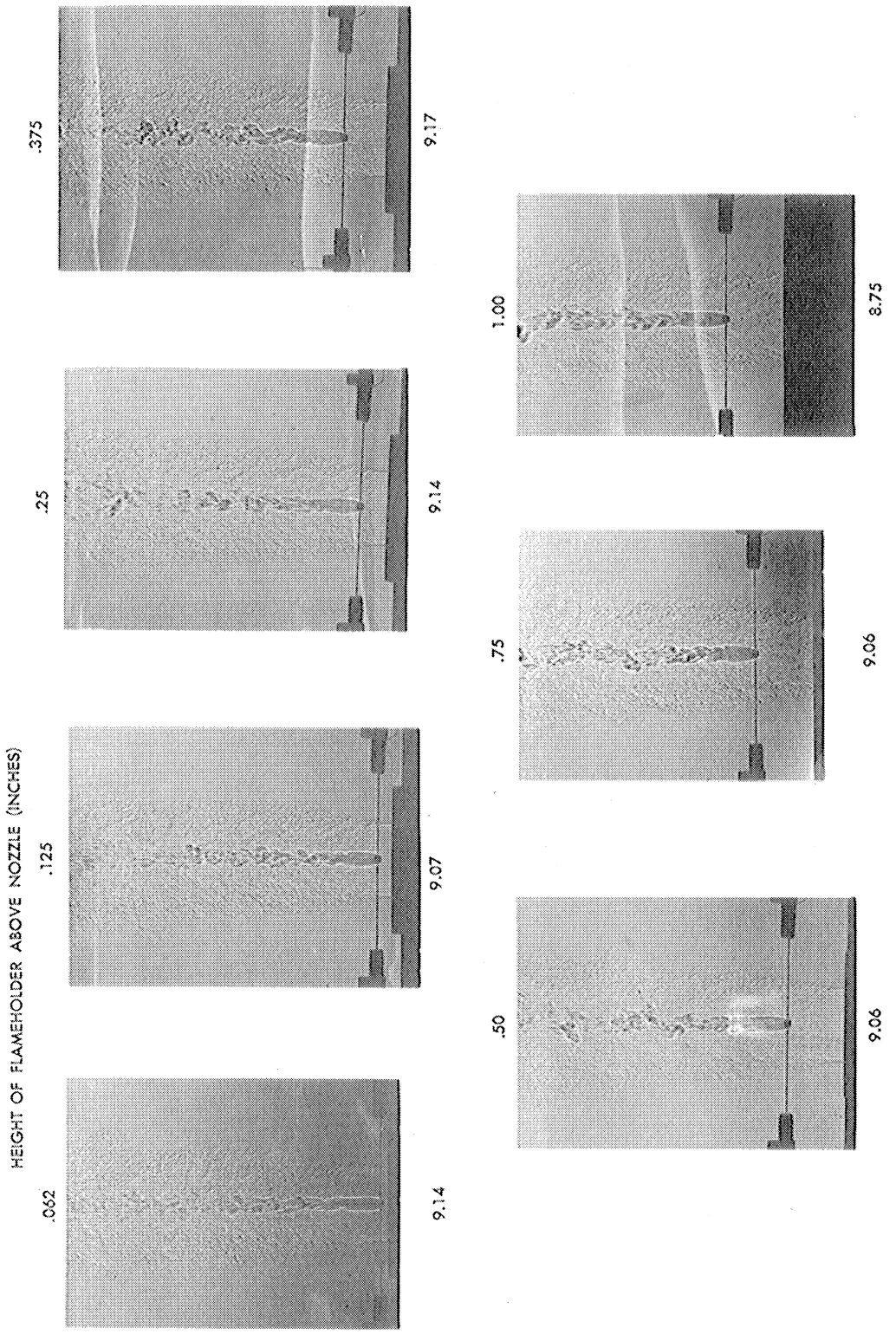

FIG. 39 SHADOWGRAPHS SHOWING EFFECT OF HEIGHT OF FLAMEHOLDER ABOVE .625" NOZZLE ON COMBUSTION FOR A MASS VELOCITY RANGE OF 8.75 - 9.17 WITH GLASS WOOL UPSTREAM OF NOZZLE.

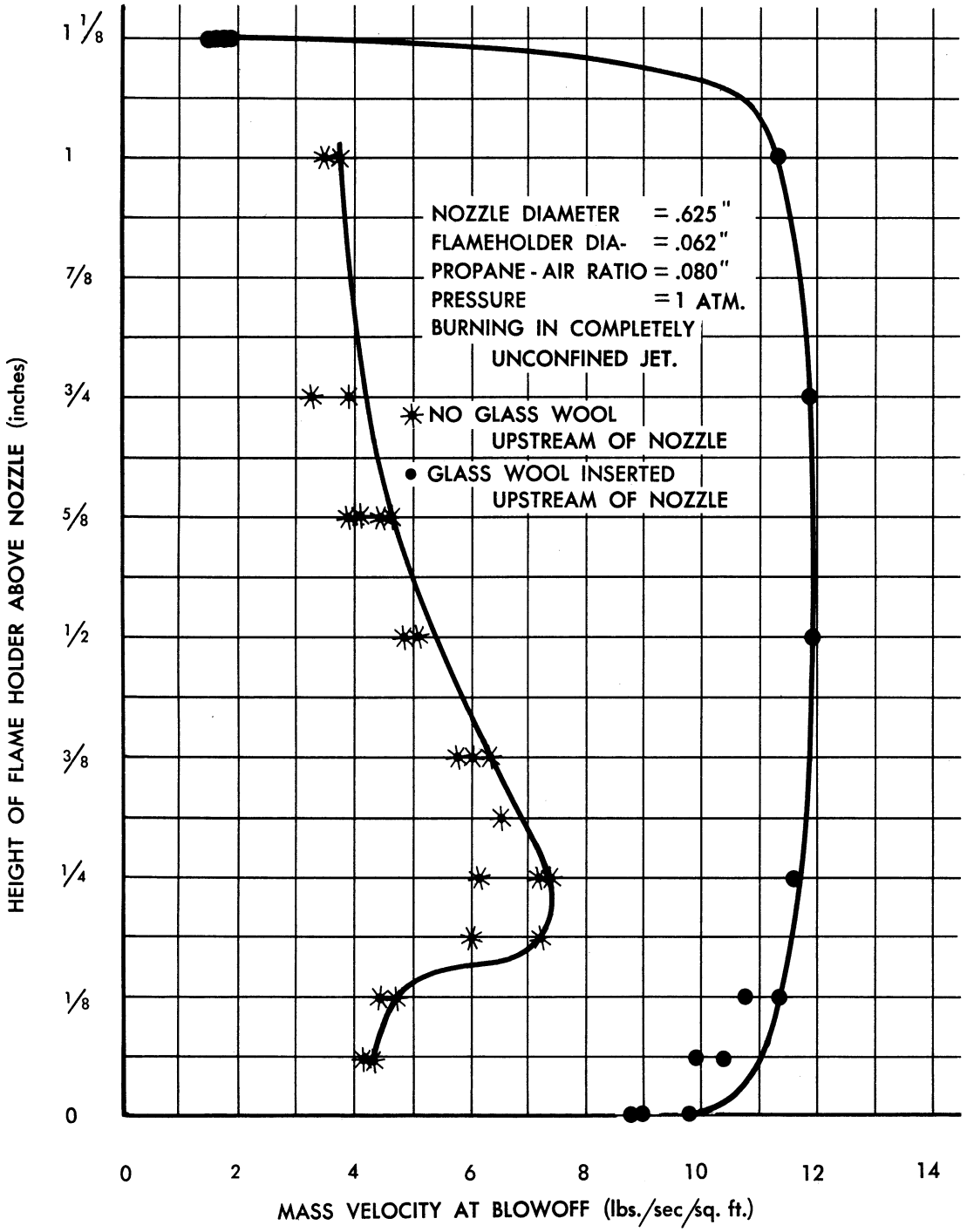

FIG. 40 EFFECT OF INSERTION OF GLASS WOOL UPSTREAM OF .675 IN. NOZZLE ON MASS VELOCITY AT BLOWOFF.

Blowoff velocities for these same conditions, except that experiments were conducted outside of the test chamber, were shown in figure 35. When glass wool is inserted upstream of the nozzle, the effect of jet confinement may easily be seen from figure 41.

The effects of jet confinement may be summarized as follows:

1. When a ratio of test chamber area to nozzle area of 1100 to 1 was used, there was no appreciable difference between that ratio and an infinite ratio (i.e. an unconfined jet) when no glass wool was inserted upstream of the nozzle, and very little difference when glass wool was inserted upstream of the nozzle.

2. When a ratio of test chamber area to nozzle area of 400 to 1 was used, it was impossible to ignite the flame when no glass wool was inserted upstream of the nozzle, and when glass wool was inserted upstream of the nozzle, the mass velocity at blowoff was ca. 1/2 the value obtained in an unconfined jet.

3. When a ratio of test chamber area to nozzle area of 36 to 1 was used (in System 1) severe explosions (at a flame holder height of 1/2 inch) resulted as the flame flashed back through the nozzle. Five such explosions occurred in System 1 before System 2 was used.

The effect of nozzle diameter may be seen in figures 32, 34, 40 and 41 which are plots of the mass velocity at blowoff versus height of the flame holder for the 3/8 inch and the 5/8 inch diameter nozzles under various conditions.

The experimental data presented in this section has indicated that the following variables have an appreciable effect on the mass velocity at blowoff: fuel-air ratio, sphere diameter, pressure, nozzle diameter, height of the flame holder above the nozzle, the degree of jet confinement, and the noise level of the flame as affected by the insertion of the glass wool upstream of the nozzle. The last four variables are all interrelated and are not easily separable. For example, the nozzle diameter and the height of the flame holder are both important in determining how much effect confinement of the jet will have on the mass velocity at blowoff. The insertion of glass wool was believed to decrease the resonance between the flame itself and the upstream tube, but no attempt was made

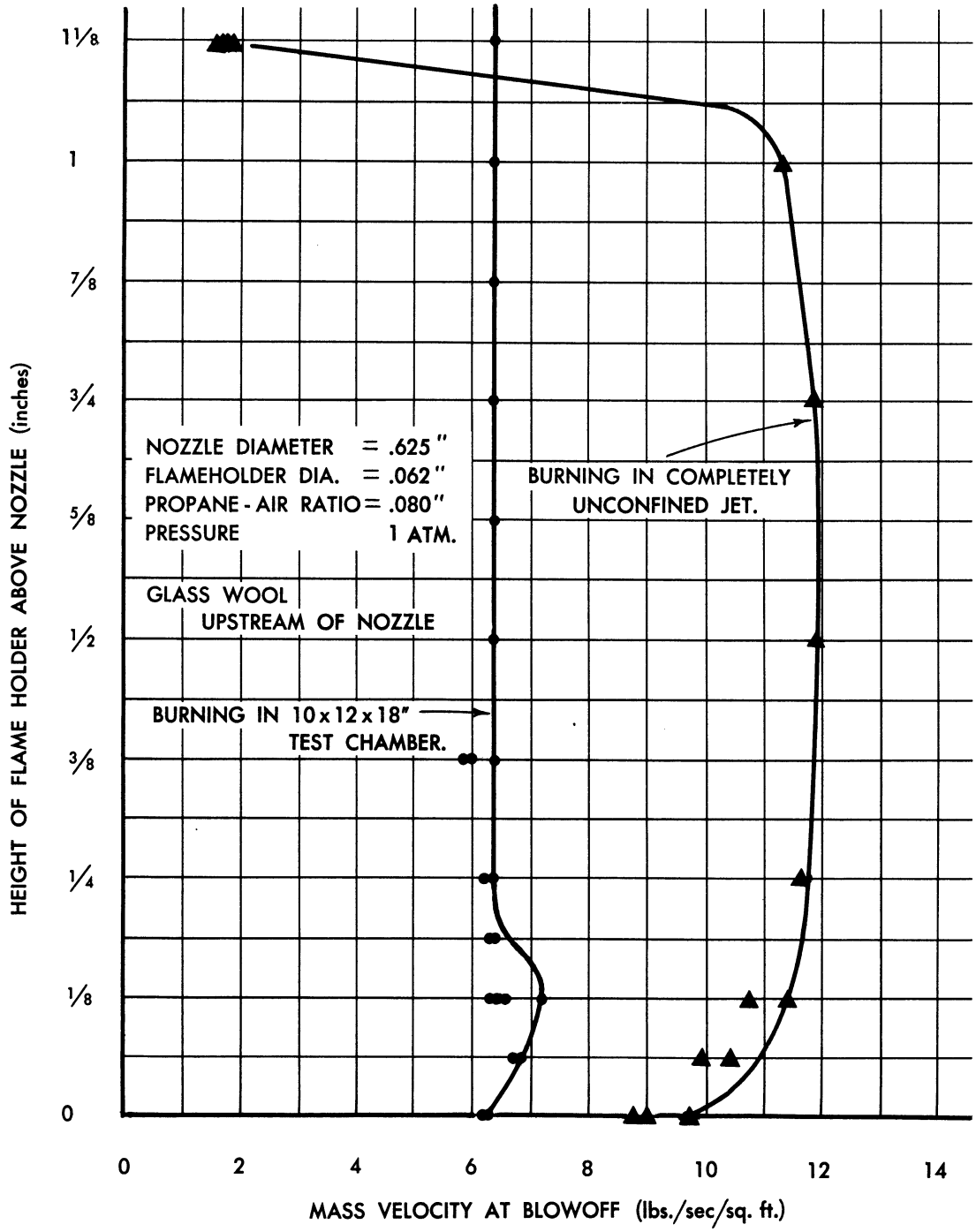

FIG. 41 EFFECT OF JET CONFINEMENT ON MASS VELOCITY AT BLOWOFF .625 IN. NOZZLE,

to determine quantitatively this decrease in resonance. Only the change in the mass velocity at blowoff was measured.

It is not possible to eliminate these system effects in ramjet combustion chambers, since there must be some degree of confinement of the jet. It is believed, therefore, that these data indicate that the system variables have an effect on the mass velocity at blowoff comparable to the effect of fuel-air ratio, pressure, or flame holder diameter.

IV. MISCELLANEOUS EXPERIMENTS

Several experiments were performed during this investigation which were not connected directly with blowoff velocities of spherical flame holders, but were connected with the more general problem of flame stabilization. They are presented here with the hope of offering other investigators new methods of attack on the general problem of flame stabilization.

A. Immersed Flame Holders

This work was performed in November, 1948, and previously reported in a progress report.[3]

The appearance of a pilot flame at high jet velocities has previously been stated. From aerodynamic considerations, it seemed that a bluff body located downstream of the spherical flame holder would provide a low velocity region and might again stabilize the flame and allow it to propagate. In figure 42 are several photographs showing the effect of insertion of a cylindrical rod in the wake. All of the photographs in figure 42 are at exactly the same conditions; namely, atmospheric pressure, 0.125 inch diameter spherical flame holder, 1 inch diameter jet, flame holder height of 1/2 inch, fuel-air ratio of 0.05 and a jet velocity of 268 ft/sec. The effect of insertion of a cylindrical rod at the critical position into the pilot flame shown in Photograph 8 may be seen in Photograph 9. The appearance of the flame when the cylinder is below the critical position is shown in Photograph 10. Photographs 11 and 12 show the appearance of the flame as the cylinder is progressively moved downstream from the spherical flame holder. Photograph 13 is a photograph of a smaller diameter cylinder inserted at the critical position in the pilot flame shown in Photograph 8, while Photograph 14 shows the appearance of the flame with the same cylinder inserted further downstream. It should be emphasized that there is a critical position for the height of the rod above the flame holder, for example the 3/8 inch diameter rod in Photograph 10 is only 3/8 inch below the optimum position shown in Photograph 9, while in Photograph 11, the 3/8 inch diameter rod is only 5/16 inch above the optimum position.

It also appears that there is a variation in the critical distance above the flame holder for a variation in cylinder size, as is shown in Photographs 10 and 13, the critical distance being 1-1/2 $\pm$ 1/16 inch for the 3/8 inch diameter rod and 1-1/4 $\pm$ 1/16 inch for the 1/8 inch diameter rod.

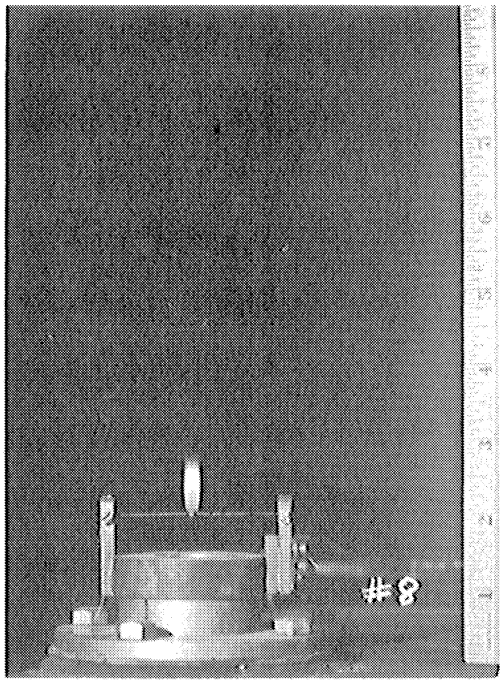

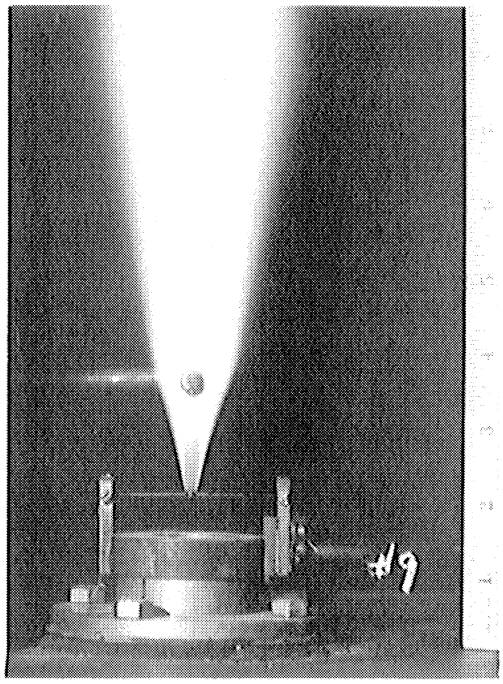

3/8" ROD — CRITICAL DISTANCE =
1 1/2"±1/16" ABOVE FLAMEHOLDER

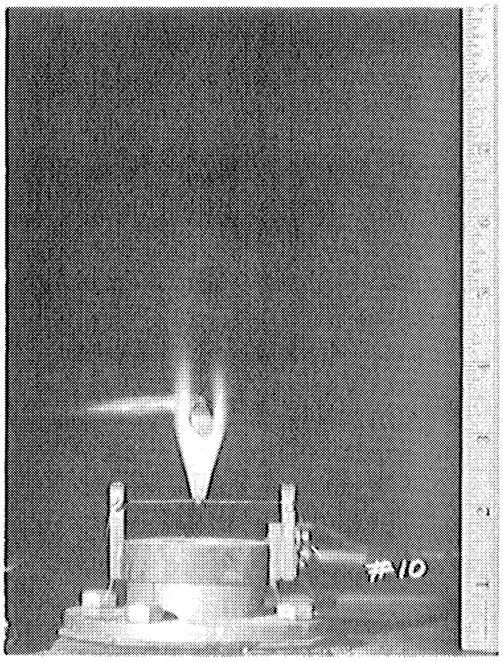

ROD 1/4 " BELOW CRITICAL DISTANCE

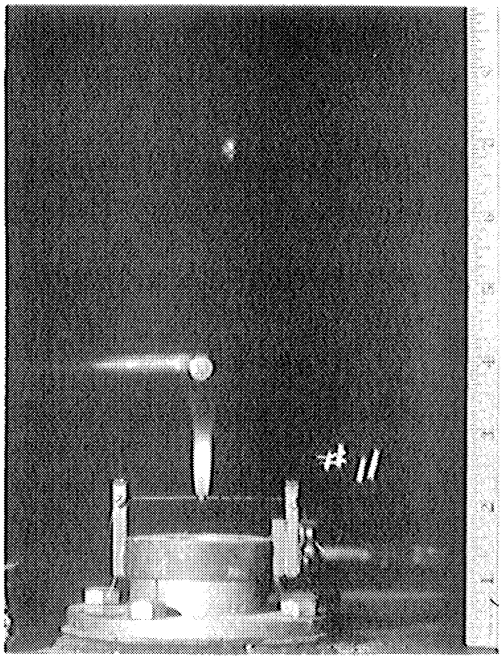

ROD 1/4 " ABOVE CRITICAL DISTANCE

FIG. 42 A EFFECT OF INSERTION OF A CYLINDRICAL ROD INTO A PILOT FLAME.

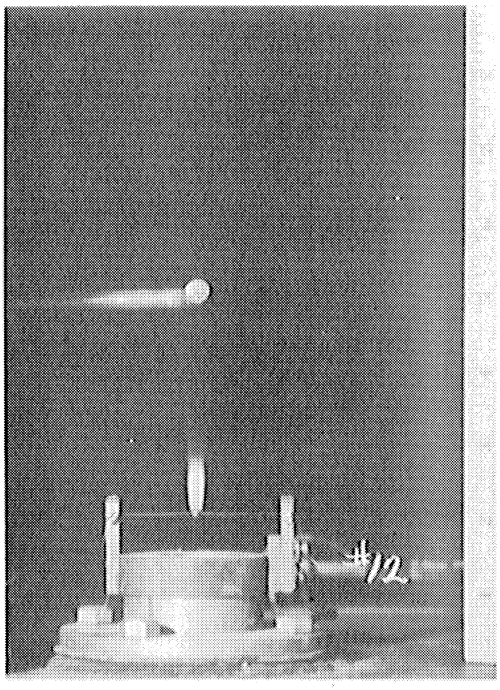

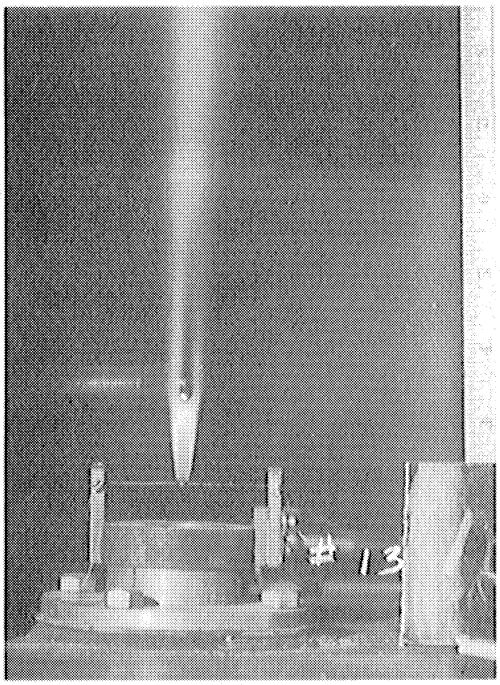

1/8" ROD — CRITICAL DISTANCE =
1 1/4" ±1/16" ABOVE FLAMEHOLDER

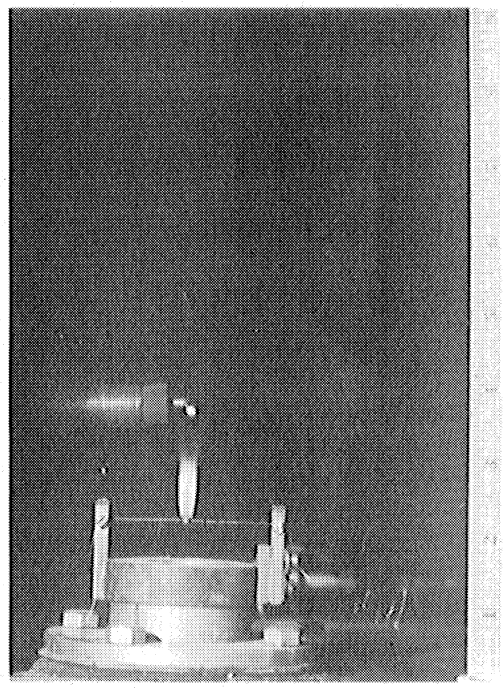

ALL PHOTOGRAPHS ARE AT SAME CONDITIONS
JET VELOCITY = 268 ft./sec.
ON MASS VELOCITY = 20 lb./sec./sq. ft. of Nozzle Area
FLAMEHOLDER DIA. = 1/8"
NOZZLE DIA. = 1"
HEIGHT OF FLAMEHOLDER = 1/2"
PRESSURE = 1 atm.
COMPLETELY UNCONFINED JET

FIG. 42 B EFFECT OF INSERTION OF A CYLINDRICAL ROD INTO A PILOT FLAME.

A few experiments were performed using a sphere instead of a cylindrical rod. The second sphere seemed to act just as an additional flame holder, that is burning occurred directly from the surface of the sphere, and its position was not critical, while the action of the rod seemed to be a more involved aerodynamic process. Fastex shadowgraphs and titanium tetrachloride smoke tracers did not shed appreciable light on the phenomenon.

B. Boundary Layer Removal Experiments

A flame holder involving surface section was constructed as is shown in figure 43. The vacuum was applied with a Nash Hytor MP 673 vacuum pump. A flow tube in the vacuum line was calibrated so that the amount of mixture removed could be measured. At full vacuum the flow through the bleed holes was ca. 2.5 cu.ft. per mm of 0.073 lbs per cu.ft. air. This value was substantiated by both the calibrated flow tube and the pump specification curve. In figure 44 in the right photograph, a flame is shown burning from the cylindrical holder with no vacuum applied at a fuel-air ratio of 0.0865 and a jet velocity of 137 ft/sec. In the left photograph, the flame at the same conditions is seen after full vacuum was applied. The flow through the ten No. 60 (0.020) dull holes is ca. 2.5 cfm. The total flow through the jet is 42 cfm. Calculations based on the Blasius solution for the order of magnitude of the thickness of the boundary layer indicates a boundary layer flow between 0.5 and 2.5 cfm. The use of titanium tetrachloride smoke tracers showed little or no disturbance of the flow pattern with vacuum on. Therefore, it is believed that most of the boundary layer is being removed with no appreciable alteration of the flow pattern about the holder.

Figure 45 is a comparative plot of the stability limits on the rich side for this type of flame holder with and without boundary layer removal. The curve for the flame holder shown in figure 43 without vacuum concurs exactly with the curve obtained for the four spheres previously tested in System 1. As may be seen in figure 45, with vacuum applied there is an appreciable decrease in the stability limits.

A further extension of this experiment is shown schematically in figure 46. A ring of 0.026 inch diameter wire was used to artifically create separation at various points along the flame holder. Three distinct regions were found, as shown in figure 46. With the ring located at any point in region 1, ignition was secured easily and the

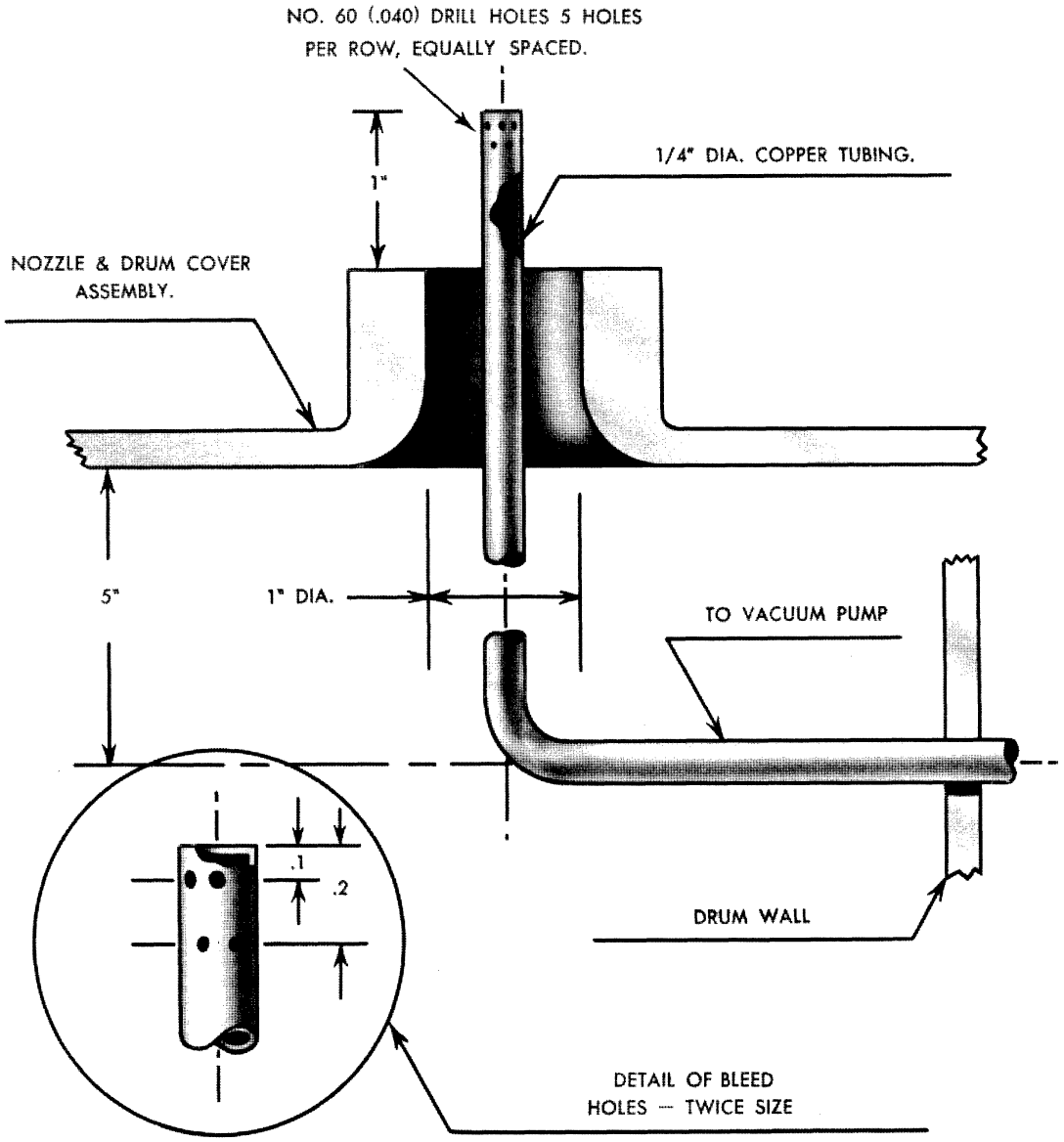

FIG. 43 SURFACE SUCTION FLAME HOLDER.

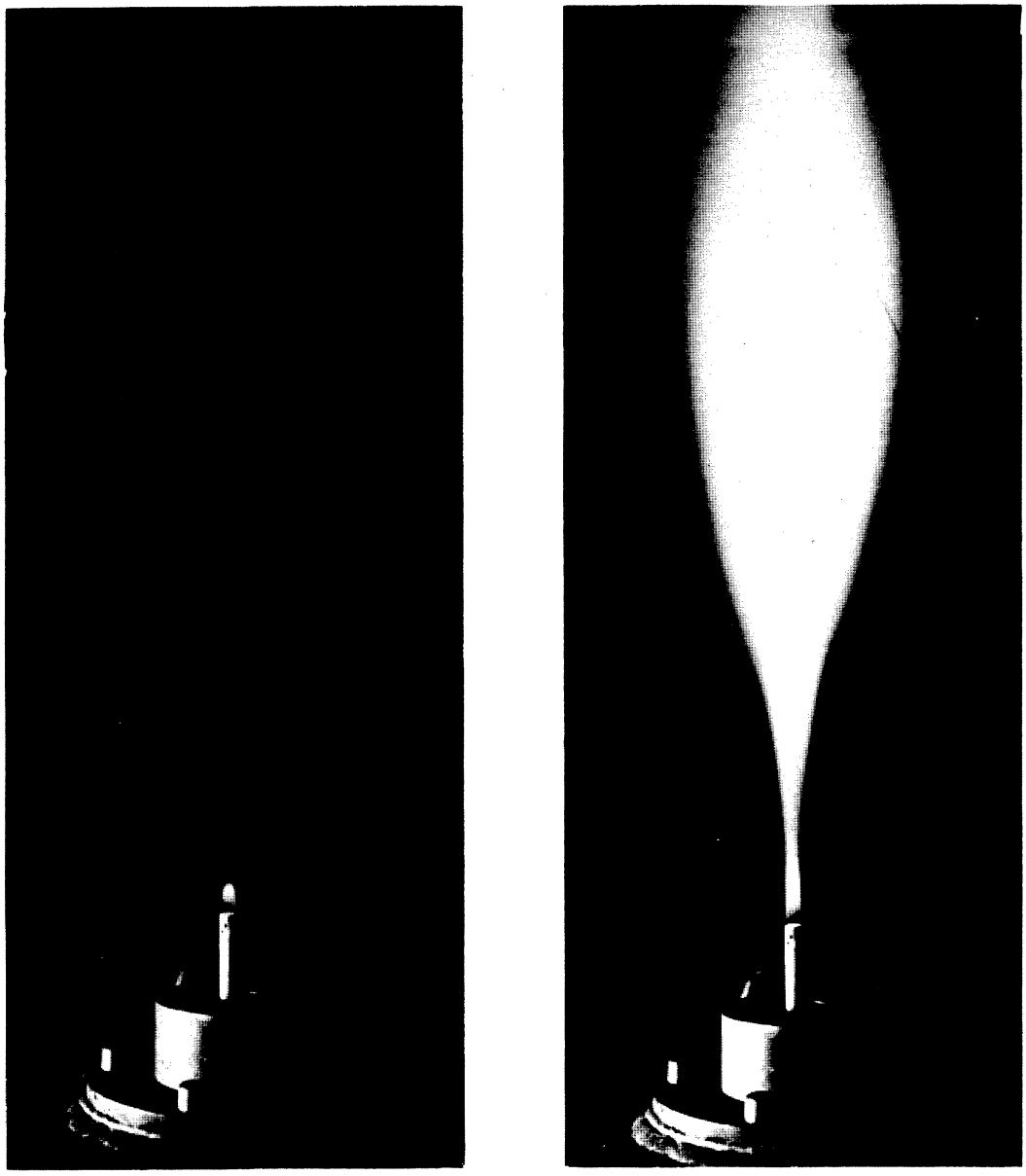

With boundary layer removal

Without boundary layer removal

PHOTOGRAPHS SHOWING EFFECTS OF
BOUNDARY LAYER REMOVAL ON FLAME

Jet velocity = 137 ft./sec.
Mass velocity = 10.4 lbs./secs./sq. ft. of nozzle area.
Nozzle dia. = 1 in.
Cylindrical flameholder dia. = .25 in.
Propane - air ratio = 0.0865
Pressure = 1 atmosphere.

FIG. 44

PHOTOGRAPHS SHOWING EFFECT OF BOUNDARY LAYER REMOVAL ON FLAME.

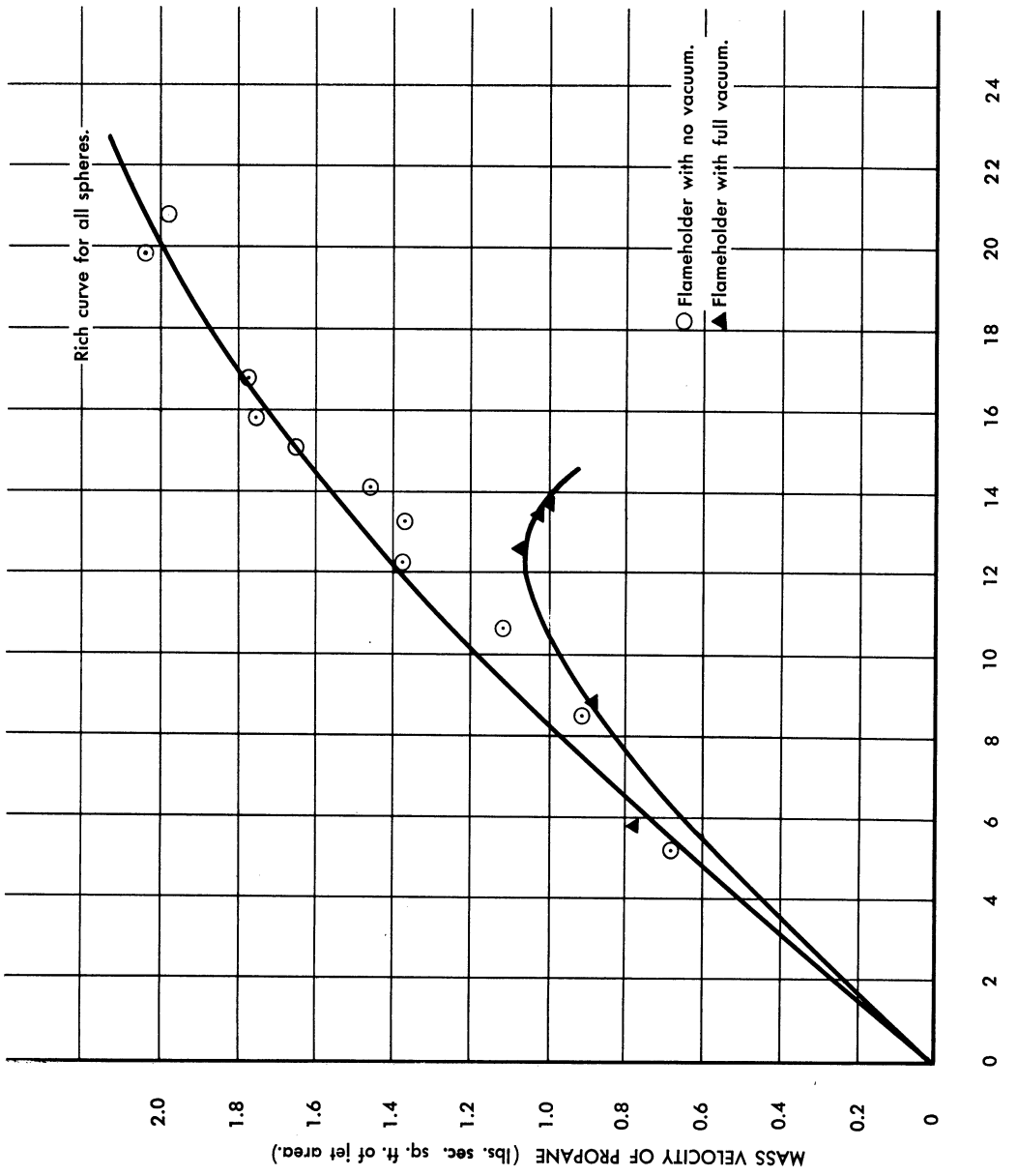

FIG. 45 BLOWOFF VELOCITY OF FLAMEHOLDER SHOWN IN FIG. 43

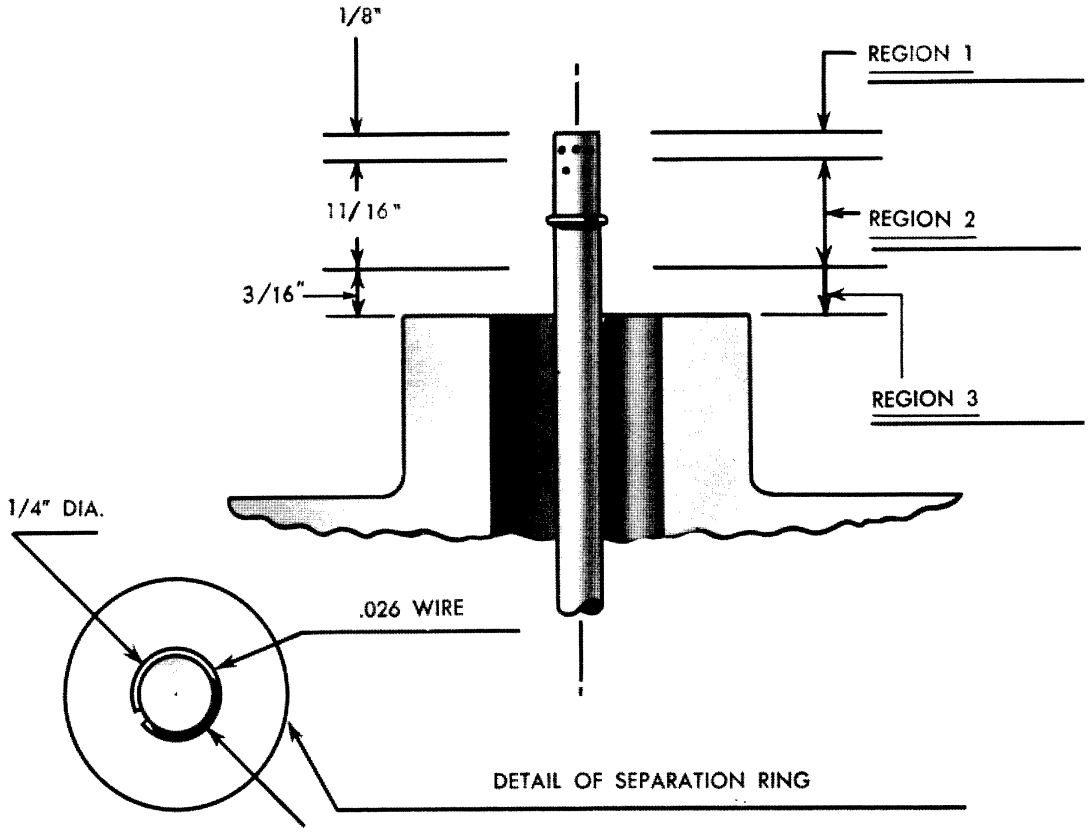

REGION 1 IGNITION & CONTINUOUS BURNING POSSIBLE, FLAME BURNS FROM WIRE.

REGION 2 IGNITION POSSIBLE, BUT STEADY BURNING IMPOSSIBLE WITHOUT USE OF SURFACE SUCTION.

REGION 3 IGNITION & STEADY BURNING POSSIBLE WITHOUT SURFACE SUCTION, FLAME BURNS FROM HOLDER.

FIG. 46 SEPARATION EXPERIMENT

flame burned stably. The zone was somewhat larger due to the fact that the flow separated at the ring. Region 1 extended a distance of 0.125 inches measured from the end of the flame holder. At the extreme point of region 1 it became impossible to ignite the mixture using the initial combination of jet velocity equal to 137 ft/sec and fuel-air ratio of 0.0826, or any other combination of fuel-air ratio and jet velocity. Region 2 represents the length in which it was impossible to obtain burning off the flame holder.

At the end of region 2, a distance of 11/16 inch from the downstream end of the holder, it again became possible to obtain ignition and steady burning. The combustion, however, appeared to be unsteady and very incomplete.

When surface suction is applied with the ring located anywhere in region 1, the flame is altered in much the same manner as is shown in the right hand photograph in figure 44. The downstream combustion ceases and only a pilot flame remains. With the ring located anywhere in region 2, ignition and steady burning is impossible without the application of vacuum. In other words, surface suction allows the stabilization of a flame behind the holder where it was not previously possible. When the ring is located anywhere in region 3, the effect of vacuum is again the same as shown in figure 35. It is to be noted that the action of surface suction becomes more effective in restabilizing the flame as the location of the ring approaches the point dividing regions 1 and 2.

The above mentioned experimental work was previously reported[4] in a progress report in July, 1949. Investigators at Battelle Memorial Institute attempted to duplicate the results shown in figure 44 but did not succeed, and their conclusion was "that the boundary layer has little or no effect on the blowoff limits and consequently, profile drag can be considered to have little or no effect on flame holding."[5] However, their apparatus[6] differed in several respects from the apparatus shown in figure 43. Although the nozzle diameter in both systems was 1 inch, the distance of the straight section following the convergent section of the nozzle was 3/4 inch in the apparatus shown in figure 43 and 2 inches in the equipment used at Battelle. Also, the latter system contained four relatively large supports at the inlet of the nozzle. These differences might tend to make the jet in the latter system more turbulent than the jet of the apparatus shown in figure 43.

The notch in the cylindrical flame holder used by Battelle might have had a separation effect similar to the effect of the wire ring shown in figure 46.

The experiments performed at Battelle Memorial Institute were designed to change the length of boundary layer build-up and not to completely remove the boundary layer immediately upstream of the flame, as in our experiments. Hence, their "full vacuum" and "no vacuum" designations did not have the same meaning as in the experiments previously described, i.e., in our experiments, full vacuum meant complete removal of the boundary layer immediately upstream of the flame, while in their experiments, full vacuum meant that the distance for boundary layer build-up was decreased by a factor of 3 or of 8, but not removed immediately before the flame.

It was found necessary in our experiments to remove ca. 2 to 5% of the total flow through the nozzle in order to obtain the results pictured in figure 44. In our 1 inch jet, this required almost the full capacity of a reasonably large vacuum pump (Nash Hytor MD 673), the use of a standard water aspirator not being sufficient. The amount of material removed in Battelle's experiments was not stated explicitly.

The data presented in section 3 indicates how sensitive flame holding is to system variables, such as the height of the flame holder, etc. The reason for the disagreement of the two experiments is probably due to some combination of the above mentioned possibilities. Since the system and the technique employed at Battelle was not identical to that used here, it is believed that their failure to reproduce the experiment, shown in figure 44, is meaningless. Since the disagreement was reported by Battelle, the experiments have been repeated in this laboratory many times, not only with the cylindrical flame holder shown, but with conical and disc flame holders as well. A rotameter installed in the vacuum line indicated that reproducible results could be obtained over a wide range of fuel-air ratios and jet velocities, and that decidedly lower blowoff velocities were obtained when the boundary layer was removed.

C. Flame Traverses

An attempt was made to obtain quantitative measurements in the region downstream of the flame holder during burning as well as in cold flow. It was believed that analytical work would be meaningless because of the length of time required to perform analysis by conventional methods, as well as the time consumed by sampling. It was also felt that a thermocouple traverse would not be very accurate because of the lack of knowledge concerning emissivity coefficients, etc., at the high temperatures involved. However, it was believed that physical measurements of pressure and electrical conductivity could be made in the flame region at various locations. For this purpose, an apparatus was constructed which permitted vertical and horizontal traverses to be made accurately. The flame holder used in the experiments was constructed from a 1/4 inch copper tube, plugged at one end and connected to a water manometer at the other. A hole, 0.040 inches in diameter, was drilled through the brass plug. The flame holder was installed axially through the nozzle (in a manner similar to the flame holder shown in figure 43), and thus a vertical cylindrical flame holder was obtained which permitted measurement of the pressure at the base of the flame. For the traverse measurements of pressure a piece of steel hypodermic tubing 0.042 inches in diameter, connected to a water manometer, was used. Measurements were made with burning and without burning using a fuel-air ratio of 0.0942 and a jet velocity of 109 ft/sec, the one inch diameter nozzle in System 1, and a completely unconfined jet at atmospheric pressure. The end of the 1/4 inch cylindrical flame holder was ca. 1-3/8 inches above the nozzle. A photograph of the flame burning under these conditions may be seen in figure 47. The pressure traverse tube orientated vertically may be seen in the right of the photograph.

Horizontal traverses were made at different heights above the flame holder to obtain pressure measurements for each of the following cases: vertical tubing with burning; vertical tubing without burning; horizontal tubing with burning; and horizontal tubing without burning. The experimental data obtained with the vertical tube traverses is shown in figure 48, while the data obtained with the horizontal tube traverses are shown in figure 49; a cross plot of this data showing the pressure measurements versus height along the flame center line is shown in figure 50. Data obtained from figures 48 and 49 was used to obtain pressure contours, and these plots, superimposed on a photograph

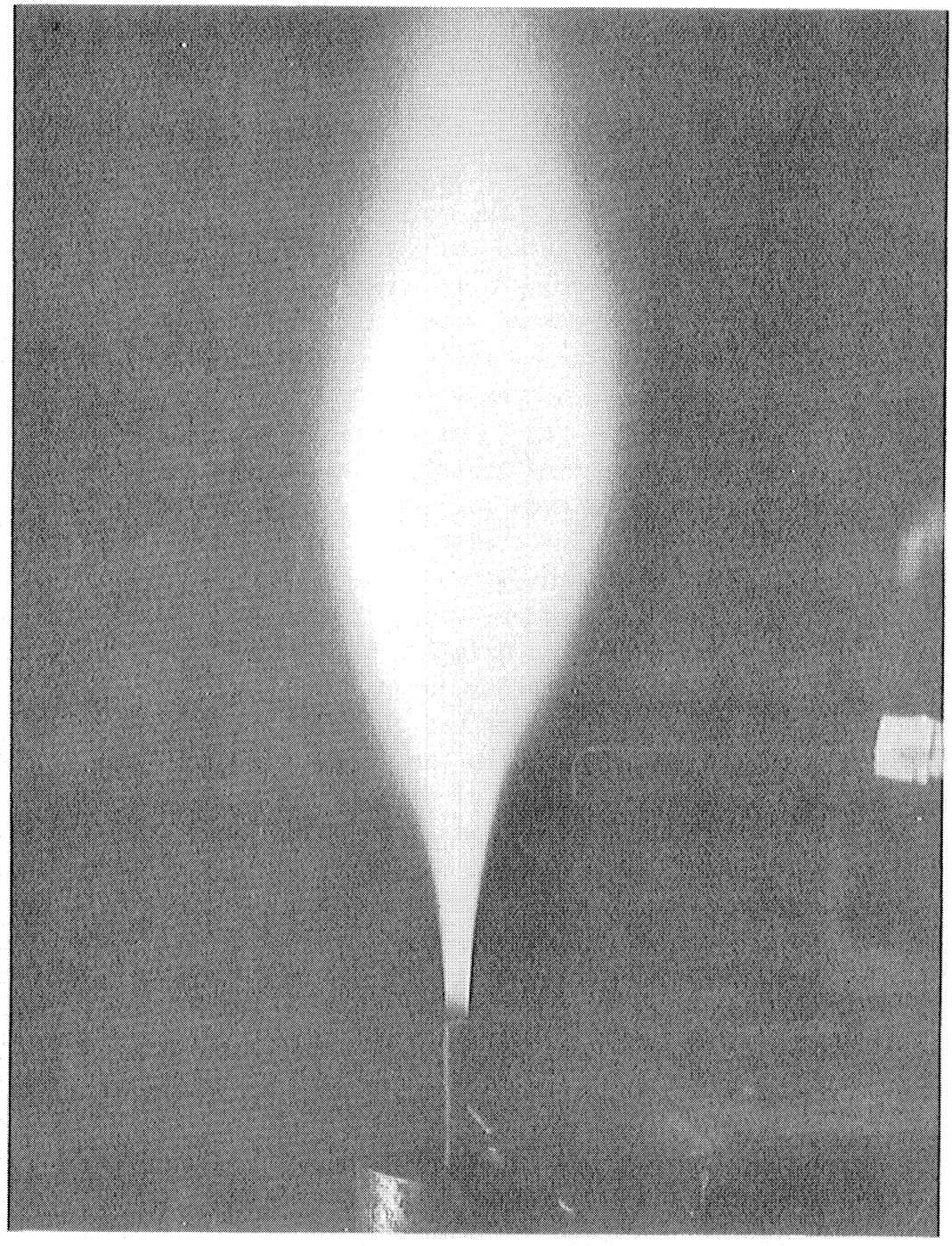

FIG. 47 PHOTOGRAPH OF FLAME AT CONDITIONS USED FOR PRESSURE TRAVERSES.

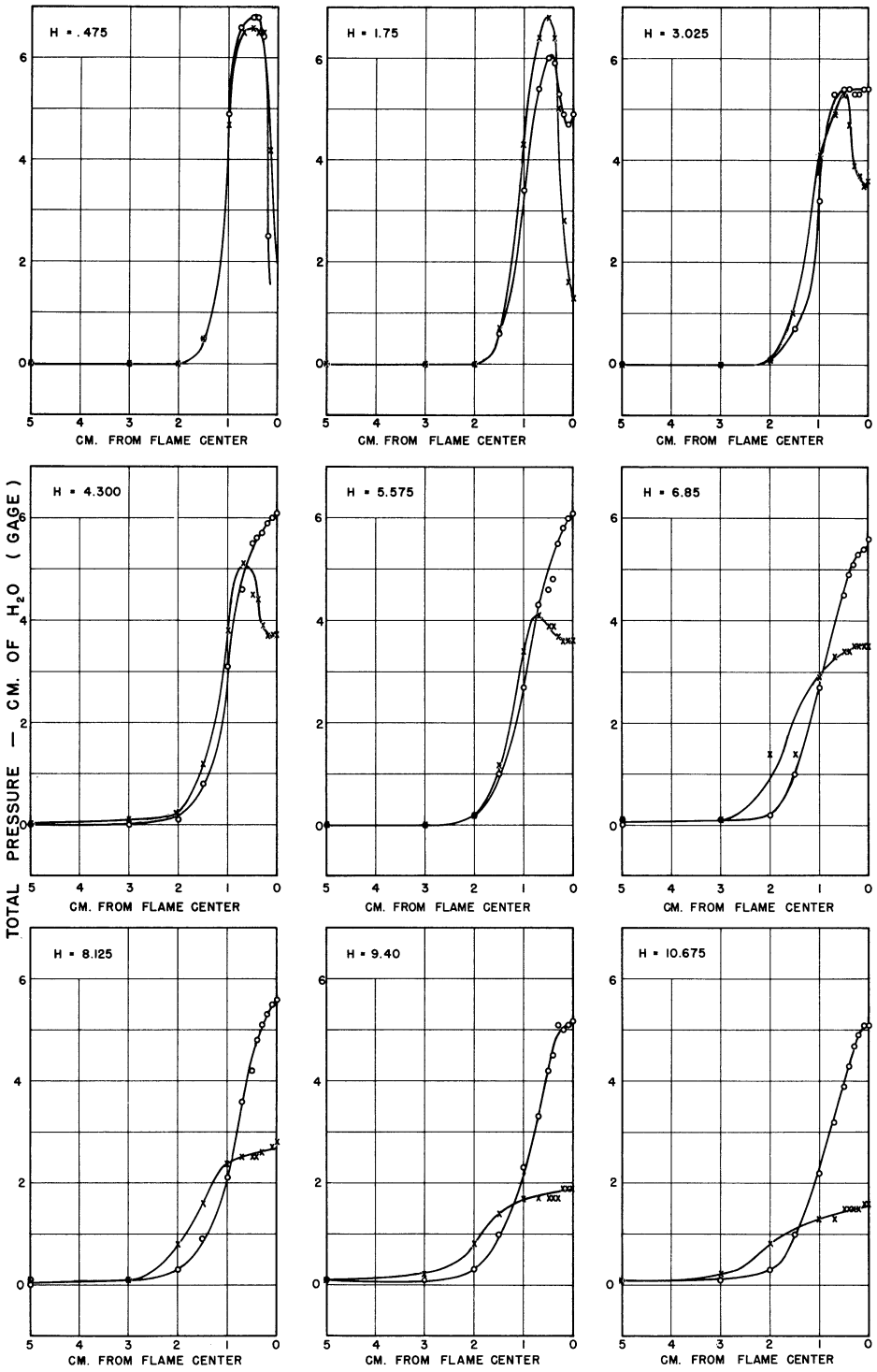

x = BURNING

o = NO BURNING

H = HEIGHT ABOVE FLAMEHOLDER BASE, CM.

TRAVERSE TAKEN AT EVERY 1/8" (.32 CM.) OF HEIGHT: SELECTED POINTS SHOWN HERE.

MASS VELOCITY = 8.3 LBS./SEC./SQ.FT.

PROPANE AIR RATIO = 0.0942

PRESSURE = 1 ATM.

NOZZLE DIAMETER = 1 INCH

CYLINDRICAL FLAME HOLDER DIA. = 1/4"

FIG. 48 VERTICAL TUBE PRESSURE TRAVERSES OF FLAME.

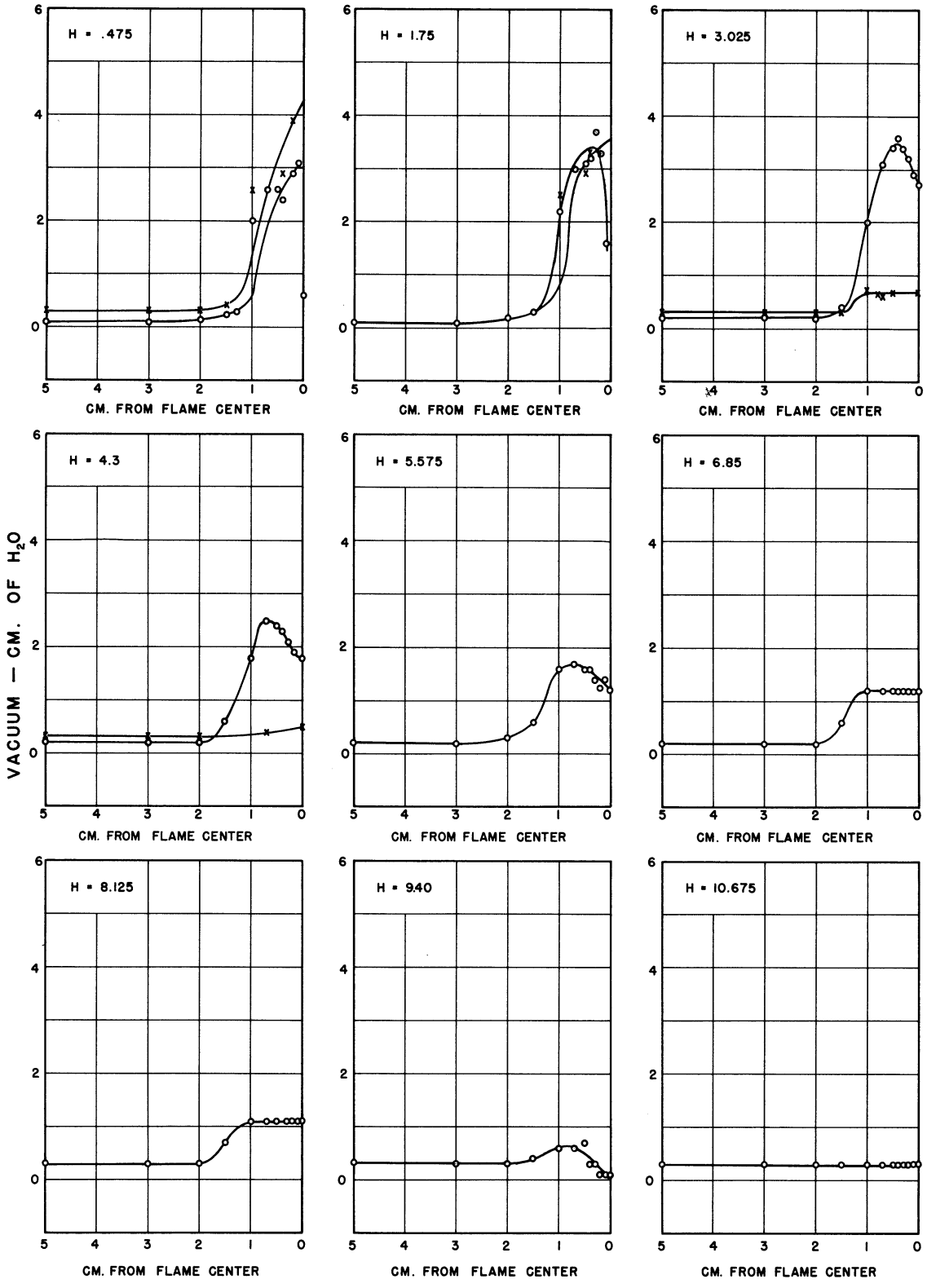

x = BURNING
o = NO BURNING
H = HEIGHT ABOVE. FLAMEHOLDER BASE, CM
TRAVERSE TAKEN AT EVERY 1/8" (32CM.) OF HEIGHT: SELECTED POINTS SHOWN HERE.

MASS VELOCITY = 8.3 LBS./SEC./SQ.FT.
PROPANE AIR RATIO = 0.0942
PRESSURE = 1 ATM.
NOZZLE DIAMETER = 1 INCH
CYLINDRICAL FLAMEHOLDER DIA. = 1/4"

FIG. 49 HORIZONTAL TUBE PRESSURE TRAVERSES OF FLAME.

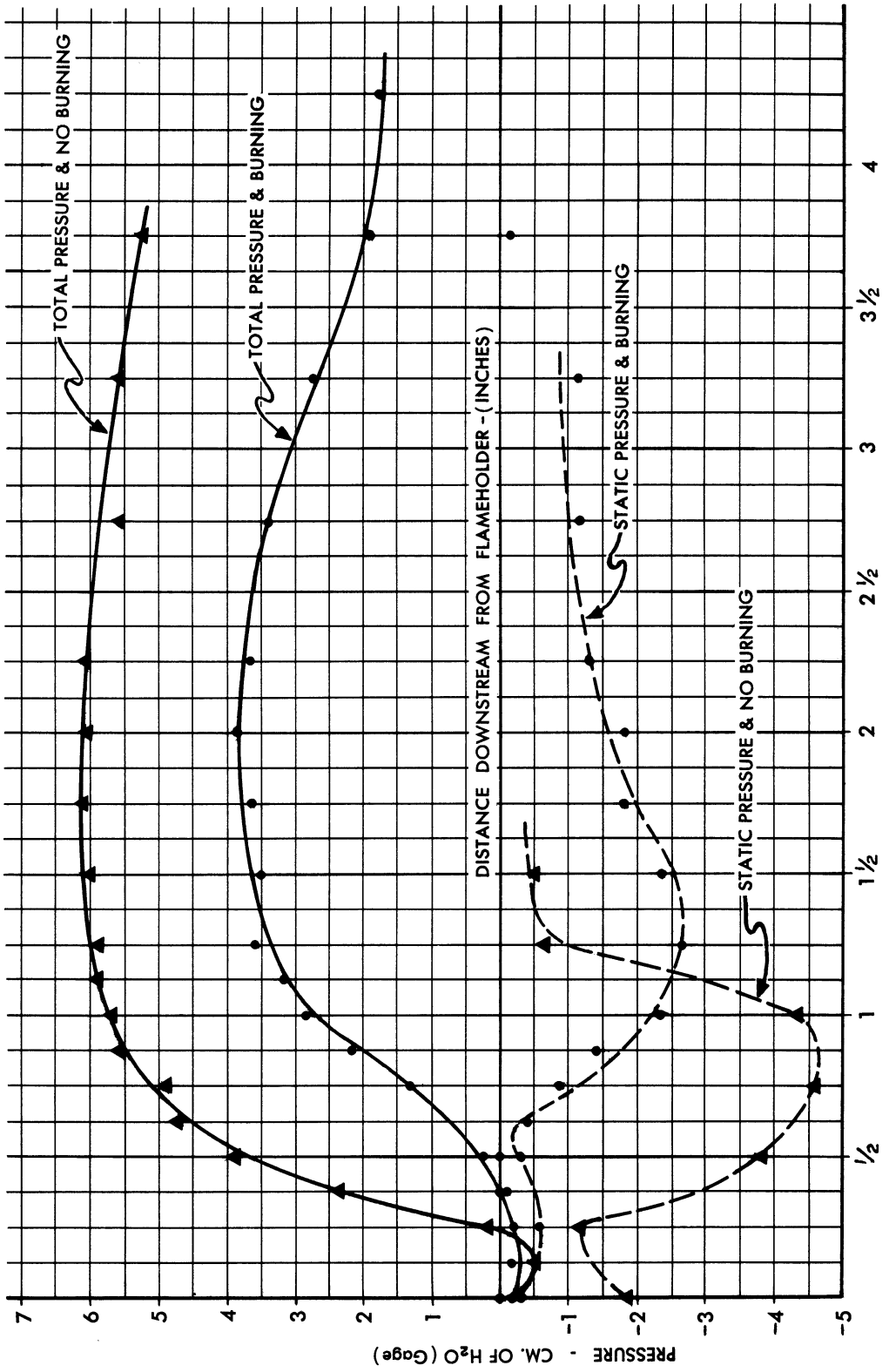

FIG. 50 PRESSURE MEASUREMENTS OF FLAME ALONG CENTER LINE.

of the flame zone, are shown in figure 51. The reading of the manometer connected to the flame holder was -0.2 cm. of water gage in the case of burning and -0.9 cm. of water gage in the case of no burning. These readings corresponded exactly to those obtained when the hypodermic tubing, orientated both vertically and horizontally, was placed directly over the hole in the flame holder.

A few experiments were performed with the tube placed vertically, but pointed in the downstream direction. Although vacuums were generally obtained, a positive pressure was observed in the center of the flame at specific heights with a few fuel-air ratios possibly indicating a flow reversal under these conditions.

Velocity calculations were not made from these measurements for several reasons. The stagnation pressure, P_{st}, has been defined[7] as the sum of the static pressure, P, and the pressure rise resulting on isentropic deceleration to zero velocity. The equation P_{st}, P, and the velocity, u, has been derived from a force balance for steady functionless flow as

$$P_{st} = P + \int_0^u \frac{\rho u du}{g_c}$$

The vertical tube measurements might be assumed to correspond to the stagnation pressure with the assumptions stated above. However, it is believed that the data obtained with the horizontal tube traverses does not correspond so closely to the static pressure because of the aspirating effect of the gas moving past the end of the horizontal tubing as well as the lack of a surface upstream in which to obtain boundary layer buildup. Had a conventional pitot tube (i.e. double walled) been used in these measurements, it is believed that the necessarily larger diameter would have seriously disturbed the flame and flow process.

As seen from the above equation, it is necessary to know the gas density as well as the static and stagnation pressures in order to compute the velocity at any point. To compute the gas density requires a knowledge of the temperature and composition of the gas as well as its static pressure. The experimental work of Morrison and Dunlap[8]

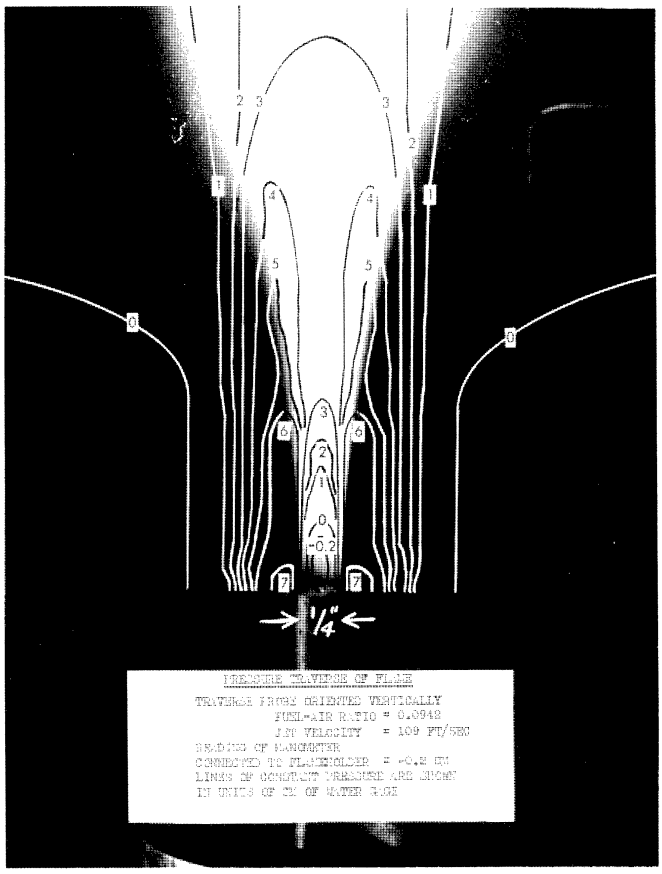

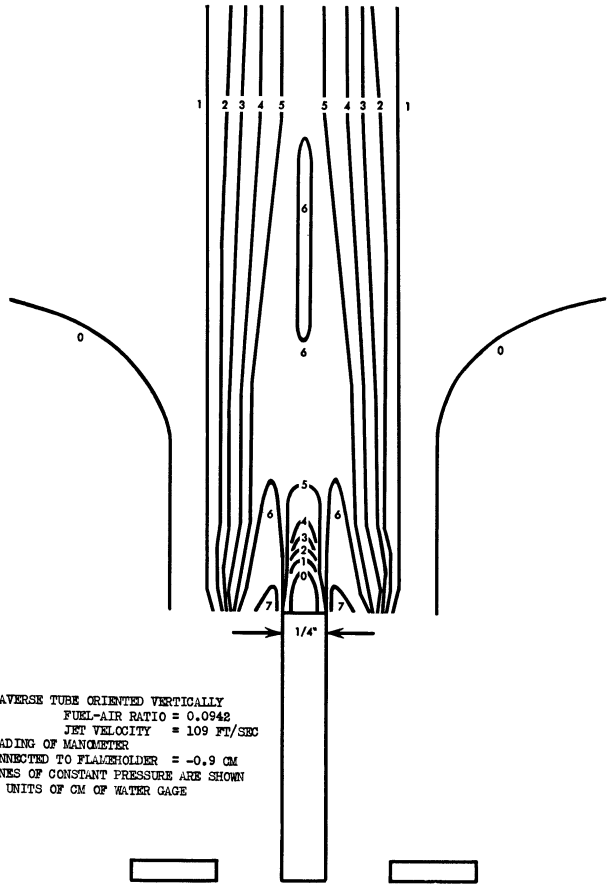

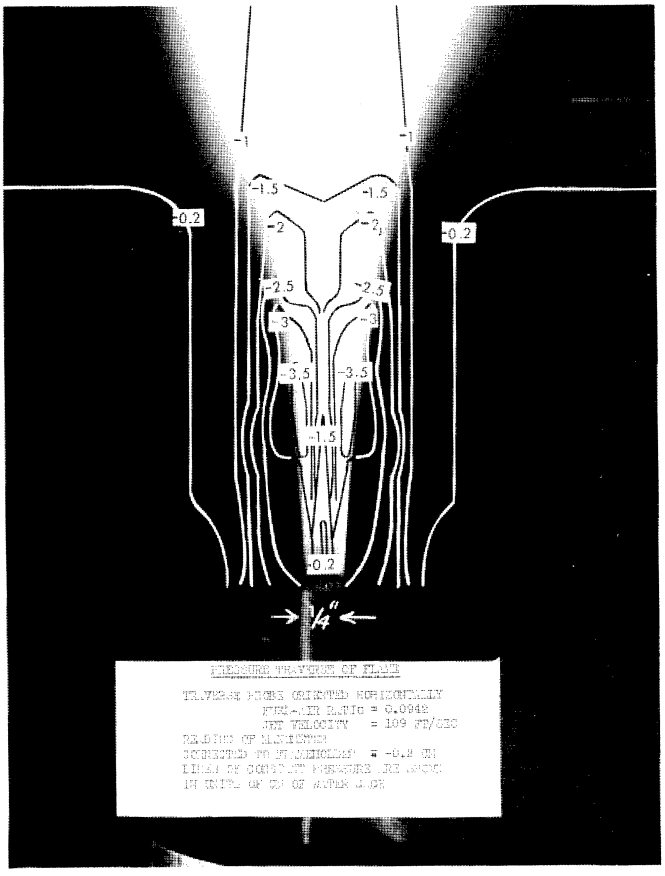

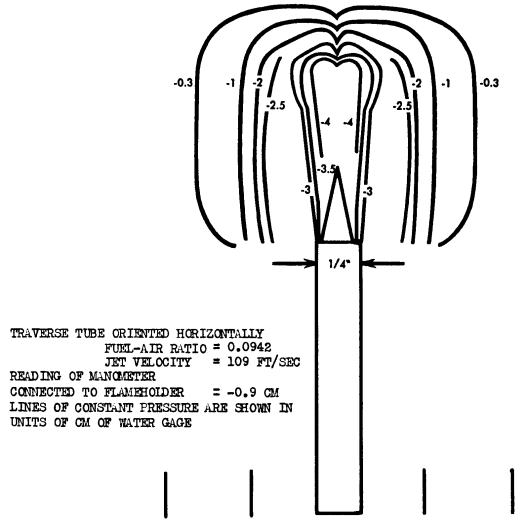

FIG. 51 PRESSURE MEASUREMENTS OF FLAME.

indicated that equilibrium conditions were not attained in propane-air flames at low jet velocities ca. 10 ft/sec and it is believed doubtful that equilibrium would be attained at all points in a flame burning in a jet with a velocity of 109 ft/sec. Thus the lack of knowledge of the gas temperature and composition as well as the uncertainty of the static pressure measurements makes a density, and, hence, a velocity, computation from these data inadvisable in the case of burning.

It has been known for more than a century that gases from flames are conductors of electricity. Volta caused a discharge of electricity from the surface of a non-conductor by passing a flame over it.[9]

An attempt was made with the present equipment to measure the conductivity of the flame at different locations. Two wires, 3/16 inch apart, were traversed through the flame area and the voltage drop between them, compared to a 10 meg. ohm resistance, was measured. A reading of 0 volts was obtained when no flame existed. The data obtained (using the 1/4 inch cylindrical flame holder in the 0.1 inch unconfined jet of System 1 at atmospheric pressure) for a fuel-air ratio of 0.0942 and a jet velocity of 109 ft/sec may be seen in figure 52. Fuel-air ratio seemingly caused greater variations in the flame conductivity than did jet velocity.

The values shown in figure 52, however, are integrated values and not point values, since the conductivity of a larger volume of gas than the volume included between the wire tips is measured. In an attempt to decrease the magnitude of this effect, it was decided to measure the resistance between two parallel flat plates with an area large in comparison with the wire area. Accordingly, two plates, ca. 2 mm by 2 mm were affixed to the wires and traversed through the flame. However, the plates were so large that they acted as secondary flame holders and no data was obtained.

It should be noted that at locations above the pilot zone, the wires became incadescent, and, therefore, contribute an additional ionizing effect to the gases surrounding them. The combination of these two ionizing sources makes it virtually impossible to differentiate between them. It would be possible to obtain an empirical correlation between conductivity and fuel-air ratio or jet velocity for a given system which might have practical application, but at the present time it is believed that this would not add materially to a better understanding of the flame holding mechanism.

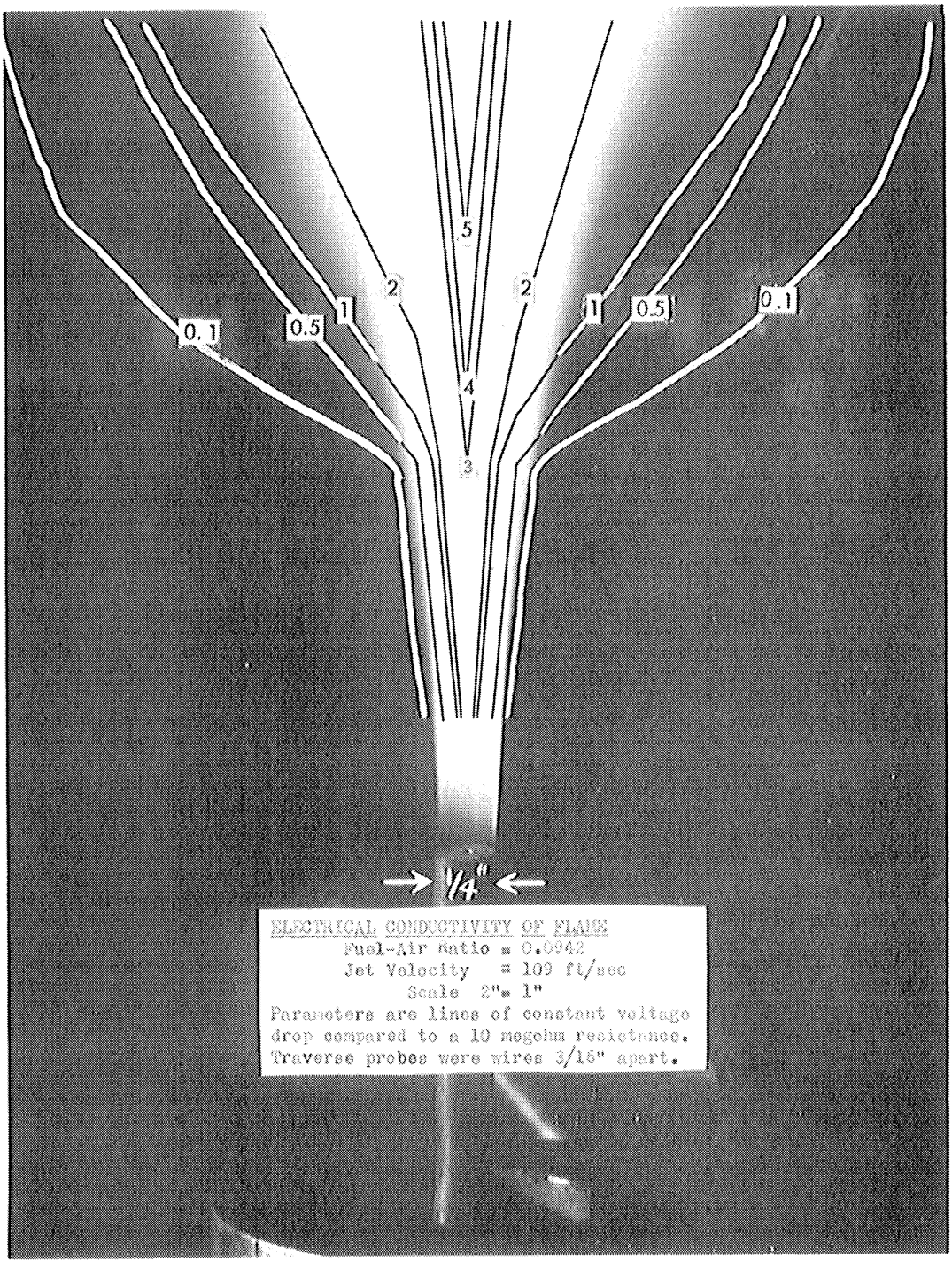

FIG. 52 ELECTRICAL CONDUCTIVITY OF FLAME.

The only conclusion obtained from these and other experiments is that it is very difficult to determine experimentally absolute values of any physical property at different points in the flame region.

The static pressure may be measured satisfactorily at one point, at the base of the flame, but the other measurements only indicate that the static pressure varies a great deal throughout the flame region, but no reliance is placed on the absolute values obtained.

The lack of temperature and composition data as well as the uncertainty of the static pressure measurements prevents computation of the velocity from the total pressure measurements.

A large number of shadow photographs were taken of flames, including Fastex shadowgraphs at 5000 pictures per second. Some of these shadowgraphs have been presented in previous progress reports[10,11,12], as well as in figures 20, 21, 22, 29, 30, 31, 37, 38, and 39 of this report. However, these shadowgraphs do not permit any absolute determination of the flow pattern in the flame area except to indicate that the flow and flame process is a function of the many variables previously mentioned. Some work was done with smoke tracers of titanium tetrachloride, but no results were expected or obtained with their use, since the work of Langmuir and Blodgett[13] indicates that solid particles do not follow the gas streamlines in the range of particle sizes and Reynolds number with which we are concerned. An attempt to determine a composition distribution by the measurement of a physical property, electrical conductivity, was not successful because of the difficulty in differentiating between the ionizing effect of the flame and the ionization caused by the emission of electrons from the hot probes. The conclusion is that it is very difficult to obtain absolute values of the flow or composition distribution in the flame region, at least with simple apparatus. It is possible that some combination of optical methods, such as the use of an interferometer and an emission spectrometer might be of value in determining absolute values of the flow and composition distribution in a flame region.

V. CORRELATION OF BLOWOFF DATA

A. Previous Attempts

It was previously reported[14] that a straight line was obtained when the fuel-air ratio at the maximum blowoff velocity (for each spherical flame holder) was plotted against $\frac{1}{\sqrt{R_e}}$

(R_e = Reynolds number = $\frac{DG}{\mu}$

D = spherical flame holder diameter

G = maximum mass velocity at blowoff

μ = viscosity of fuel-air mixture issuing from nozzle)

This straight line was obtained with the use of data from System 1 (1 in. nozzle) at atmospheric pressure. Because of the relationship between $\frac{1}{\sqrt{R_e}}$ and the thickness of a boundary layer, this type of plot led to the boundary layer experiments reported in Section IV. However, when experimental data was obtained under vacuum with System 2 using a 3/8 in. diameter nozzle, a series of similar curves (for different pressures) was obtained rather than one straight line. These may be seen in figure 53. As may be seen from this plot, the 1/16 inch diameter spherical flame holder data does not fall on the straight line obtained with the other three spherical flame holders.

Straight lines were obtained, however, when the Reynolds number was plotted against sphere diameter, for maximum blowoff velocity. These lines all intersect at $R_e = 0$, D = 0.04 inches as may be seen in figure 54, which might indicate that sphere diameters smaller than 0.04 inches would not hold a flame. It was noted under vacuum with the 0.0625 inch diameter sphere, that burning occurred sometimes as a Bunsen flame, rather than from the flame holder. Experiments were not performed with smaller flame holders, however.

Calculations were made to determine the amount of chemical energy of the fuel contained in the boundary layer flow. This "heat release

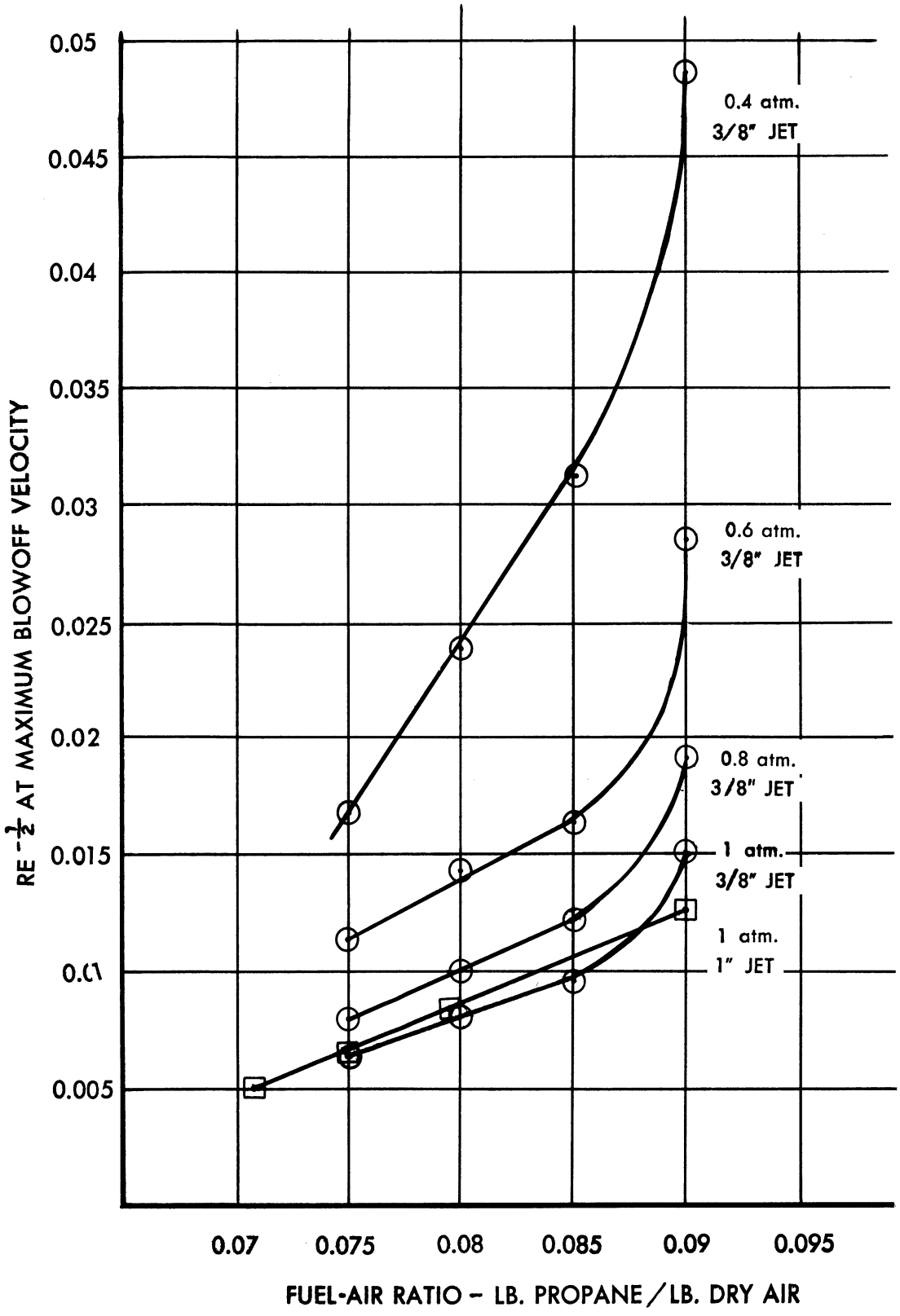

FIG. 53 FUEL-AIR RATIO VERSUS $\frac{1}{\sqrt{\text{REYNOLDS NO.}}}$ AT MAXIMUM BLOWOFF VELOCITY.

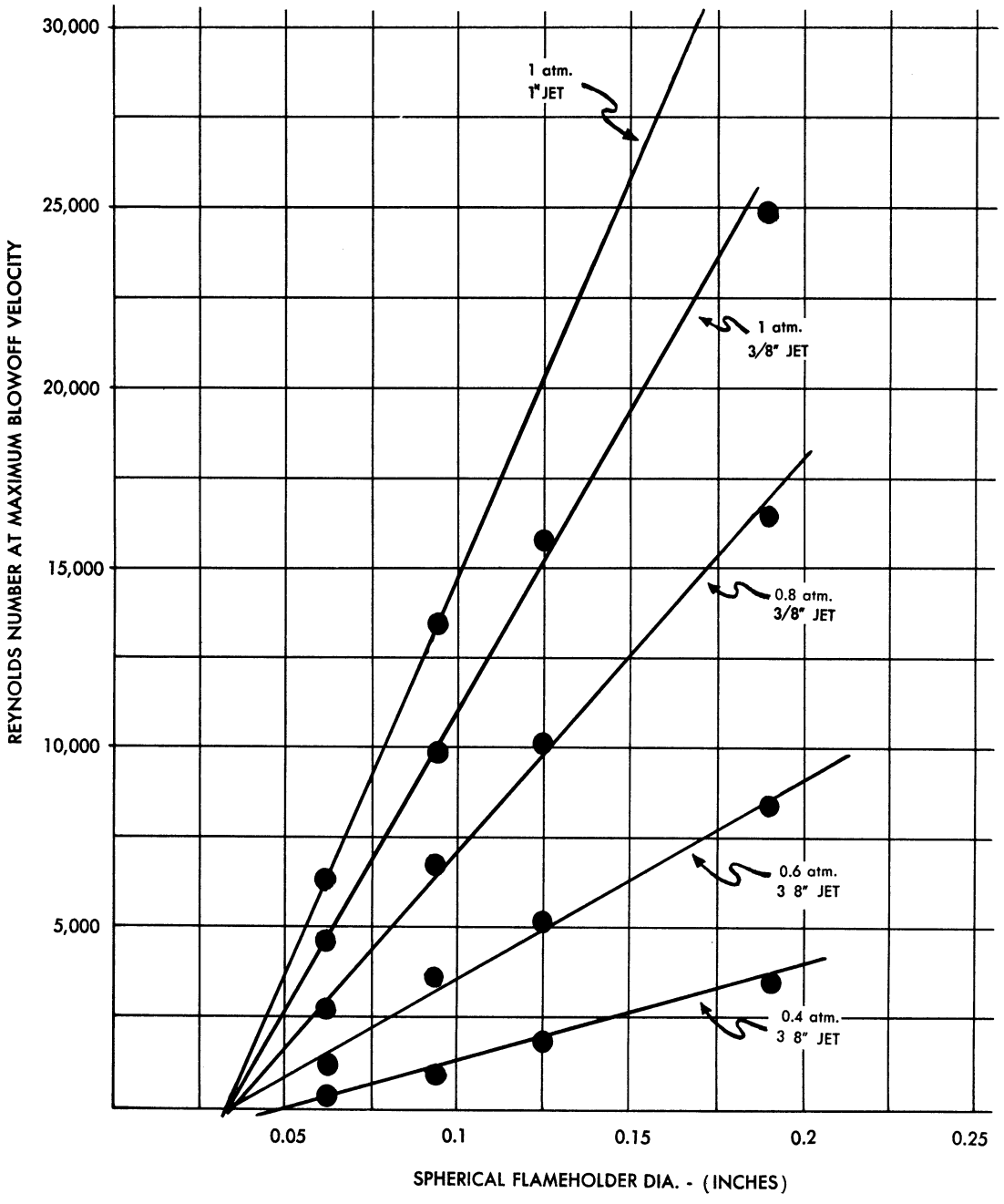

FIG. 54 REYNOLDS NUMBER AT MAXIMUM BLOWOFF VELOCITY VERSUS FLAME HOLDER DIAMETER FOR VARIOUS PRESSURES.

of the boundary layer", (BTU/sec) was plotted against the mass velocity at blowoff to obtain a straight line from the origin for all fuel-air ratios. However, different lines were obtained for each sphere tested. The slope of these lines was extremely sensitive to the value of ΔH (enthalpy change) used to determine the "heat release of the boundary layer." Equilibrium values as well as values calculated from the experimental ρ_b / ρ_u data of Morrison and Dunlap[15] were used. However, when the data was plotted as indicated by dimensional analysis ($\frac{V_b}{\sqrt{\Delta H}}$ vs $\frac{\mu}{D\rho\sqrt{\Delta H}}$ on log-log paper) four lines, one for each of the spheres tested were obtained rather than a single line for all spheres.

Other investigators have obtained limited correlation of blowoff data. Scurlock[16] attempted to correlate his data as well as the blowoff data of Longwell, and the data of Lewis and Von Elbe by plotting the log of $\frac{V_{bo}}{D^{0.45}}$ against a generalized oxidant fraction (i.e. a function of fuel-air ratio so computed that a stoichimetric mixture of all fuels is 0.5). Different curves were obtained for the different fuels as well as the data obtained in different systems. Scurlock did not obtain correlation with different fuels in the same system by plotting

$$\frac{V_{bo}}{D^{0.45}} \cdot V_f \cdot (T_b - T_o) \text{ vs. generalized oxidant fraction}$$

V_{bo} = blowoff velocity, ft/sec

D = flame holder characteristic dimension

V_f = laminar flame speed

$T_b - T_o$ = temperature rise due to burning.

Scurlock did, however, succeed in correlating the data obtained in his system at atmospheric pressure by plotting $\frac{V_b}{D^{0.45}}$ versus fuel-air ratio to obtain a single curve for different flame holder sizes and spheres. This data was obtained in a confined test chamber, 3 inches by 3 inches by 17 inches long, the flame holder being nine inches above the 3 inch square nozzle. De Zubay[17] obtained a similar type of correlation,

but including pressure, by plotting fuel-air ratio vs. log $\frac{V_b}{D^{0.85} P^{0.95}}$

V_b = blowoff velocity, ft/sec

D = disc diameter, inches

P = pressure, psia

to obtain a single curve for three different diameter discs (1/4 inch, 1/2 inch, and 1 inch diameter). This data was obtained in a 2-3/4 inch diameter cylindrical test chamber with the disc being held 2 inches from the inlet of the 4 inch long test chamber. A water spray nozzle was inserted in the flame ca. 2 inches downstream of the holder. Jensen and Miesso[18] found that separate equations were necessary to characterize fuel rich and lean blowoff. For 1/4 and 1/8 inch diameter spheres and discs, for propane, isobutane, and ethane, the equation for the lean blowoff was found to be

$$(Pe_f)^2 = \frac{1}{16.7} \frac{Pe_v \left(\frac{C_p \mu}{k}\right)^2}{\left(\frac{D_j}{D}\right)^{0.3} C_D^{0.5}}$$

while the equation for the fuel rich side was found to be

$$\sqrt{Pe_f} \doteq \frac{1}{10,300} \frac{Pe_v \left(\frac{D_j}{D}\right)^{0.6}}{\sqrt[4]{C_D}}$$

in which

Pe_f = Peclet number based on flame speed,

Pe_v = Peclet number based on blowoff velocity,

C_D = drag coefficient,

$\frac{C_p \mu}{k}$ = Prandlt number of fuel-air mixture,

D_j = nozzle diameter = 1 inch,

D^j = flame holder diameter.

However, the Peclet number is merely the product of the Reynolds number and the Prandlt number, and the Prandlt number is essentially a constant for the fuel-air mixtures used. The density and viscosity vary only slightly (since the data is obtained at atmospheric pressure); D_j is a constant, since only one nozzle was used in the experiments, so that the lean equation may be reduced to

$$(D\ V_f)^2 = K \frac{D\ V_b\ D^{0.3}}{C_D^{0.5}}$$

$$\text{or} \quad (V_f)^2 = \frac{K\ V_b}{D^{1.7}\ C_D^{0.5}}$$

while the rich blowoff equation may similarly be reduced, in terms of actual experimental variables to

$$\sqrt{V_f} = K \frac{V_b}{D^{0.1}\ C_D^{0.25}}$$

This data was obtained in a one inch diameter nozzle in an unconfined jet with a 3 inch diameter plenium chamber upstream of the nozzle. The height of the flame holder above the nozzle was not stated.

As may now be seen, three different investigators obtained similar type correlations of blowoff data, i.e.

Scurlock - F/A $\alpha \left(\frac{V_b}{D^a} \right)$
at 1 atm in partially confined jet

$a = 0.45$

De Zubay F/A $\alpha \left(\frac{V_b}{D^a P^b} \right)$
under vacuum in partially confined jet

$a = 0.85$
$b = 0.95$

Jensen and Miesso - at 1 atm in unconfined jet for lean blowoff

$$(V_f)^2 \propto (F/A)^2 \propto \frac{V_b}{D^a C_D^c}$$

$$a = 1.3$$
$$c = 0.5$$

for rich blowoff

$$\sqrt{V_f} \propto \sqrt{F/A} \propto \frac{V_b}{D^a C_D^c}$$

$$a = 0.1$$
$$c = 0.25$$

However, none of these investigators succeeded in obtaining any straight line correlation involving fuel-air ratio, nor did any of them include such variables as nozzle diameter or height of the flame holder above the nozzle. In addition, Scurlock and De Zubay obtained their data in a partially confined jet. The wide variation in the exponent of the flame holder diameter (0.1; 0.45; 0.85; 1.3) could probably be attributed in part to the differences in the testing systems, but is also a function of fuel-air ratio, as may later be seen. Some of the data obtained during this investigation could be represented by the correlation obtained by the 3 previous investigators (i.e. $F/A \propto \frac{V_b}{D^a P^b C_D^c}$) but no one equation would represent the data when the system variables were imposed.

A great many unsuccessful attempts were made to apply dimensional analysis to the experimental data obtained at this laboratory, and no one theoretical equation could be found which represented all of the data. It is difficult to evaluate such terms, for example as viscosity, which affects the flow pattern around the holder, but which varies from point to point due to temperature and composition changes.

Since previous correlations proved inadequate, and because no theoretical equation was found which represented all of the experimental data obtained, an empirical equation was developed which represented the experimental data obtained. This equation, for a completely unconfined jet, spherical flame holders, and propane-air mixtures, includes the following experimental variables

	G,	the mass velocity at blowoff
	D,	the spherical flame holder diameter
	F/A,	the fuel-air ratio
	P,	the absolute pressure
	D_j,	the nozzle diameter
and	h_j,	the height of the flame holder above the nozzle.

This equation is

$$G = \left(\frac{P}{100}\right)^{\alpha} \left(\frac{0.29}{D}\right)^{B} \left[\frac{-7.2 + 17.32\, D_j - 4\Gamma}{8.42\,(1-\Gamma)}\right]$$

in which

$$\alpha = \frac{1}{1.15\, D + 6.6\, F/A - 0.255}$$

$$B = \frac{(0.100/F/A)^{3.11}}{-0.91}$$

$$\Gamma = \frac{1.42\, D_j - 1.54}{\left(\frac{h}{D_j} - D_j^{1.84}\right)^2 - 0.60}$$

The development of this equation and its limitations are presented on the following pages.

B. Development of Empirical Correlation

The mass velocity at blowoff (G, (lbs/sec/sq.ft. of nozzle area)) was plotted against the absolute pressure P, in mm Hg. on log-log paper to obtain a straight line of slope a. An example of this plot may be seen in figure 55 which is for a 1/16 inch diameter spherical flame holder, the 3/8 inch diameter nozzle in System 2, at a flame holder height of 3/16 inch. Plots similar to figure 55 were constructed for all of the vacuum data obtained in System 2, i.e. for flame holder diameters of 1/16, 3/32, 1/8, and 0.189 inches, each flame holder being tested at nine fuel-air ratios from 0.06 to 0.100. The values of a, the slope of the line on figure 55 and similar figures, were then plotted against fuel-air ratio as is shown in figure 56. As may be seen in figure 56, the slopes of the lines for the four spheres are the same, 6.6, so that the equation of lines on figure B is

$$(1) \quad a = 6.6\,(F/A) + b$$

in which b is the intercept at F/A = 0 and is a function of sphere diameter. The values of b are plotted against sphere diameter in figure 57 to obtain a straight line whose slope is 1.15 and whose intercept at D = 0 is -0.255. Hence, the equation of the line in figure 57 is

$$(2) \quad b = 1.15\,D - 0.255$$

substituting this value of b in equation (1) we obtain

$$(3) \quad a = 6.6\,(F/A) + 1.15\,D - 0.255$$

Hence, referring to figure 55, we have

$$(4) \quad \log \left(\frac{P}{100}\right) = a \log G + c^1$$

$$(5) \quad \text{or} \quad \log G = \log \left(\frac{P}{100}\right)^{1/a} - c^1$$

Values of $\left(\frac{P}{100}\right)^{1/a}$ were then calculated for all of the vacuum points obtained in System 2. Log-log plots of $\left(\frac{P}{100}\right)^{1/a}$ vs. G were then drawn

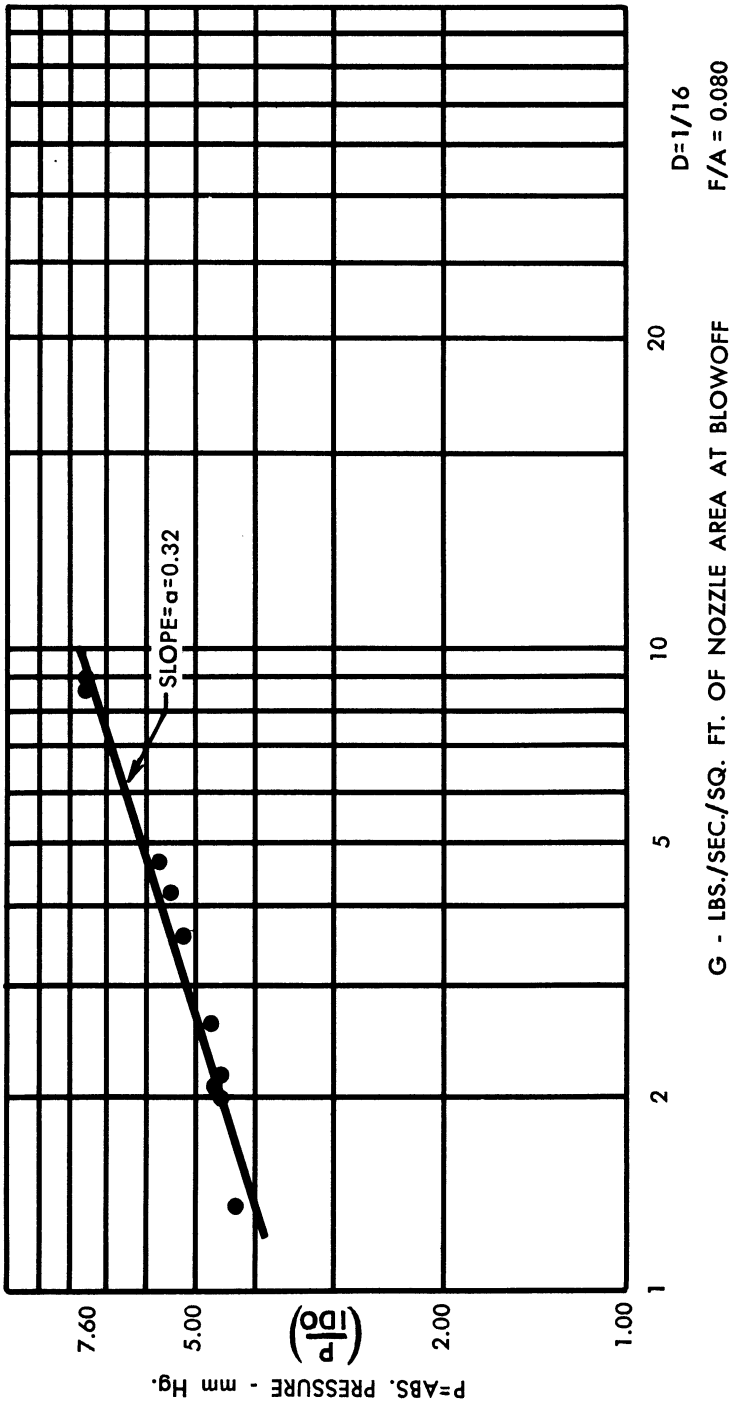

FIG. 55 DEVELOPMENT OF CORRELATION LOG G VERSUS LOG P

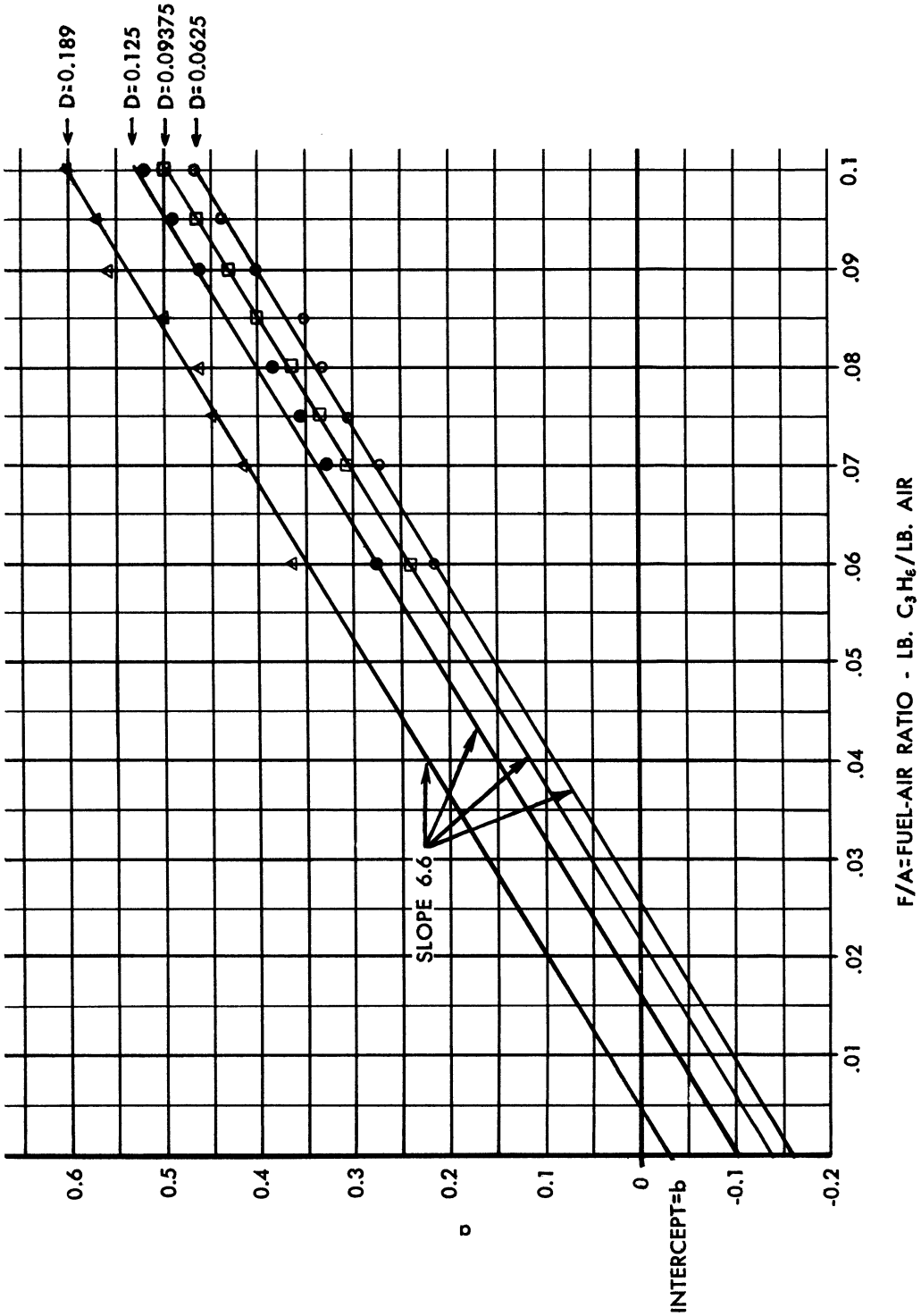

FIG. 56 DEVELOPMENT OF CORRELATION FUEL AIR RATIO VERSUS σ

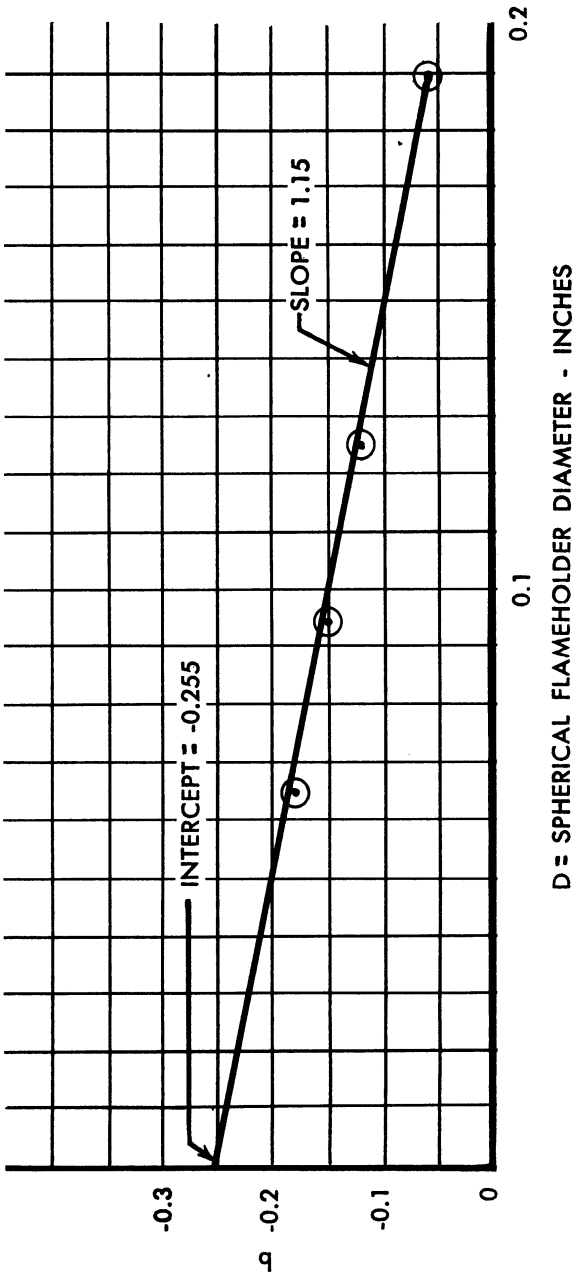

FIG. 57 DEVELOPMENT OF CORRELATION FLAME HOLDER DIAMETER VERSUS b

with a slope of 1 for each of the four spheres and their nine fuel-air ratios. An example of one of these plots may be seen in figure 58 which is for a fuel-air ratio of 0.080 and a sphere diameter of 1/16 inch. The intercepts at G = 1 (∴ log G = 0) were obtained from figure 58 and similar plots. Equation (5) may be written as

$$(6) \quad \log G = \log \left(\frac{P}{100}\right)^{1/a} - \log c$$

or

$$(7) \quad G = \frac{\left(\frac{P}{100}\right)^{1/a}}{c}$$

in which c is the intercept obtained at G = 1 from figure 58 and similar figures. The values of c obtained were plotted vs. D (sphere diameter) on log-log paper as is shown in figure 59. As may be seen from figure 59, the lines of constant fuel-air ratio intersect at a common point, D = 0.29 and c = 1.4. The equations for these lines may then be written

$$(8) \quad \log (0.29) - \log D = d (\log 1.4 - \log c)$$

or

$$(9) \quad \log \left(\frac{0.29}{D}\right) = d \left(\log \frac{1.4}{c}\right)$$

Values of the slope d were then plotted against F/A to give a straight line on log-log paper as may be seen in figure 60. The slope of this line is 3.11 and one point on this line is F/A = 0.100 at d = -0.91. Hence, the equation for the line shown in figure 60 may be written as

$$(10) \quad \text{slope} = 3.11 = \frac{\log - 0.91 - \log d}{\log 0.1 - \log F/A}$$

or

$$(11) \quad 3.11 \log \frac{0.1}{F/A} = \log \frac{- 0.91}{d}$$

or

$$(12) \quad d = \frac{-0.91}{\left(\frac{0.1}{F/A}\right)^{3.11}}$$

Substituting this value of d in equation (9) and solving for c, we obtain

$$(13) \quad c = \frac{1.4}{\left(\frac{0.29}{D}\right)^{\left(\frac{0.1/FA}{-.91}\right)^{3.11}}}$$

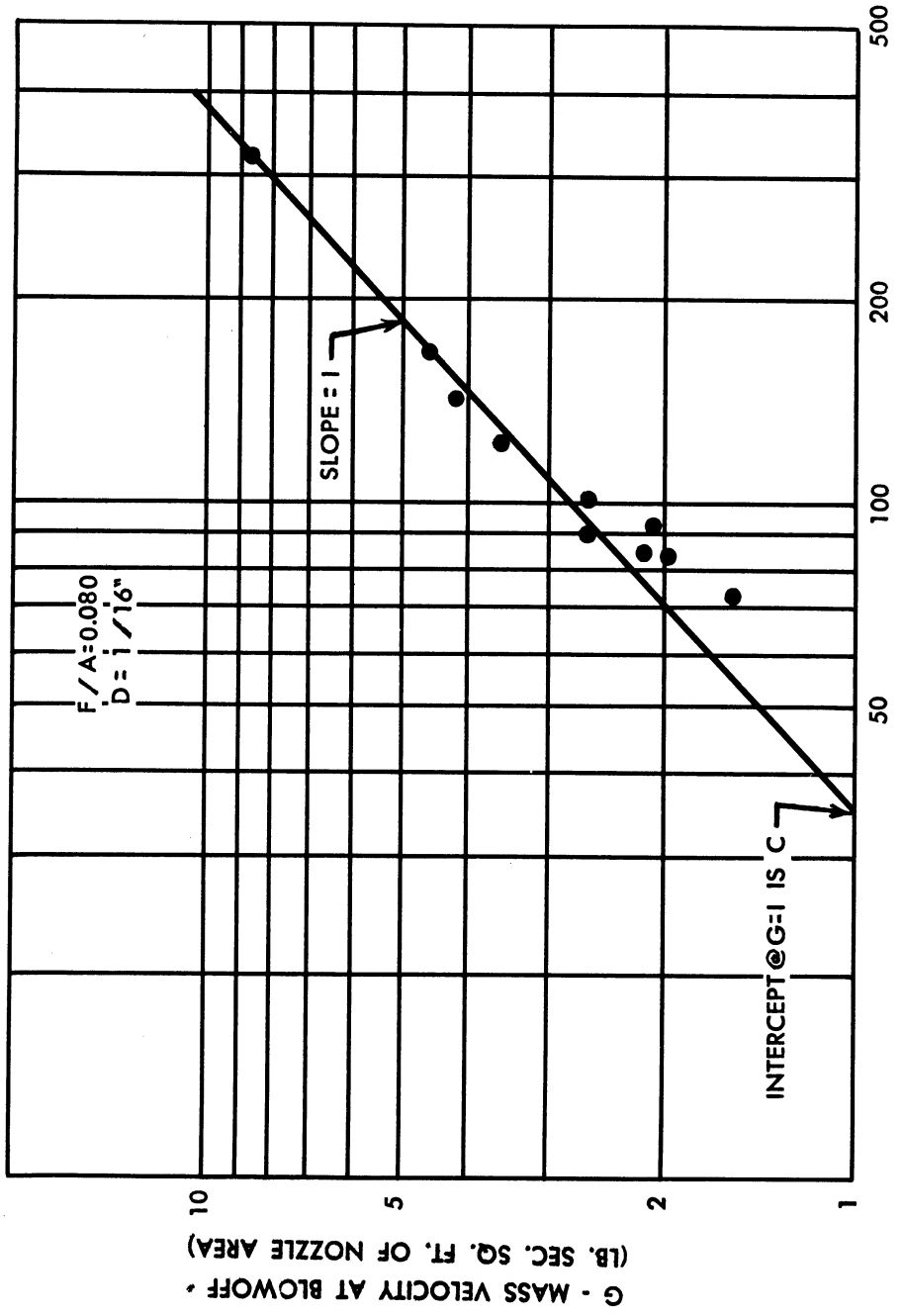

FIG. 58 DEVELOPMENT OF CORRELATION LOG G VERSUS LOG $\left(\frac{P}{100}\right)^{\frac{1}{a}}$

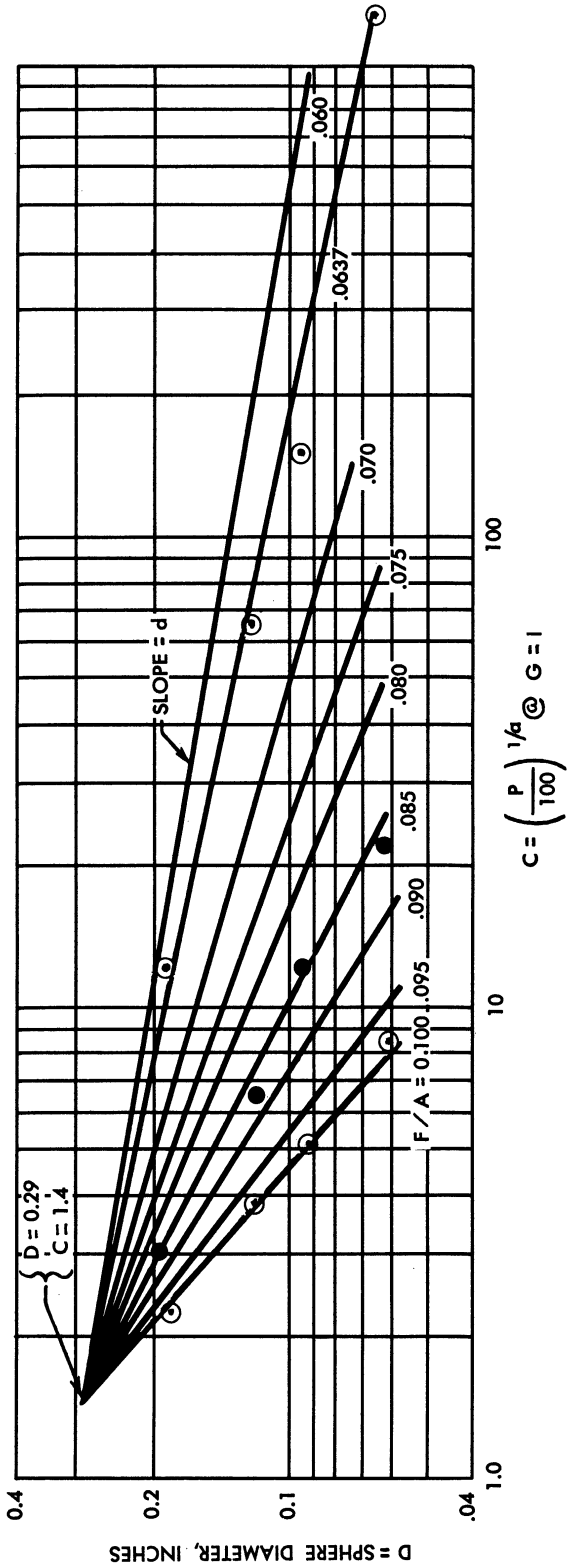

FIG. 59 DEVELOPMENT OF CORRELATION LOG D VERSUS c

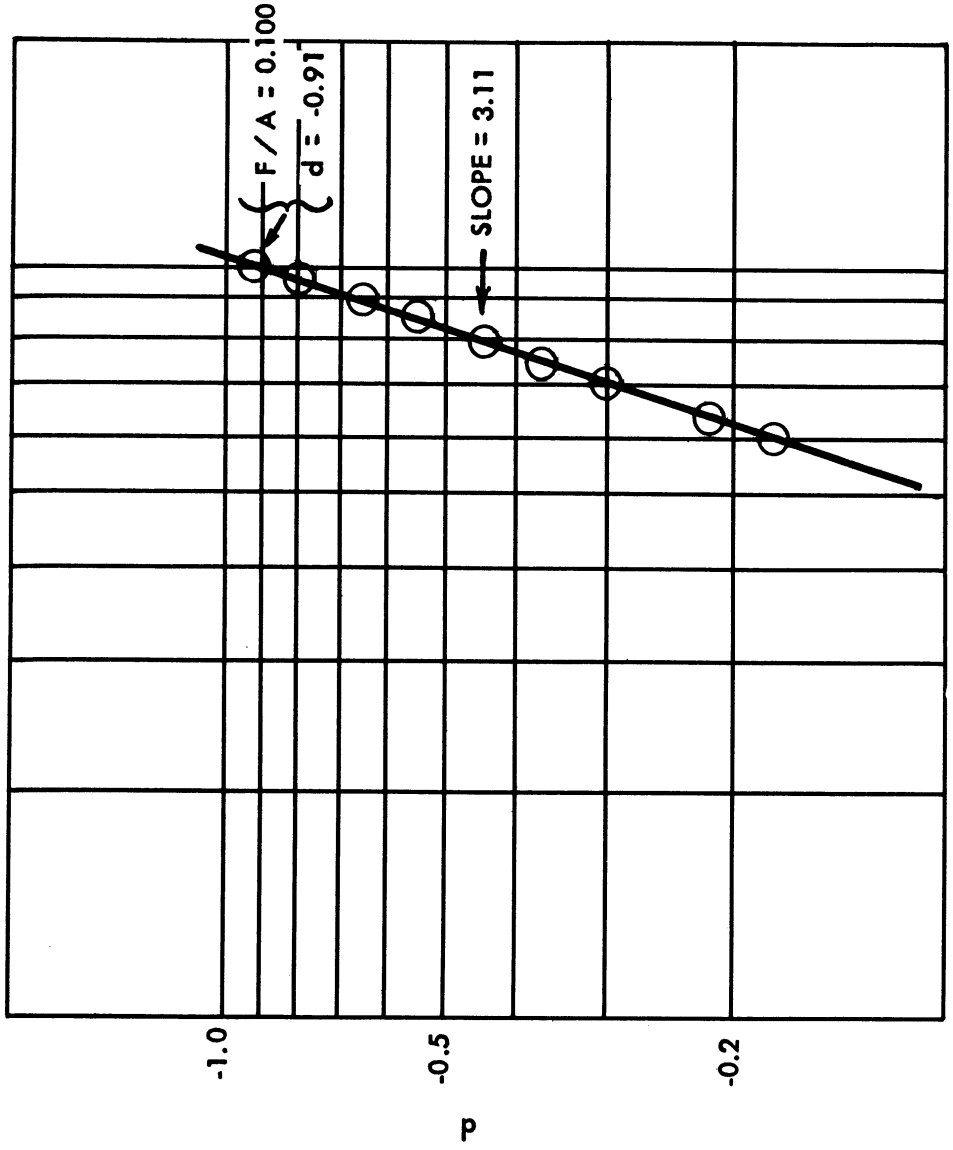

DEVELOPMENT OF CORRELATION LOG D VERSUS LOG FUEL AIR RATIO

FIG. 60

and substituting this value of c in equation (7), we find

$$(14) \qquad G = \frac{\left(\frac{P}{100}\right)^{\alpha} \left(\frac{0.29}{D}\right)^{B}}{1.4}$$

in which

$$\alpha = \frac{1}{a} = \frac{1}{1.15\ D + 6.6\ (F/A)\ -0.255}$$

and

$$B = \frac{1}{d} = \frac{(0.1/F/A)^{3.11}}{-0.91}$$

Equation (14) should be valid for spherical flame holder diameters (D) from 0.0625 to 0.189 inches in diameter, for propane-air (F/A) ratios from 0.06 to 0.100, and for pressures (P) from 760 to 200 mm Hg abs. It is, however, valid only for the above conditions when used in a 3/8 inch diameter nozzle at a flame holder diameter of 3/16 inch, when tested in a system in which the ratio of test chamber area to nozzle area is at least 1100 to 1. Thus, in order to determine the mass velocity at blowoff (G) which would be obtained if the system geometry was varied, additional terms must be added to equation (14). The effect of nozzle diameter and height of the flame holder upon the mass velocity at blowoff was presented in Section III. In this correlation, no attempt was made to incorporate the data obtained with the use of glass wool upstream of the nozzle or to consider the effects of jet confinement. The problems of jet confinement and the resonance change induced by glass wool are intimately connected with flame stabilization, but resonance effects in confined jets have been considered in a previous report[2] from these laboratories, and not enough quantitative data was obtained in this investigation to include these effects in a correlation. Hence, the nozzle diameter and height of the flame holder are the only system variables which are to be incorporated into equation (14). Figure 61 shows the effects of the height of the flame holder upon the mass velocity at blowoff for a 3/8 inch and a 5/8 inch diameter nozzle in an unconfined jet. (The data used in equation (14) was obtained with a 3/8 inch nozzle in a 10 x 12 x 18 inch test chamber. However, as was previously shown, and, as may be seen in figure 61, there is essentially no difference between this degree of confinement, $\left(\frac{\text{test chamber area}}{\text{nozzle area}} = 1100/1\right)$, and a completely unconfined jet.)

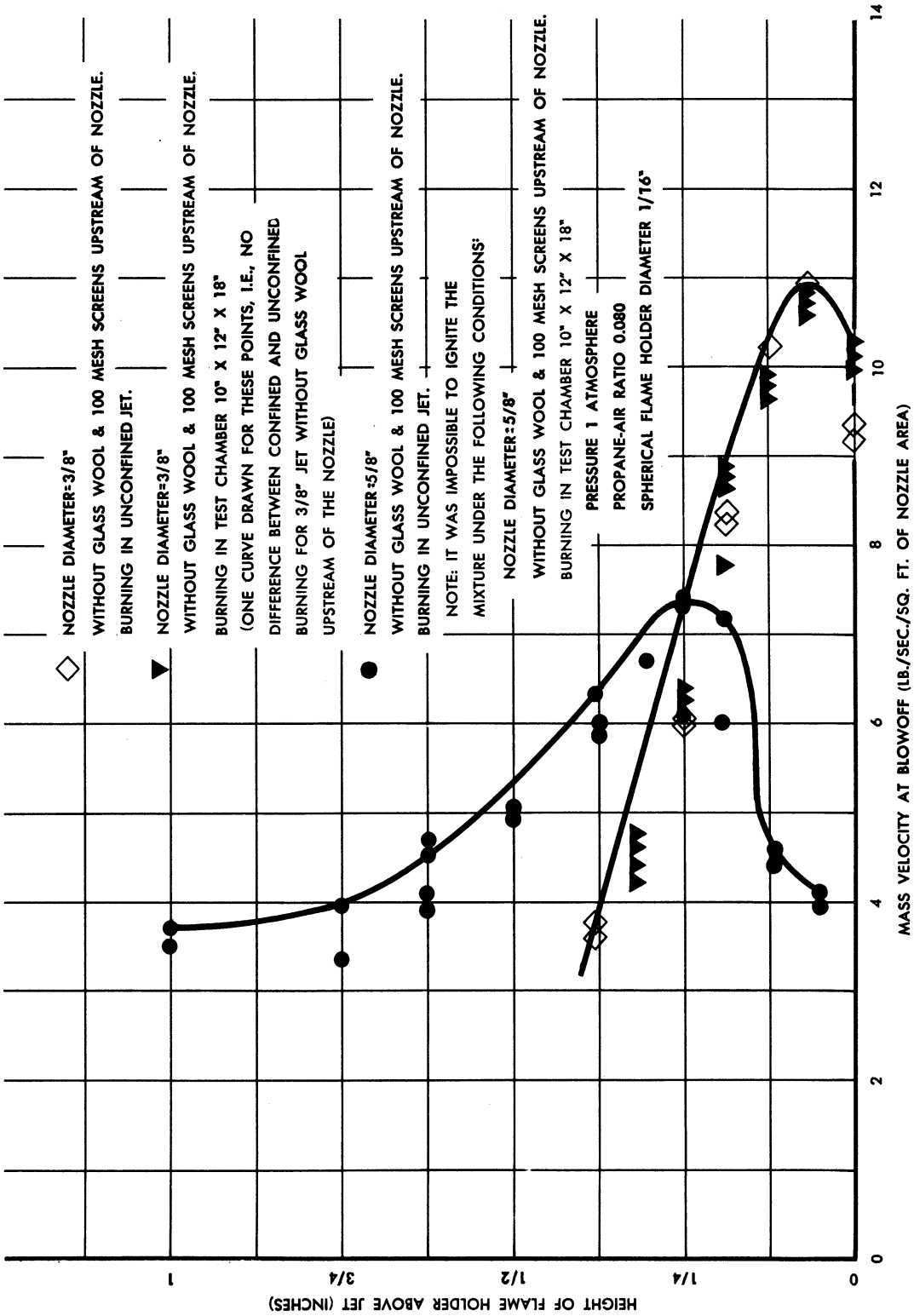

FIG. 61 EFFECT OF NOZZLE DIAMETER ON MASS VELOCITY AT BLOWOFF

Figure 61 indicates that there is a maximum height for the flame holder, and that this maximum height is some function of the nozzle diameter. For the 3/8 inch and the 5/8 inch diameter nozzles, the optimum $\frac{h}{D_j}$ was found to equal numerically $D_j^{1.85}$ in which h is the height of the flame holder, and D_j is the nozzle diameter, both expressed in inches. It was found that the experimental data shown in figure 61 could be fitted to a parabolic type of curve (i.e. $(g-k)^2 = 4p\,(x-j)$). Straight lines were obtained for both nozzles when G, the mass velocity at blowoff, was plotted against

$$\frac{G - 4}{\left(\frac{h}{D_j} - \left(\frac{h}{D_j}\right)_{max}\right)^2 - 0.6} = \left(\frac{G - 4}{\left[\left(\frac{h}{D_j}\right) - D_j^{1.84}\right]^2 - 0.6} = \frac{G - 4}{H} \right)$$

Straight lines so obtained are shown in figure 62. As may be seen, the two lines intersect at G = 11.6, $\frac{G - 4}{H} = -12.2$. If the slope of these lines (f) (which is some function of nozzle diameter) were known, the equation of these lines would be represented as

$$(15) \quad f = \frac{11.6 - G}{-12.2 - \frac{G - 4}{H}}$$

or rearranging

$$(16) \quad G = \frac{12.2f - 4\frac{f}{H} + 11.6}{1 - f/H}$$

Although complete height vs. G data is available for only two nozzle diameters, 3/8 inch and 5/8 inch, data was obtained at $\frac{h}{D_j} = 0.5$ for 7/16, 1/2, and 1 inch diameter nozzles. The use of this data would give one point for each of these three nozzles on figure 62. If the assumption were made that lines representing other $\frac{h}{D_j}$ for these nozzles

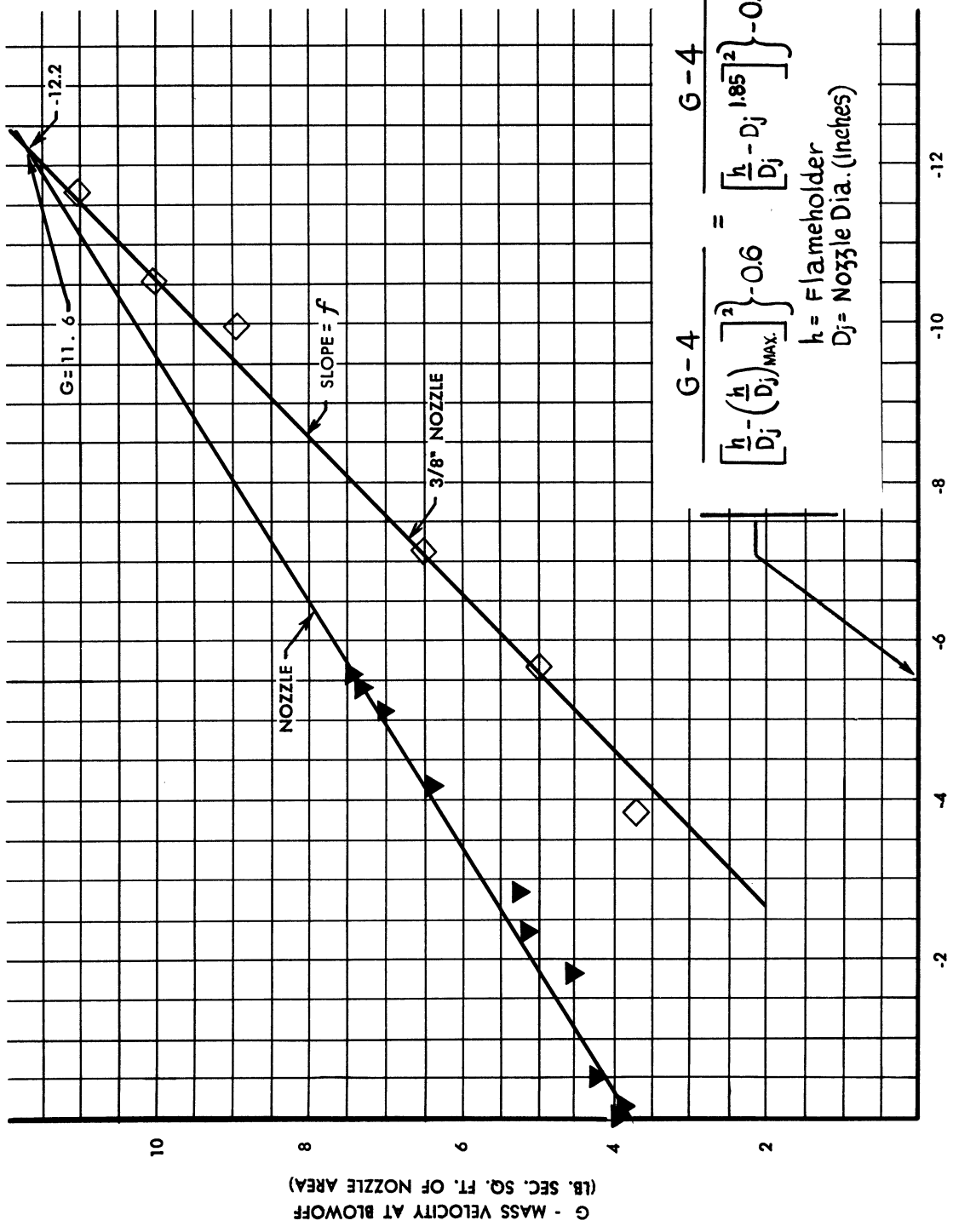

FIG. 62 DEVELOPMENT OF CORRELATION G VERSUS $\frac{G-4}{\left(\frac{h}{D_j}-D_j^{1.84}\right)^2}-0.6$

also passed through the intersection point of the 3/8 and 5/8 inch nozzle, then the slope (f) could be determined for these nozzles as well as for the 3/8 and 5/8 nozzles for which more complete data is available. This was done and the values of f were plotted against D_j in figure 63 to obtain a straight line whose equation is

$$(17) \qquad f = 1.42\ D_j - 1.54$$

This value of f was substituted in equation (16) to obtain the expression for G shown below

$$(18) \qquad G = \frac{-7.2 + 17.32\ D_j - 4\ \frac{f}{H}}{1 - f/H}$$

in which

$$\frac{f}{H} = \frac{1.42\ D_j - 1.54}{\left(\frac{h}{D_j} - D_j^{1.84}\right)^2 - 0.6}$$

The values of G, the mass velocity at blowoff, predicted by equation (18), are compared with the experimental values obtained, in Table 2. In general the highest experimental value obtained was used to draw the curves shown in figures 61 and other blowoff curves.

As may be seen from Table 2, equation (18) represents the experimental data reasonably well, except in the 1/8 inch and possibly in the 1/4 inch nozzle. This deviation of the smaller nozzles could perhaps be explained by blocking of the nozzle by the flame holder. Thus, a correction for nozzle diameter and flame holder height may be applied to equation (14) to obtain the following expression

$$(19) \qquad G = \frac{\left(\frac{P}{100}\right)^{\alpha} \left(\frac{0.29}{D}\right)^{B}}{1.4} \left[\frac{-7.2 + 17.32\ D_j - 4\ \Gamma}{8.42\ (1 - \Gamma)}\right]$$

TABLE 2

COMPARISON OF EXPERIMENTAL VALUES OF THE MASS VELOCITY AT BLOWOFF WITH THE VALUES OBTAINED FROM EQUATION 18

Sphere Diameter = 0.0625 inches
F/A = 0.080 lb/C_3H_8/lb air
Completely Unconfined Jet
No Glass Wool Upstream of Nozzle

Nozzle Diameter Inches D_j	Height of Flame Holder / Nozzle Diameter h/D_j	Mass Velocity at Blowoff lbs/sec/sq.ft. G Experimental	G from Eq. 18
1	0.5	13.5	13.3
5/8	0.5	6.4 - 7.0	7.8
1/2	0.5	7.1 - 8.9	9.0
7/16	0.5	7.8 - 8.2	8.7
3/8	0.5	7.8 - 8.9	8.4
1/4	0.5	6.5 - 7.1	8.2
1/8	0.5	4.2 - 4.6	7.1
3/8	0.1667	10.5 - 10.9	10.9
3/8	0.333	9.6 - 10.2	10.2
3/8	0.5	7.8 - 8.9	8.4
3/8	0.667	6.0 - 6.5	6.5
3/8	0.833	4.3 - 4.9	4.9
3/8	1	3.5 - 3.7	4.5
5/8	0.1	4.0 - 4.4	5.0
5/8	0.2	4.3 - 4.8	6.0
5/8	0.3	6.0 - 7.3	7.3
5/8	0.4	6.0 - 7.3	8
5/8	0.5	6.5 - 7.0	7.8
5/8	0.6	5.8 - 6.4	6.5
5/8	0.8	4.9 - 5.3	4.9
5/8	1.0	3.9 - 4.7	4.3
5/8	1.2	3.8 - 4.0	4.0
5/8	1.6	3.5 - 3.8	3.8

in which

$$\alpha = \frac{1}{a} = \frac{1}{1.15\ D + 6.6\ (F/A) - 0.255}$$

$$B = \frac{1}{d} = \frac{\left[0.100/(F/A)\right]^{3.11}}{-0.91}$$

$$\Gamma = \frac{f}{H} = \frac{1.42\ D_j - 1.54}{\left(\frac{h}{D_j} - D_j^{1.84}\right)^2} - 0.60$$

when the variables are expressed in the following units

G = mass velocity at blowoff lbs/sec/sq.ft. of nozzle area

P = absolute pressure, mm of Hg

D = spherical flame holder diameter, inches

F/A = lb propane/lb air

D_j = nozzle diameter, inches

h = height of flame holder above nozzle, inches

This equation, then, is valid for fuel-air ratios from 0.06 to 0.100, sphere diameters from 0.0625 to 0.189 inches, and pressures from 200 mm to 760 mm Hg abs, in a 3/8 inch diameter nozzle with h/D = 0.5. It is also valid for a F/A of 0.080, D = 0.0625, for nozzle diameters from 1/8 to 1 inch, at h/D = 0.5, and for 3/8 and 5/8 inch nozzles from h/D = 0 to h/D = 1.6. It is conceivable that the equation would predict the mass velocity at blowoff for other conditions, but no experimental data is available to test the equation. The equation is valid for completely unconfined jets, or at least jets in which the area of the test section to the nozzle area is at least 1100 to 1. It is known that a greater degree of jet confinement reduces the mass velocity at blowoff considerably due to resonance and other effects. The size of the plenium chamber upstream of the nozzle, as well as insertion of glass wool immediately upstream of the nozzle, also changes the mass velocity at blowoff, probably because of resonance between the flame and the upstream chamber. The representation of all the experimental data obtained by equation (19) may be seen in figure 64.

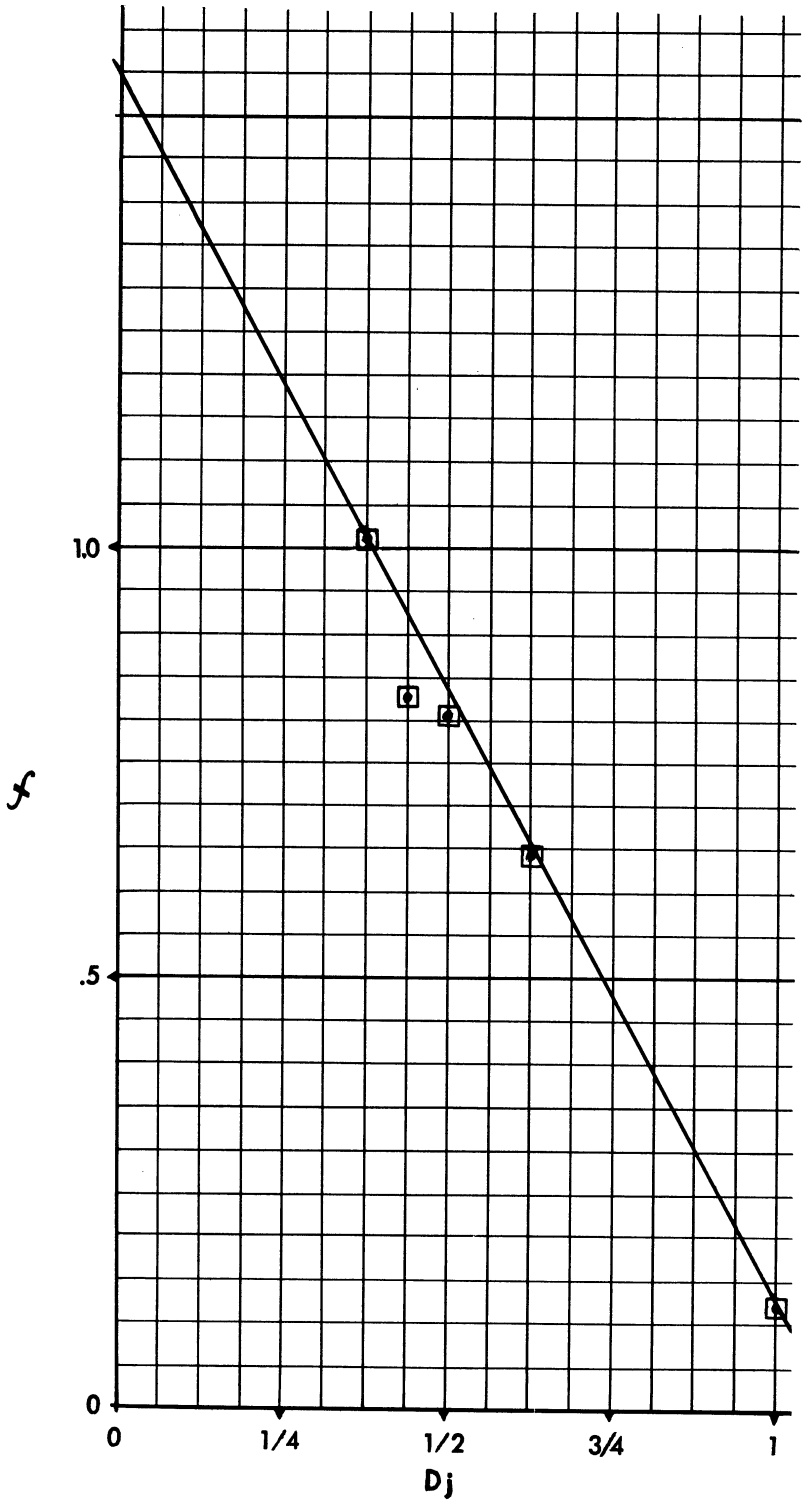

FIG. 63 DEVELOPMENT OF CORRELATION D_j VERSUS f

CORRELATION OF EXPERIMENTAL BLOWOFF DATA FOR

IN. $D = 3/8"$, $\frac{h}{D_j} = 0.5$

- PROPANE-AIR RATIOS (F/A) FROM 0.06 TO 0.100
- SPHERICAL FLAMEHOLDER DIAMETER (D) FROM 0.0625 TO 0.189 INCHES
- ABSOLUTE PRESSURES (P) FROM 200 TO 760 MM. HG.

AND

$D = 0.0625$, $F/A = 0.08$, $P = 760$ M.M.

- NOZZLE DIAMETERS (D_j) FROM 1/8" TO 1"
- FLAMEHOLDER HEIGHTS (h) FROM 0" TO 1-1/8"

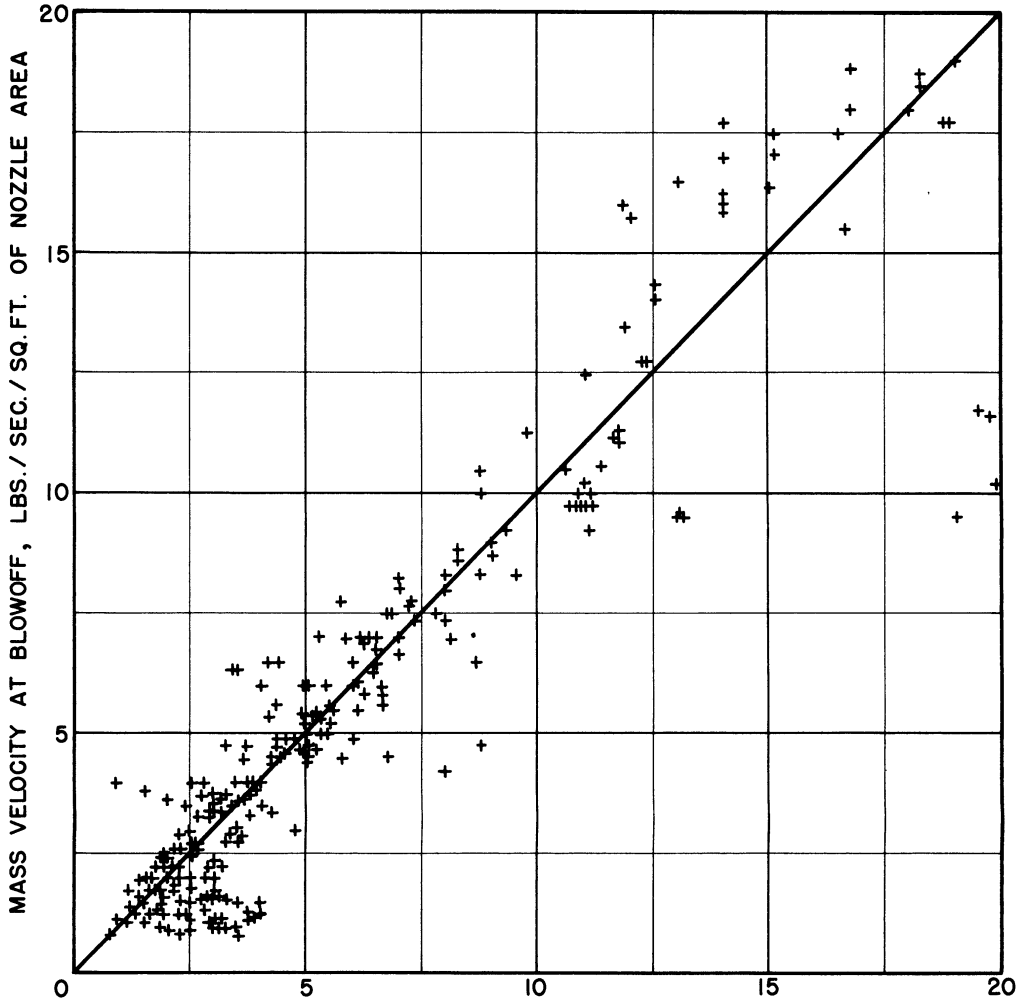

$$\frac{\left(\frac{P}{100}\right)^{\alpha}\left(\frac{0.29}{D}\right)^{\beta}}{1.4}\left[\frac{-7.2 + 17.32\,D_j - 4\Gamma}{8.42\,(1-\Gamma)}\right]$$

IN WHICH:

$$\alpha = \frac{1}{1.15\,D + 6.6\,(F/A - 0.255)}$$

$$\beta = \frac{\left[0.100/F/A\right]^{3.11}}{-.091}$$

$$\Gamma = \frac{1.42\,D_j - 1.54}{\left(\frac{h}{D_j} - D_j^{1.84}\right)^2 - 0.60}$$

FIG. 64 CORRELATION OF EXPERIMENTAL BLOWOFF DATA

BIBLIOGRAPHY

No.

1 Hougen and Watson, "Chemical Process Principles, Part 2, Thermodynamics," John Wiley and Sons, New York, New York, 1947, p. 489.

2 University of Michigan External Memorandum No. 43, "Resonance of a Flame in a Parallel Walled Combustion Chamber," R. A. Dunlap.

3 University of Michigan UMR-27, Progress Report No. 3, AAF Contract W33-038-ac-2100, pp. 3 - 12.

4 University of Michigan UMR-33, Progress Report No. 6, AAF Contract W33-038-ac-2100, pp. 3 - 10.

5 Battelle Memorial Institute, Progress Report No. 30, "Aerodynamic Conditions Affecting Blowoff of Burners," AMC Contract AF-33-038-2038

6 Ibid, figure 161.

7 Hottel, Williams, and Satterfield, "Thermodynamic Charts for Combustion Processes, Part One, Text," John Wiley and Sons, New York, New York, 1949.

8 University of Michigan External Memorandum No. 21, "Measurement of Flame Speeds with the V-Flame," R. B. Morrison and R. A. Dunlap, 1947.

9 Thomsen and Thomsen, "Conduction of Electricity Through Gases, Vol. I," Cambridge, 1928.

10 University of Michigan UMR-33, Progress Report No. 6, AAF Contract W33-038-ac-2100, figure 1, p. 5.

11 University of Michigan UMR-31, Progress Report No. 5, AAF Contract W33-038-ac-2100, figure 1.

12 Ibid, figure 2.

13 Langmuir and Blodgett, USAF Technical Report No. 5418, February 19, 1946, Graph Reported in Perry, "Chemical Engineer's Handbook," Third Edition, McGraw Hill Book Co., New York, 1950, p. 1022.

14 University of Michigan UMR-29, Progress Report No. 4, AAF Contract, W33-038-ac-2100.

15 University of Michigan External Memorandum No. 21, "Measurement of Flame Speeds with the V-Flame," R. B. Morrison and R. A. Dunlap, 1948, figure 17, p. 27.

BIBLIOGRAPHY (CONTINUED)

No.

16 A. C. Scurlock, "Flame Stabilization and Propagation in High Velocity Gas Streams," Meteor Report No. 19, MIT Guided Missiles Program, May 1948.

17 E. A. De Zubay, "Flame Stability Characteristics of Circular Discs," Scientific Paper No. 1506, Westinghouse Research Laboratories, Westinghouse Electric Corp., March 9, 1950.

18 Summary Report to AMC, Contract AF-33-038-2038, Battelle Memorial Institute, Section on "Aerodynamic and Other Conditions Affecting Blowoff of Burners," R. A. Jensen and C. A. Miesso, May 15, 1950.

DISTRIBUTION

Distribution of this report is made in accordance with AMC letter dated 8 April 1949.